The Dissertation Committee for Amy Ann Mrazek Certifies that this is the approved version of the following dissertation:

Preclinical Development of a Pharmacologic Agent for the Treatment of Recurrent Acute Pancreatitis

Celia Chao, M.D., Chair

Mark R. Hellmich, Ph.D., Mentor

Miriam Falzon, Ph.D.

Jia Zhou, Ph.D.

Dai H. Chung, M.D.

Taylor S. Riall, M.D., Ph.D.

Committee:

Dean, Graduate School

Preclinical Development of a Pharmacologic Agent for the Treatment of Recurrent Acute Pancreatitis

by

Amy Ann Mrazek, M.D., B.S.

Dissertation

Presented to the Faculty of the Graduate School of

The University of Texas Medical Branch

in Partial Fulfillment

of the Requirements

for the Degree of

Human Pathophysiology and Translational Medicine (HPTM)

Doctor of Philosophy

The University of Texas Medical Branch

August, 2015

Dedication

This dissertation is dedicated to my mother, Nancy Mrazek, who I am forever grateful for her encouragement and support throughout my academic pursuits.

Acknowledgements

I am appreciative of the mentorship by Drs. Mark R. Hellmich and Celia Chao over the past three years. I am grateful for the opportunity to have developed valuable collaborations with Drs. Jia Zhou, Miriam Falzon, Vandanajay Bhatia, Judith Aronson, and Heidi Spratt. Finally, I am much obliged to the current UTMB Department of Surgery chairman, Dr. Douglas S. Tyler, former chairman, Dr. Courtney M. Townsend, Jr., and general surgery residency program director, Dr. Kristene K. Gugliuzza, for their support of my research endeavors and development as a surgeon scientist.

Preclinical Development of a Pharmacologic Agent for the Treatment of Recurrent Acute Pancreatitis

Publication No._____

Amy Ann Mrazek, Ph.D.

The University of Texas Medical Branch, 2015

Supervisor: Celia Chao

ABSTRACT - Chronic pancreatitis (CP) is an irreversible disease process defined by acinar cell necrosis, inflammation and fibrosis. With disease progression, patients develop pancreatic insufficiency secondary to the destruction of functional pancreatic tissue and its replacement with scarring. Patients with CP have a poor quality of life, and their treatment options are limited to supportive care and symptom palliation. There are currently no drugs on the market directly targeting the pathogenesis of CP. The objective of this research is to develop a pharmacologic agent for the treatment of recurrent acute pancreatitis (RAP), thereby limiting progression to CP. Apigenin is a natural compound with known anti-inflammatory, anti-proliferative, and pro-apoptotic properties. In a mouse model of RAP, the natural compound, apigenin, protected the pancreas from histologic damage while minimizing fibrosis. It was hypothesized that apigenin minimized the sequelae of RAP by inhibiting the inflammatory and fibrotic response to recurrent injury. Parathyroid hormone related protein (PTHrP) is a pro-inflammatory and pro-fibrotic mediator of acute and CP. The first aim was to identify PTHrP-related mechanisms by which apigenin limits inflammation in acinar cells. Apigenin reduced activation of the MAPK/ERK and NF-κB

pathways, leading to suppression of PTHrP P3 promoter activity and IL-6 transcription. The second aim was to determine how apigenin limits pancreatic stellate cell (PSC)-mediated fibrosis. Apigenin inhibited PSC proliferation, induced PSC death, reduced PSC transcription of extracellular matrix proteins collagen and fibronectin, proliferative cofactor PCNA, and cytokines TGF-β, IL-6, and IL-8. The last aim was to develop apigenin-like compounds with more favorable drug-like properties. Analogs with improved aqueous solubility were tested *in vitro* and *in vivo* for increased potency. Analog HJC 05-61 was more potent than apigenin at limiting PSC viability and inducing PSC apoptosis. In a proof-of-concept RAP mouse study, apigenin derivatives were as effective as apigenin in preserving pancreatic architecture and limiting fibrosis. Thus, apigenin and analogs protect the pancreas during RAP by limiting the pro-inflammatory and pro-fibrotic response to pancreatic injury. This is in part mediated through down-regulation of PTHrP and PSC activity, both of which participate in autocrine and paracrine signaling that perpetuates pancreatitis.

TABLE OF CONTENTS

LIST OF FIGURES

LIST OF TABLES

LIST OF ABBREVIATIONS

α-SMA	alpha smooth muscle actin
Ab	antibody
AC	adenylate cyclase
ACh	acetylcholine
AKA	also known as
Akt	Ak strain transforming retrovirus (aka protein kinase B)
ANOVA	analysis of variance
ANTICPATE	ANTI-oxidant therapy for painful Chronic Pancreatitis Therapy Evaluation trial
AP	acute pancreatitis
AP-1	activating protein 1
ATP	adenosine triphosphate
bFGF	basic fibroblast growth factor
Ca^{2+}	calcium
cAMP	cyclic AMP (adenosine monophosphate)
CBP	CREB (cAMP-response element-binding protein)-binding protein
CCK	cholecystokinin
CCKR	cholecystokinin receptor
cDNA	complementary deoxyribonucleic acid
CFTR	cystic fibrosis transmembrane regulator
CHOP	C/EBP (CCAAT/enhancer binding protein) homologous protein
CINC	cytokine-induced neutrophil chemoattractant
cLogP	calculated logarithm of the partition-coefficient
CR	cerulein
CP	chronic pancreatitis
d	days
DAG	1,2-diacylglycerol
DAMP	danger-associated molecular pattern
DBTC	dibutyltin dichloride

DMSO	dimethyl sulfoxide
DNA	deoxyribonucleic acid
EC_{50}	half maximal effective concentration
ECL	enhanced chemiluminescence
ECM	extracellular matrix
ELISA	enzyme-linked immunosorbent assay
ERCP	endoscopic retrograde cholangiopancreatography
ERK	extracellular signal-regulated kinase (aka p42/p44)
FAEE	fatty acid ethyl ester
FBS	fetal bovine serum
FN	fibronectin
FR	free radical
GFAP	glial fibrillary acidic protein
GRP78	78 kDa glucose-related protein (aka binding immunoglobulin protein, BiP)
H&E	hematoxylin and eosin
HMB1	high-mobility protein B1
HP	hereditary pancreatitis
HPLC	high performance liquid chromatography
hr	hour(s)
HRP	horseradish peroxidase
IACUC	Animal Care and Use Committee
IC_{50}	half maximal inhibitory concentration
ICAM-1	intracellular adhesion molecule-1
ICC	immunocytochemistry
IHC	immunohistochemistry
IκB	inhibitor of NF-κB
IKK	IκB kinase
IL	interleukin
IP_3	inositol 1,4,5-triphosphate
IP	intraperitoneal
irPSCc3	immortalized rat pancreatic stellate clone 3

KO	knockout
JNK	c-Jun N-terminal kinase (aka stress-activated protein kinase)
LPS	lipopolysaccharide
LY	LY294002, PI3K inhibitor
MANNHEIM	multiple risk factors; alcohol; nicotine; nutritional; hereditary; efferent duct; immunologic; and miscellaneous and rare metabolic disorders
MAPK	mitogen activated protein kinase
MC	methylcellulose
MCP-1	monocyte chemoattract protein-1
min	minute(s)
mL	milliliter
mM	millimolar
MMP	matrix metalloproteinase
MPO	myeloperoxidase
MQ	Milli-Q water
mRNA	messenger ribonucleic acid
ms	millisecond(s)
mTOR	mammalian target of rapamycin
MTT	3-(4,5-dimethylthiazol-2-yl)-2,5-diphenyltetrazolium bromide
N	number
N21I	asparagine to isoleucine substitution at codon #21
N34S	asparagine to serine at codon #34
NF-κB	nuclear factor-kappa B
NLRP3	NACHT, LRR, and PYD domains-containing protein 3
OS	oxidative stress
PAF	platelet activating factor
PAR-2	protease activated receptor-2
PBS-T	phosphate buffered saline with Tween 20
PD	PD98059, MAPK inhibitor
PDGF	platelet derived growth factor
pH	potential of hydrogen

PI3K	phosphatidylinositol 3-kinase
PIP_2	phosphatidylinositol 4,5-bisphosphate
PKC	protein kinase C
PLC	phospholipase C
PRSS,1	protease serine, 1 (aka cationic trypsinogen)
PSC	pancreatic stellate cell
PSP	pancreatic stone protein (aka lithostathine)
PSTI	pancreatic secretory trypsin inhibitor
PTHrP	parathyroid hormone-related protein
PTP	pancreatic thread protein
PVDF	polyvinylidene fluoride
qPCR	real-time polymerase chain reaction
Q-Q	quantile-quantile
R117H	arginine to histidine substitution at residue #117
RAP	Recurrent Acute Pancreatitis
RANTES	regulated on activation normal T cell expressed and secreted (aka CCL5)
RNA	ribonucleic acid
ROI	region of interest (Image J command)
ROS	reactive oxygen species
RT	room temperature (20-25˚C)
RT-PCR	reverse transcription polymerase chain reaction
SAPE	Sentinel Acute Pancreatitis Event
SDS-PAGE	Sodium Dodecyl Sulfate-PolyAcrylamide Gel Electrophoresis
SEM	standard error of the mean
SPINK1	serine protease inhibitor, Kazal type 1 (aka pancreatic secretory trypsin inhibitor)
TBS-T	tris buffered saline with Tween 20
TIGAR-O	toxic-metabolic; idiopathic; genetic; autoimmune; recurrent and severe AP-associated CP; obstructive
TIMP	tissue inhibitors of matrix metalloproteinase
TGF-β	transforming growth factor-beta

TLR	toll-like receptor
TNF-α	tumor necrosis factor-alpha
tPSA	topological polar surface area
TUNEL	dUTP nick end labeling
µg	microgram
µL	microliter
UPR	unfolded protein response
UTMB	University of Texas Medical Branch
V	volts
VEGF	vascular endothelial growth factor
VIP	vasoactive intestinal peptide
WB	Western blot
WBN/Kob	Wistar Bonn/Kobori (rats)
wk	week(s)
WT	wild-type
ZG	zymogen granule

CHAPTER 1:

BACKGROUND

1.1 Introduction

Chronic pancreatitis (CP) is a progressive disease characterized by irreversible histologic damage and pancreatic insufficiency. CP is the result of recurrent acute pancreatitis (RAP), where the physiologic response to acinar cell injury becomes pathologic. Repeated pancreatic injury induces glandular atrophy, chronic inflammation, and pancreatic stellate cell (PSC)-mediated scarring. Current treatment options for CP are limited to supportive care and symptom palliation rather than targeting disease pathogenesis. The overall objective of this dissertation was to develop a novel therapeutic that reduces the severity of RAP, thereby preventing or delaying progression to CP.

The natural flavanoid, apigenin, was identified as a promising lead compound. When tested in a preclinical mouse model of RAP, we found that apigenin therapy induced a protective phenotype, preserving pancreatic architecture while limiting histologic damage. Therefore, we hypothesized that apigenin decreased the sequelae of recurrent acute pancreatitis (RAP) by inhibiting inflammatory signaling and fibrotic activity of PSCs. Apigenin's anti-inflammatory activity was, in part, mediated through inhibition of parathyroid hormone related protein (PTHrP), mitogen activated protein kinase (MAPK) and nuclear factor-kappa B (NF-κB) pathway activation. Apigenin's anti-fibrotic activity was, in part, mediated through growth inhibition, apoptosis induction, and suppression of PTHrP-mediated PSC response to pancreatic injury. Lastly, apigenin analogs were developed with more favorable drug-like properties and screened *in vitro* for improved anti-proliferative and pro-apoptotic activity in PSCs. In a proof-of-concept study, analogs were found to be as effective as apigenin in limiting the fibrotic response to RAP. This dissertation provides mechanistic and preclinical evidence supporting further optimization, preclinical and clinical testing of apigenin-like compounds in RAP to facilitate their transition from bench to bedside.

Within the first chapter of this dissertation, a scholarly review of the literature is provided. Normal pancreatic anatomy and physiology are reviewed. Focus is placed on the exocrine pancreas with a description of normal acinar cell biology and molecular signaling. The disease of CP is defined and its pathogenic mechanisms are analyzed through a

historical review of multiple theories, leading up to the current concept of RAP. Pancreatitis-induced changes in acinar cell and PSC physiology are reviewed. Both *in vitro* and *in vivo* experimental models of pancreatitis are discussed. My central objective and aims are presented and followed by a discussion on selection of apigenin as my lead compound for analog development.

1.2 Pancreatic Anatomy and Physiology

The pancreas is a critical part of both energy metabolism and digestion. This abdominal organ is divided into the following regions: head and uncinate process, neck, body, and tail. The pancreas is a retroperitoneal gland spanning from the first part of the small intestines (duodenum) to the spleen. Digestive juices are primarily drained through the main pancreatic duct of Wirsung, which joins the common hepatic duct carrying biliary drainage from the gallbladder and liver. The common bile duct ends at the sphincter of Oddi, which controls excretion through the ampulla of Vater into the duodenum. The accessory pancreatic duct of Santorini provides alternative drainage directly into the small intestines (1, 2).

The endocrine pancreas accounts for 2% of the pancreatic mass (2). The islets of Langerhans are comprised of the following major cell types, each of which is listed with the hormone it produces: beta (insulin), alpha (glucagon), delta (somatostatin), delta-2 (vasoactive intestinal peptide, VIP), and F cells (pancreatic polypeptide) (3). The hormones are secreted directly into the bloodstream, altering the metabolism and storage of carbohydrates, lipids, and protein. The exocrine pancreas is comprised of centroacinar, ductal, and acinar cells (**Figure 1**). The centroacinar and ductal cells secrete water, bicarbonate, and other electrolytes, responding to hormones like secretin, cholecystokinin (CCK), and the neurotransmitter acetylcholine (ACh). Acinar cells synthesize, store, and secrete digestive enzymes into the pancreatic juices, which assist with the digestion of food in the small intestines. The exocrine pancreas will be a primary focus of this dissertation.

1.2.1 Acinar Cell Biology

Acinar cells are the predominate cell of the pancreatic parenchyma. Digestive enzymes produced by the pancreas include amylase, lipase, trypsin, chymotrypsin, elastase, carboxypeptidases, ribonuclease, and deoxyribonuclease. Most of these secretory proteins are synthesized and processed in the endoplasmic reticulum as zymogens, requiring proteolytic cleavage to become activated. Amylase and lipase are exceptions to the proenzyme rule as they are secreted in their active form.

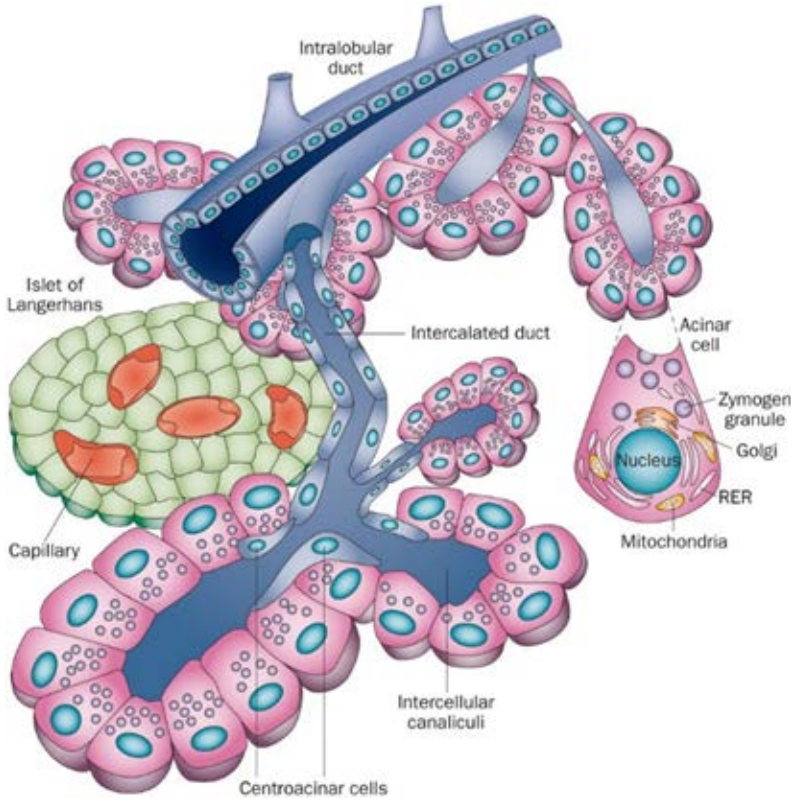

FIGURE 1. **Diagram of pancreatic structure**.
The functional structure of the exocrine pancreas is the acinus, which is composed of a grape-like cluster of acinar cells surrounding a lumen. Acini secrete digestive enzymes along the apical membrane. The centroacinar and ductal cells secrete water and electrolytes, providing a basic solution for the pancreatic juices. Secretions travel through a system of intercalated and intralobular ducts, which lead to the main pancreatic duct. Reproduced with permission from: Logsdon CD, Ji B. The role of protein synthesis and digestive enzymes in acinar cell injury. Nat Rev Gastroenterol Hepatol. 2013;10(6):362-370.

Within the Golgi apparatus, the newly synthesized digestive enzymes are modified and packaged into zymogen granules (ZGs). The ZGs are then transported to the apical surface of the acinar cell and their contents are excreted by exocytosis into the lumen of the acinus. The digestive proenzymes are transported through a system of ducts that lead to the small intestines (**Figure 1**). Enterokinases within the duodenum initially cleave an 8 amino acid N-terminal peptide from trypsinogen, leading to its proteolytic activation. Trypsin is

the primary enzyme responsible for catalyzing the activation of other proenzymes and additional trypsinogen activation (4).

Multiple fail-safe mechanisms exist to prevent premature intrapancreatic activation of trypsinogen. Digestive enzymes are synthesized as inactive proenzymes and kept isolated in membrane-bound organelles. The spatial and temporal intracellular trafficking of ZGs to the apical membrane of acini is a highly regulated process involving calcium (Ca^{2+}) oscillations, the maintenance of optimal pH and cytoskeletal structure (5). Trypsinogen and trypsin inhibitors such as pancreatic secretory trypsin inhibitor (PSTI), mesotrypsin, and enzyme Y are synthesized by acini as part of a negative feedback mechanism (6). Trypsin also possesses a cleavage site (Arg 117) for hydrolytic auto-inactivation (6). Thus, various fail-safe mechanisms exist to provide protection against pancreatic autodigestion.

1.2.2 Acinar Cell Molecular Signaling

Acini respond to hormonal and neural input through the expression of basolateral cell-surface receptors for secretagogues like ACh, CCK, secretin, and VIP. I will be focusing on CCK stimulation. The use of cerulein (CR), a CCK analog, is a well-characterized model to study secretagogue-induced pancreatitis (7). CCK binds to the CCK receptor (CCKR), which is a seven transmembrane G-protein coupled receptor that activates several intracellular signaling cascades (**Figure 2**) (8). Phospholipase C (PLC) catalyzes the formation of the secondary messenger 1,4,5-triphosphate (IP_3), which diffuses to the apical endoplasmic reticulum membrane and opens IP_3-sensitive calcium channels (9). The influx of cytosolic calcium stimulates the following: opening of ryanodine receptors, which increases the release of calcium stores; mitochondrial ATP synthesis, which is needed to fuel cell membrane ATPase calcium pumps; reuptake of calcium by the endoplasmic reticulum; and ZG exocytosis at the acinar cell's apical pole (9, 10). Activated adenylyl cyclase catalyzes the formation of cyclic AMP (cAMP), which has been shown to increase ZG sensitivity to calcium, inducing granule-to-granule fusion and luminal exocytosis (11).

CCK has been shown to activate several other intracellular signaling pathways, but their relationship to the acinar cell secretory function has yet to be established. The mitogen activated protein kinases (MAPKs) is divided into three major families: extracellular signal-regulated kinase (ERK), c-Jun N-terminal kinase (JNK), and p38 MAPK (**Figure 2**). The MAPK pathways are involved in the regulation of cellular synthetic activity (12), proliferation, differentiation, survival, apoptosis, inflammation and generation of a stress response (8). A protective negative feedback loop has been identified, where intrapancreatic trypsin activates protease activated receptor-2 (PAR-2), which leads to the down-regulation of the MAPK pathway, through the activation MAP kinase phosphatases (13).

Both diacylglycerol (DAG) and calcium activate protein kinase c (PKC), which in turn stimulates NF-κB uncoupling from and degradation of its inhibitor (IκB) (**Figure 2**). Activated NF-κB then translocates to the nucleus, where it stimulates the transcription of genes related to inflammation and cell survival (8). Through the use of pharmacologic protease inhibitors (14), adenoviral-induced NF-κB over-expression (15), and genetically modified mice lacking trypsinogen (16), NF-κB pathway activation can occur independently of trypsinogen activation.

Lastly, the phosphatidylinositol 3-kinase (PI3K) pathway leads to activation of protein kinase B (AKT) and mammalian target of rapamycin (mTOR) (**Figure 2**), which regulate cell proliferation, metabolism, survival, and regulation of an immune response (17). Inhibition of the PI3K by wortmannin has been shown to decrease colocalization of ZGs and lysosomes, which contain proteases like cathepsin B that can activate trypsinogen prematurely (18). Cross-talk does exist between the signaling pathways, such as a relationship between PKC and Ras/Raf in the MAPK pathway (19). Overall, additional research is needed to determine the relationship between stimuli-induced activation of the MAPK, PI3K, and NF-κB pathways and acinar cell secretory response.

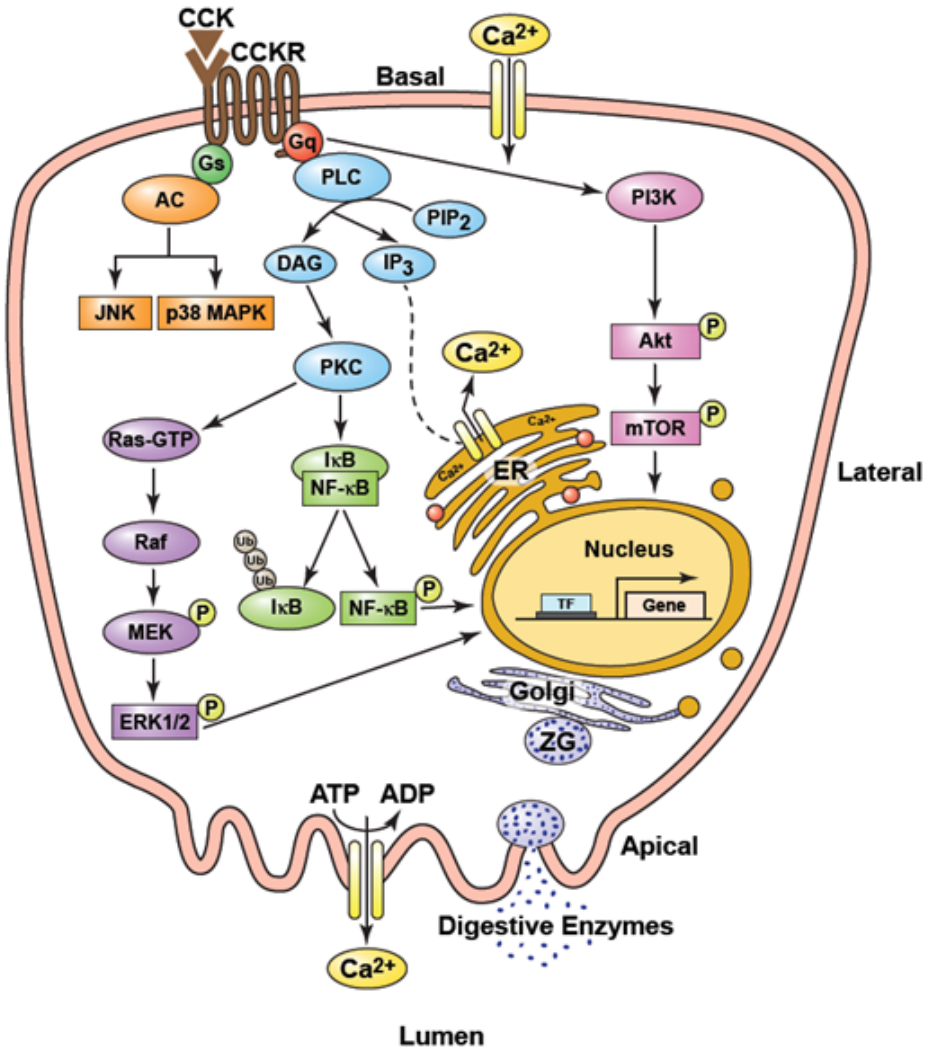

FIGURE 2. Cholecystokinin receptor (CCKR) activation of intra-acinar signaling pathways.

Binding of CCK to the CCK1R G protein-coupled receptor induces a conformational change and dissociation of secondary messenger G-proteins Gs and Gq. Gs activates adenylyl cyclase (AC) and downstream c-Jun N-terminal kinase (JNK) and p38 mitogen activated protein kinase (MAPK). Gq activates phospholipase C (PLC) and the phosphatidylinositol 3-kinase (PI3K) pathways. PI3K activates protein kinase B (Akt) and mammalian target of rapamycin (mTOR). PLC cleaves phospholipid phosphatidylinositol 4,5-bisphosphate (PIP_2) into 1,2-diacylglycerol (DAG) and inositol 1,4,5-triphosphate (IP_3). IP_3 diffuses to the endoplasmic reticulum (ER) and binds to open calcium (Ca^{2+}) channels. DAG activates protein kinase C (PKC), which activates the MAPK/extracellular signal-regulated kinase (ERK) and nuclear factor-kappa B (NF-κB) pathways. The Ras GTPase activates a series of kinases: Raf, MEK, and ERK1/2. PKC signals ubiquitination (Ub) of the inhibitor of NF-κB (IκB). ERK, Akt, and NF-κB diffuse to the nucleus where they regulate the phosphorylation (P) and binding of transcription factors, inducing target gene expression. Digestives enzymes are synthesized in the ER, packaged into zymogen granules (ZGs) within the Golgi apparatus, and transported to the apical surface for exocytosis.

1.3 Chronic Pancreatitis (CP)

CP is a progressive disease characterized by pancreatic atrophy, chronic inflammation, and stromal fibrosis. With repeated pancreatic injury, functional exocrine and endocrine tissue is damaged and replaced with scarring. Pancreatic insufficiency is manifested as impaired digestion, nutritional deficiencies, diarrhea, anorexia, and diabetes mellitus (20). Patients report a poor quality of life burdened by chronic abdominal pain and disease complications such as pseudocyst formation, biliary or duodenal obstruction, infection, organ failure, and an increased risk of pancreatic cancer (21).

CP has no cure, and treatment options are confined to supportive care and symptom palliation. Initial medical management includes analgesics, enzyme replacement, nutritional supplementation, glucose control, and lifestyle changes (22). With disease progression and failure of conservative therapies, invasive procedures are incorporated into the treatment plan (23). Endoscopic procedures may include nerve blocks/neurolysis, sphincterotomy, stricture dilatation, ductal stenting, stone retrieval, or lithotripsy (22, 24). Surgical intervention aims to improve symptomology through decompression, denervation, resection, bypass, and/or total pancreatectomy with islet cell transplantation (25). Current treatment options are directed at the symptomatology of CP rather than targeting disease pathogenesis.

CP has a reported incidence of 4.4 to 11.9 per 100,000 and prevalence of 36. 9 to 41.8 per 100,000 individuals (26). The estimated annual cost of pancreatitis in the United States is $3.7 billion due to multiple long-term hospital admissions, frequent physician visits, and supportive care (27). Disease morbidity is associated with impaired functional status, an increased rate of unemployment and early retirement (28). The various etiologic risk factors of CP can be categorized using systems such as the TIGAR-O (24) and MANNHEIM (29) classifications (**Table 1**). Within industrialized nations, alcohol abuse has been identified as a common factor in 44-65% cases of CP (26); however, CP develops in only 10-15% of alcoholics (30). Heavy alcohol consumption is thought to act as disease modifier, and the development of CP most likely involves an interplay of environmental factors and biologic predisposition (31).

Classification for CP Etiology
Traditional
Alcohol, idiopathic, hereditary, obstructive, hyperlipidemia
TIGAR-O
Toxic-metabolic: alcohol, tobacco smoking, hypercalcemia, hyperlipidemia, chronic renal failure, medications, toxins Idiopathic: early onset, late onset, tropical Genetic mutations: *PRSS1*, *CFTR*, *SPINK1*, others Autoimmune: isolated, syndromic Recurrent and severe AP-associated CP: postnecrotic (severe AP), vascular disease/ischemic, postirradiation Obstructive: pancreas divisum, sphincter of Oddi disorders, duct obstruction (eg, tumor), posttraumatic pancreatic duct scars
MANNHEIM
M indicates multiple risk factors including: Alcohol consumption: excessive (>80 g/d), increased (20–80 g/d), moderate (<20 g/d) Nicotine consumption Nutritional factors: high calorie proportion of fat and protein, hyperlipidemia Hereditary factors: hereditary, familial, idiopathic (early onset, late onset), tropical Miscellaneous and rare metabolic disorders: hypercalcemia, hyperparathyroidism, chronic renal failure, drugs, toxins

TABLE 1. Nomenclature classifying the etiologies of CP. Reproduced with permission (26).

Even though there is overlap between the causative factors of acute pancreatitis (AP) and CP, there are distinct differences between the two inflammatory conditions. Gallstone disease is the top etiology of AP (41%), which is followed closely by alcoholic-induced AP (31.7%) (30). AP is more prevalent than CP, ranking as the top diagnosis recorded in gastrointestinal-related hospital admissions within the United States (32). AP generally involves increased serum amylase and lipase levels; the resolution of an acute attack is associated with complete clinical recovery and restoration of normal pancreatic histology (23). This differs from CP, where recurrent pancreatic injury induces disease progression over years, resulting in irreversible histologic damage, fibrosis, and the development of exocrine and endocrine insufficiency.

1.4 Pathogenic Mechanisms of CP

Historically speaking, multiple mechanistic theories have been proposed to explain the pathogenesis of CP. Early theories focused on specific etiologies or risk factors for pancreatitis, and scientific evidence was often limited to clinical observation of disease progression and the histologic analysis of pancreatic tissue post-mortem. A major conceptual downfall of the early theories was evaluating the pathogenic mechanisms in

isolation, as mutually exclusive phenomena. Furthermore, *in vitro* and *in vivo* experimental design and resulting interpretation established correlation rather than causation.

Advances in scientific methods, incorporation of preclinical animal models of pancreatitis with reproducible results, and the characterization of genetic mutations involved in hereditary pancreatitis have provided the strongest evidence in support of the RAP model. Irrespective of the etiology of pancreatitis, injury is initiated within the acinar cell. This induces a sequence of pancreatic autodigestion, generation of immune response, and stimulation of a reparative 'wound-healing' response. The pancreas is able to recover from a bout of pancreatitis; however, recurrent pancreatic injury interferes with physiologic repair and recovery, shifting homeostasis toward a pro-inflammatory, pro-fibrotic state. Thus, current clinical, experimental, and genetic evidence support the idea that pancreatitis is a continuum of disease where progression occurs with repeated pancreatic injury.

1.4.1 Toxic Metabolic Hypothesis

Bordalo *et al* are credited with the development of the toxic metabolic hypothesis after studying surgical biopsies in chronic alcoholics with pancreatitis and normal lipid profiles. Fatty degeneration of acini was observed by electron microscopy, which was considered a consequence of cellular toxicity induced by ethanol and its metabolites (33). Acinar cells can metabolize ethanol by oxidative and non-oxidative pathways, producing acetaldehyde and fatty acid ethyl esters (FAEEs), respectively (34). Moreover, chronic alcohol use has been shown to inhibit alcohol dehydrogenase, favoring the formation of FAEEs; this shift in ethanol metabolism is accompanied by a reduction in acinar cell proliferation and viability as well as an induction of apoptosis and necrosis (35). Rats infused with FAEEs generated acute pancreatic toxicity as evidenced by edema, ectopic trypsinogen activation, vacuolization and steatosis of acini (36). Yet, epidemiologic and animal studies fail to show that alcohol toxicity alone consistently induces CP. Only 10-15% of alcoholics develop symptomatic CP (30). Therefore, excessive ethanol consumption is now thought to act a sensitizer to pancreatic injury. The toxicity of ethanol and its metabolites serve as a 'second hit' of recurrent pancreatic injury, facilitating disease progression to the irreversible damage of CP (23, 26).

1.4.2 Oxidative Stress Theory

Free radicals (FRs) are generated from physiologic redox reactions involved in cytochrome P450 metabolism, the regulation of calcium channels, and mitochondrial function (37). FRs can induce pathologic injury through lipid peroxidation, nucleic acid modification, protein oxidation, increasing cytosolic calcium levels, and propagation of a local and systemic inflammatory response (38). Oxidative stress (OS) develops when there is an imbalance between pro-oxidant conditions and antioxidant activity. Braganza *et al* advocated the OS theory after finding increased FR oxidation products in the biliary and duodenal secretions of patients with CP (39, 40). Chronic ethanol feeding in rats produced increased pancreatic levels of malonaldehyde, which is an end-product of lipid peroxidation, but failed to induce histologic damage characteristic of pancreatitis (41). This reinforces the overlap of theories, where ethanol metabolism generates reactive oxygen species (ROS) that induce cellular injury by damaging phospholipid membranes.

OS is further compounded by the exhaustion of antioxidant pools and their limited replacement due to malabsorption and malnutrition. Compared to control patients and patients who had recovered from a bout of AP, significant antioxidant deficiencies were identified in patients with CP (42). The evidence presented above supports the role of OS as mediator of pancreatitis. OS is a pathologic response to injury rather than a cause thereof, and this is, in part, reflected in the failure of clinical trials, such as the ANTICPATE study (43), in establishing a benefit of antioxidant therapies in pancreatitis (44, 45).

1.4.3 Intraductal Obstruction Theory

At the 1963 Marseille meeting on pancreatitis, experts noted differences in the risk factors and epidemiologic presentation of AP and CP, thus considering AP and CP as two distinct entities (31). Sahel and Sarles reported a hypersecretion of proteins without changes in the volume of pancreatic juices attained from alcoholics with CP. These conditions were favorable for the precipitation of proteins and obstruction of intrapancreatic ducts (46). This obstruction theory was supported by the pathogenesis of chronic calcifying pancreatitis. Concentrated proteins precipitate as plugs or pancreatic calculi that obstruct small ducts; this initiates a cascade of damage to ductal epithelium, stasis of pancreatic enzymes, intraductal hypertension, periductal inflammation, fibrosis, ductal stricturing and dilation with retention cyst formation (rather than pseudocysts) (47).

A proposed mechanism of calcium lithiasis was down-regulation of pancreatic stone protein (PSP, aka lithostathine), which was thought to function as a calcium stabilizer (48, 49); however, PSP was later identified as the product of regeneration protein degradation by trypsin, which polymerizes into the insoluble pancreatic thread protein (PTP) (50, 51). The intraductal obstruction theory describes a phenomena of lithogenesis that occurs late in disease progression and is not present in all forms of CP (52). However, elements of this theory are incorporated into the RAP model, as the degradation of intrapancreatic trypsin leads to the formation of PTP, which can polymerize and build to a point of ductal obstruction with recurrent pancreatic injury.

1.4.4 Necrosis Fibrosis Theory

Kloppel and Maillet developed the necrosis fibrosis theory after studying the histopathology of alcoholic CP in humans (53). They thought CP resulted from relapsing AP, which induced interstitial periductal necrosis followed by perilobular fibrosis, interlobular duct obstruction, and intralobular fibrosis (52, 53). Thus, injury started at the level of the ducts, and the fibrotic healing response was pathologic, producing ductal strictures, obstruction, digestive enzyme stasis, and acinar cell atrophy. A large, 30-year prospective study of alcoholic pancreatitis found that progression to CP was related to the

incidence and severity of AP (54). Morphological changes were followed in a subset of these patients. Necrosis, mild fibrosis, pseudocyst formation, and a lack of calculi were noted in the early stages of alcoholic CP, whereas progressive fibrosis and pancreatic insufficiency occurred late in the evolution of CP (55). Morphologic analysis of pancreatectomy and autopsy specimens revealed that pseudocysts were common in CP and reflected the same autodigestive necrosis seen in AP. Serial sectioning of pancreatic tissue allowed better characterization of cystic cavities. This enabled differentiation between pseudocysts and epithelial-lined ductal dilations, dismissing the retention cyst aspect of the ductal theory while providing evidence for the evolution of AP to CP (56).

Critics of this theory argue that severe acute biliary pancreatitis can induce significant pancreatic necrosis that resolves without histologic evidence of fibrosis or progression to CP (52). Also, the necrosis fibrosis theory considers acinar cell injury as a consequence of fibrosis and does not account for the direct toxicity of ethanol and its metabolites on acinar cells and PSCs. The RAP model includes elements of necrosis, fibrosis, and repeated injury in the pathogenesis of pancreatitis, but injury is initiated at the level of the acini rather than the ducts. Acinar cell injury generates an inflammatory response and activates PSC-mediated fibrosis.

1.4.5 Sentinel Acute Pancreatitis Event (SAPE) Theory

The Sentinel Acute Pancreatitis Event (SAPE) model provides a framework for the progression of acute to recurrent pancreatitis and finally to CP. The first episode of AP is referred to as the sentinel event since it “foresees the potential development of CP” (57). Acinar cell injury activates a sequence of events that initiates inflammatory response through cytokine generation, activation of resident macrophages and mast cells, and recruitment of lymphocytes and monocytes (**Figure 3**). Premature intrapancreatic zymogen activation leads to parenchymal autodigestion, further amplifying the inflammatory response. As part of physiologic wound-healing mechanisms, PSCs respond by secreting extracellular matrix (ECM) proteins such as collagen and fibronectin (FN) (58). The pancreas is able to recover from an isolated bout of AP. Recurrent acinar cell injury interferes with physiologic repair mechanisms and recovery, shifting pancreatic

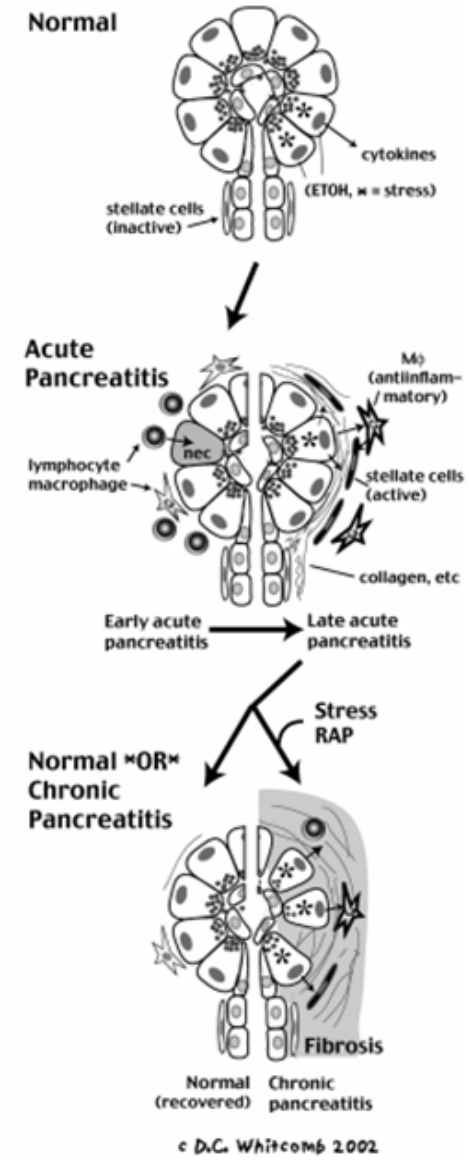

FIGURE 3. Sentinel Acute Pancreatitis Event (SAPE) Theory. Reproduced with permission (31).

homeostasis toward a pro-inflammatory, pro-fibrotic state (31, 59). RAP results in the progressive acinar cell atrophy, inflammation, and stromal fibrosis. The SAPE theory does not focus on the cause of pancreatic injury but rather than the idea of the sentinel event of AP priming the pancreas for response to repeated injury and progression to irreversible damage.

1.4.6 Recurrent Acute Pancreatitis (RAP)

In a case-series of twenty-nine patients with chronic relapsing pancreatitis, Comfort *et al* first proposed the idea that CP is the result RAP (60). The authors noted how the patients mutually shared a disease course of "recurring, acute exacerbations, separated by short or long periods of relative clinical quiescence" (60). The recurrent nature of AP was also an element of the necrosis fibrosis theory, where progressive damage was due to repeated episodes of AP.

The concept of RAP is further supported by the genetic pathogenesis and clinical course of hereditary pancreatitis (HP). Using human genome sequencing, familial linkage analysis, and mutational screening, Whitcomb identified a gain-of-function point mutation in the cationic trypsinogen gene [protease serine, 1 (*PRSS1*)] (6). Molecular modeling and x-ray crystallography revealed that the arginine to histidine substitution (R117H) modified the Arg117 cleavage site on trypsin, rendering it resistant to inactivation by proteases and autolysis (6). A second cationic trypsinogen mutation (*N21I*) was discovered in an

unrelated family with HP who lacked the *R117H* mutation, rendering members predisposed to RAP (5).

The serine protease inhibitor, Kazal type 1 (*SPINK*1) mutation has been identified in cases of idiopathic, familial, tropical pancreatitis that lacked the *PRSS1* mutation (57). It involves a loss-of-function missense mutation (*N34S*) in the pancreatic secretory trypsin inhibitor (*PSTI*), eliminating a fail-safe mechanism to autodigestion by physically blocking trypsinogen's active site (61). Mutations in both the *PSTI* and cystic fibrosis transmembrane regulator (*CFTR*) genes compound the risk for idiopathic CP by 500-fold due to decreased trypsin inhibition and mucoid pancreatic secretions impairing ductal flow (62).

These genetic disorders share a common theme of mutated trypsin activity, a predisposition to repeated bouts of AP in early childhood (before exposure to risk factors like alcohol and nicotine), and progression of the majority of cases to CP by early adulthood (63). The development of a transgenic mouse model for the *SPINK1* mutation has enabled verification of acinar cell initiated pancreatic injury rather than ductal injury as described in the necrosis fibrosis theory (64).

1.5 Acinar Cell Injury in Pancreatitis

Hyperstimulation of the acini with secretagogue, toxic ethanol metabolites, oxidative stress, and bile salts have been shown to induce a sustained pathologic increase in intra-acinar calcium (65). Physiologic calcium oscillations generally originate from the apical secretory pole and spread to the remainder of the cell; however, this spatial polarity of calcium signaling is disrupted in pancreatitis (66), contributing to intrapancreatic trypsinogen activation (67).

Elevated intracellular calcium, ROS, and toxic metabolites induce mitochondrial injury that disrupts cellular bioenergetics and alters acinar cell fate. Depolarization of the mitochondrial membrane affects the respiratory chain, leading to a depletion of cellular adenosine triphosphate (ATP) (68). The calcium ATPase pumps within the endoplasmic reticulum and plasma membrane lack the fuel to function, which exacerbates the acinar cell

calcium overload. Increased mitochondrial permeability opens membrane pores, which facilitate the release of ROS and cytochrome c, triggering necrotic and pro-apoptotic pathways (69). Thus, mitochondrial damage contributes to the acinar cell atrophy seen in CP.

Acini are already subjected to endoplasmic reticulum stress because of their significantly high rate of protein synthesis. A protective unfolded protein response (UPR) is generated early on by cells to reestablish homeostasis by decreasing protein load and activating chaperone GRP78-mediated repair of misfolded proteins. Studies utilizing the L-arginine and CCK mouse models of pancreatitis (**Section 1.7**) have helped identify how severe endoplasmic reticulum stress and a chronic UPR activation leads to programmed cell death via transcriptional activation of C/EBP homologous protein (CHOP) and the caspase cascade (70, 71). Immunohistochemistry (IHC) of human tissues indicates diffuse acinar cell overexpression of GRP78 and endoplasmic reticulum stress in CP (72). Pathologic endoplasmic reticulum stress and UPR play a role in acinar cell death.

During experimental models of secretogogue-induced pancreatitis, there is a shift from apical to basolateral degranulation of digestive enzymes into the interstitium (73). Alterations in both calcium signaling and acinar cell ultrastructure contribute to the disruption of polarized vesicular transport towards the luminal membrane. *In vitro* stimulation of primary acini with high doses of CR, a CCK analog, resulted in a loss of the apical microfilament web and intermediate filament bands (74). Other investigators have coupled electron microscopy with immunolocalization and immunoblotting to analyze the pancreata of rats subjected to CR-induced pancreatitis, observing the progressive disassembly and degradation of cytoskeletal structure while providing a mechanism behind the dysregulated trafficking and exocytosis of ZGs.

Saluja and colleagues utilized differential cell fractionation and immunolabeling to determine that the pathologic mechanism behind acinar cell vacuolation is the colocalization of lysosomes with ZGs (75). Autophagic flux has been found to be impaired in pancreatitis, favoring an imbalance between cathepsin B (which activates trypsinogen) and cathepsin L (which degrades trypsinogen and trypsin) (76). Once trypsin is prematurely

activated, it is able to activate other digestive proenzymes within the ZGs and amplify the degree of pancreatic damage. Lipase, which is synthesized in its active form, exacerbates the fatty acinar necrosis.

Necrotic acini release intracellular components such as nucleic acids, ATP, mitochondria, and heat-shock proteins into the extracellular space and are collectively referred to as danger-associated molecular patterns (DAMPs). Immune cells and acinic express toll-like receptors (TLRs) that recognize DAMPs, triggering the induction of NLRP3 (NACHT, LRR, and PYD domains-containing protein 3) inflammasome and its effectors, caspase 1 and 11, IL-1β, IL-18, and cytokine high-mobility protein B1 (HMB1) (77). Local tissue damage incites acinar cell up-regulation of the MAPK signaling pathways and transcription factors NF-κB, activating factor-1 (AP-1), and STAT along with a down-regulation of phosphatases (78). This leads to acinar cell synthesis and secretion of the following: cytokines TNF-α, TGF-β , IL-1β, IL-6, and IL-10; chemokines monocyte chemoattract protein-1 (MCP-1), mob-1, cytokine-induced neutrophil chemoattractant (CINC), regulated on activation normal T cell expressed and secreted (RANTES), and platelet activating factor (PAF); intracellular adhesion molecule (ICAM-1) (78, 79); and parathyroid hormone-related protein (PTHrP) (80, 81). Thus, inflammation amplifies the autocrine, acinar cell, and paracrine, PSC, response to pancreatic injury.

1.6 Pancreatic Stellate Cell (PSC) Activity in Pancreatitis

PSCs account for 4% of the pancreatic cells (82) and reside within the stromal compartment of the pancreas. They have a peri-acinar (basolateral), peri-ductal, peri-lobular, and peri-vascular distribution (82, 83). PSCs normally maintain a quiescent phenotype, which is identified by a stellate morphology, cytoplasmic lipid droplets rich in vitamin A, and positive immunostaining for intermediate filament proteins vimentin, glial fibrillary acidic protein (GFAP), desmin, and nestin (82). The non-activated PSCs display limited proliferation, migration, and ECM synthetic activity (82). PSCs harbor the capacity to remodel the ECM through the synthesis and secretion of matrix metalloproteinases (MMPs) -2, -9, and -13 and their tissue inhibitors of metalloproteinases (TIMPs) -1 and 2

(84). Hence, PSCs are responsible for the secretion, degradation, and remodeling of the ECM to maintain normal pancreatic architecture.

In response to pancreatic injury and inflammation, PSCs undergo a myofibroblastic transformation that is accompanied by several morphologic and physiologic changes. Activated PSCs assume a spindle shape. Activation of PSCs is associated with the loss of the vitamin-A droplets and gain in alpha smooth muscle actin (α-SMA) expression (82). Some investigators consider increases in desmin and nestin IHC staining indicative of PSC activation, but there has been variability in expression of these markers reported within the literature. Activated PSCs exhibit increased proliferation and migration to areas of injury. Their enlarged nuclei and prominent rough endoplasmic reticulum reflect their active synthesis of ECM components FN, collagen types I and III, procollagen type II, and laminin - all of which are highly expressed in CP (85). ECM turnover is altered by an imbalance in the MMP/TIMP ratio (84). Thus, PSC activation favors the disorganized, heterogenous accumulation of ECM.

The theories of CP pathogenesis also apply to the activation of PSCs. Like acinar cells, PSCs possess inducible alcohol dehydrogenase and can metabolize ethanol. Apte *et al* have shown that PSCs exposed to ethanol and acetaldehyde become activated with increased α-SMA expression and collagen synthesis (86). Similarly, incubation of PSCs with pro-oxidant compound $FeSO_4$/ascorbic acid resulted in the generation of malondialdehyde, a product of lipid peroxidation, and OS-induced activation of the PSCs, which were prevented by treatment with the antioxidant Vitamin E (86). PSCs express NADPH oxidase, which can generate ROS; diphenyleneiodonium inhibition of NADPH oxidase activity significantly reduced fibrosis in experimental models of spontaneous CP, using Wistar Bonn/Kobori (WBN/Kob) rats, and in dibutyltin dichloride (DBTC)-induced CP. In conjunction with the intraductal obstruction theory and increased tissue pressures noted in CP (87), Watanabe and colleagues placed flasks of primary PSCs in a pressure-loading apparatus and subjected them to increased mechanical stress through the infusion of compressed helium. They found that increased pressure induced PSC proliferation, α-SMA expression, MAPK pathway (p44/42 and p38) activation, and TGF-β1 and collagen secretion (88).

In accordance with the necrosis fibrosis theory, PSCs express receptors enabling their response to autocrine and paracrine inflammatory signaling from injured acini, platelets, endothelial, and immune cells. PSCs also contribute to the inflammatory response in pancreatitis by producing multiple signaling mediators: growth factors [TGF-β, TNF-α basic fibroblast growth factor (bFGF), connective tissue growth factor (CTGF), platelet derived growth factor (PDGF), vascular endothelial growth factor (VEGF), and angiopoietin]; pro-inflammatory cytokines [IL-1β, IL-6, IL-8, IL-23, IL-24, IL-32, and IL-33]; anti-inflammatory cytokines [IL-10]; chemokines [RANTES, MCP-1, and intracellular adhesion molecule-1 (ICAM-1)]; and vasoconstrictor endothelin-1 (89, 90). PSCs have been shown to express toll-like receptors (TLRs), which can activate the innate immune response (91). Lastly, activated PSCs exhibit phagocytic activity, expressing CD36 and phosphatidylserine receptors that are involved in the engulfment of apoptotic polymorphonuclear neutrophils and necrotic acini (92). Thus, PSCs respond to and perpetuate the inflammatory component of pancreatitis.

The RAP model captures how recurrent pancreatic injury leads to repeated PSC activation, shifting from physiologic ECM turnover to pathologic fibrosis. Various molecular signaling pathways have been shown to be activated in PSCs, including the MAPK/ERK, PI3K/AKT, JNK/p38 MAPK, janus activated kinase/signal induced activation of transcription (JAK/STAT), transcription factor NF-κB, and AP-1 (93). The top stimulatory signals for PSCs include pro-fibrotic TGF-β and PDGF, which induces PSC mitogenesis and chemotaxis (93). Since multiple signaling pathways are shared between acinar and PSCs, such redundancy can be targeted in therapeutic drug development.

1.7 Experimental Models of Pancreatitis

The isolation and culture of primary acini is an ideal but impractical approach to repeated experimentation. Primary cells undergo senescence, failing to grow indefinitely in culture. The only commercially available cell line for the study of acinar cell function is AR42Js. The acinar cell line was initially established from a transplantable exocrine tumor generated by azaserine treatment of Wistar/Lewis rats (94); however, the immortalized cell line maintains a differentiated exocrine phenotype in culture.

Treating AR42J acinar cells with CR is a well-established *in vitro* model of pancreatitis. CR is a decapeptide and CCK analog originally derived from the Australian tree frog *Litorea caerulea*. CR induces aberrant digestive enzyme secretion and histologic damage characteristic of pancreatitis (73). Both acinar cells and PSCs (95, 96) express the CCK G-protein-coupled receptor. High doses of CR hyper-stimulate the CCK receptor and activate multiple intracellular processes observed in human disease, which include the following (7): calcium mobilization, cytoskeleton disruption (19), dysregulated discharge of ZGs along the basolateral membrane (97), MAPK/ERK and PI3K/AKT cascade activation, ROS generation, apoptosis induction, regulation of transcription factors like NF-κB, synthesis of PTHrP (80, 81) and cytokines like interleukins IL-6, IL-8 and TGF-β. In conclusion, the *in vitro* study of pancreatic cells in isolation or as co-cultures enables mechanistic insight into pancreatitis.

CR-induced pancreatitis is the most widely utilized *in vivo* model due to its reliability, reproducibility, and extensive characterization. Lampel and Kern first described how acute infusion of CR in rats caused pancreatic edema with immune cell infiltration, acinar cell vacuolization, disturbance in the secretory pathway with premature basolateral discharge of ZGs, and hyperamylasemia (73). The secretagogue-induced model has been modified over the years to include repeated intraperitoneal (IP) administration of supraoptimal doses of CR in mice over time. The dose, frequency, and duration of CR administration can be changed to alter the severity of pancreatitis studied. Evidence of repeated pancreatic injury induced include the intrapancreatic activation of proteases (98), acinar atrophy, formation of pseudotubular complexes, fibrogenesis with colocalization of

procollagen α1 messenger ribonucleic acid (mRNA) and activated PSCs, and the development of interstitial infiltrate (99, 100). The CR model alone is insufficient at inducing endocrine insufficiency, and the incorporation of an additional trigger, like LPS, is needed to reproduce pancreatogenic diabetes (101). RAP induction by serial CR injections will be employed in the experiments described in **Chapters 3** and **4**.

Intraperitoneal injections of the essential amino acid, L-arginine, was first developed as a rodent model of severe necrotizing pancreatitis (102). L-arginine produces histologic damage of CP, including selective acinar cell necrosis, in a dose-dependent manner (103), a severe inflammatory response, and increased mortality. The pathogenic mechanism of this model is not as well-characterized as the CR model. It is thought to involve "inhibition of protein synthesis, excessive nitric oxide production, or increased lipid peroxidation" (104). Furthermore, the L-arginine model has questionable disease relevance.

The stimulus utilized by *in vivo* models of CP can be used to categorize them. Mechanical obstruction can be simulated through the ductal ligation model or the intraductal injection of occlusive foreign materials like acrylate. Since the mouse pancreas consists of three lobes, each of which has its own duct, selective ligation of pancreatic outflow allows inclusion of an internal control lobe. Watanabe performed splenic lobe ductal ligation in mice and documented the progressive pathologic changes seen in the mice over sixteen weeks (wk). Ductal obstruction resulted in acute inflammation and edema followed by progressive fatty degeneration and death of acini, ductal cell proliferation, and the deposition of connective tissue (105).

Lieber and DeCarli first proposed an alcohol feeding model (106) that was later applied to the study of alcoholic pancreatitis. Sixty percent of rats chronically fed ethanol for 20 to 30 months developed pancreatic lesions consistent with CP (107). The inconsistent induction of CP is a common critique of the ethanol feeding model, along with confounding systemic effects on organs such as the liver and kidneys (101). Genetic research into hereditary pancreatitis has facilitated the development of transgenic and knockout mouse models with *PRSS1*, *SPINK1*, and *CFTR* mutations. Lastly, modalities

can be combined to produce more severe pancreatic injury and examples include the use of serial CR injections with additional administration of toxic agents like lipopolysaccharides (LPS), cyclosporin A, DBTC, or ethanol (101). The different models enable the preclinical evaluation of different etiologies in CP.

1.8 Objective and Aims

CP is a progressive disease defined by glandular atrophy, chronic inflammation and fibrosis. Patients with CP have a poor quality of life, and their treatment options are limited to supportive care and symptom palliation. There are currently no drugs targeting the pathogenesis of CP. Irrespective of the etiology of pancreatitis, acinar cell injury initiates an autodigestive cascade of events that stimulates an inflammatory and fibrotic response; this process becomes pathologic with repeated pancreatic injury. My central hypothesis is that **the development of a novel therapeutic that reduces the severity of RAP will prevent or delay progression to CP.** Theoretically speaking, an ideal therapeutic for RAP would limit inflammatory signaling, reduce PSC-mediated fibrosis, and promote pancreatic regeneration. Therefore, the specific aims of my dissertation will include:

(1) To determine the effects of apigenin treatment on pancreatic injury and inflammation (**Chapter 2**);
(2) To determine the effects of apigenin in limiting PSC function (**Chapter 3**);
(3) To optimize apigenin's chemical structure and properties for potential therapeutic use in RAP (**Chapter 4**).

The *in vitro* and *in vivo* studies presented in this dissertation provide novel information regarding apigenin's mechanism(s) of action in preventing recurrent pancreatitis and bring us closer to the clinical testing of apigenin analogs in humans at risk for CP.

1.9 Apigenin (4',5,7-Trihydroxyflavone)

Since there is no cure for CP, a potential target for pharmaceutical development is at the early stages of RAP, thereby preventing progression to irreversible pancreatic damage. The literature was reviewed, searching for a small molecule that would limit the pathologic inflammatory and fibrotic response to recurrent pancreatic injury while preserving pancreatic function. Apigenin was identified as a promising lead compound due to its anti-inflammatory, anti-oxidant, anti-proliferative, and pro-apoptotic properties reported in the literature (108). Apigenin suppressed NF-κB, ROS, IL-6, IL-8, and ICAM-1 in gastric adenocarcinoma cells (109). Apigenin has been shown to induce cell death through cell cycle arrest and the activation of intrinsic and extrinsic apoptotic pathways (108). To my knowledge, there is only one study to date that tested apigenin in a bilio-pancreatic model of AP in rats. Lampropoulos and colleagues found that a one-time, 5 mg oral dose of apigenin minimized the histologic severity of pancreatitis and myeloperoxidase activity (MPO), which is a measure of neutrophil immune response (110).

Apigenin is a plant-derived polyphenolic flavanoid (**Figure 4**) with low intrinsic toxicity. Dietary sources of apigenin include citrus fruits, green-leafy vegetables like celery, herbs like parsley, peppermint, and thyme, grains, and beverages. Chamomile tea contains the highest dietary concentration of apigenin. The clinical application of apigenin is limited by its poor drug-like properties of limited bioavailability, hydrophobicity, and metabolic instability (111). Data regarding the synthesis and development of apigenin analogs will be discussed in **Chapter 4**.

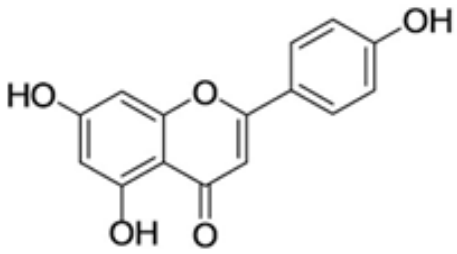

FIGURE 4: Chemical structure of apigenin.

CHAPTER 2:

APIGENIN AND ACINAR CELL-MEDIATED INFLAMMATION

2.1 Introduction

2.1.1 Parathyroid Hormone Related Protein (PTHrP) and Pancreatitis

PTHrP has been identified as a pro-inflammatory and pro-fibrogenic mediator of AP and CP (80, 81). Pancreatic acini, islets of Langerhans, and PSCs express the protein's G protein-coupled receptor (PTH1R) (80, 112, 113). Immunohistochemical staining of pancreatic tissue from animal models of acute and CP as well as patients with CP have demonstrated diffuse acinar cell and PSC up-regulation of PTHrP expression (80, 81). This phenomena has also been reproduced *in vitro* using primary cell isolates and established cell lines AR42J and immortalized rat pancreatic stellate clone 3 (irPSCc3) (114). PTHrP treatment of acinar cells has up-regulated mRNA levels of inflammatory mediators IL-6 and ICAM-1 (80). CR and ethanol treatment of primary PSCs and irPSCc3 induced increases in mRNA levels of α-SMA, which is a measure of stellate cell activation, and secretory ECM components procollagen I and FN (80).

Falzon *et al* generated an acinar-specific inducible PTHrP knockout, which provided protection from chronic pancreatic injury induced by both the CR model of RAP and the ductal ligation model in mice (81). The PTHrP knockout mice showed a decrease in all of the following parameters induced by chronic pancreatic injury: histologic damage (edema, vacuolization, and necrotic debris), amylase levels, positive α-SMA staining of PSCs localized to areas of fibrosis, periacinar and periductal collagen deposition, IL-6 expression, and NF-κB activity (81). Thus, we hypothesized that apigenin's anti-inflammatory effects may be, in part, mediated through PTHrP inhibition. This chapter will focus on the acinar cell, which is initially injured in the RAP model, generating the inflammatory and fibrotic response.

2.2 Materials and Methods

2.2.1 Materials

Apigenin (95% purity) and methylcellulose (MC) were purchased from Sigma-Aldrich (St. Louis, MO). The CR peptide was from Bachem (Torrance, CA). PTHrP (1-36) was obtained from PolyPeptide Laboratories (San Diego, CA). TGF-β and TNF-α were

from R&D Systems (Minneapolis, MN). MAPK kinase inhibitor PD98059 was purchased from Life Technologies (Carlsbad, CA), and the PI3K inhibitor LY294002 was from Selleck Chemicals (Houston, TX). Tamoxifen was from Cayman Chemical (Ann Arbor, MI). The anesthetic isoflurane was purchased from Piramal Healthcare (Bethlehem, PA). The *PTHrP*$^{flox/flox}$*; Cre*$^{+}$ mice were attained from breeding colonies in Dr. Falzon's lab, and control mice consisted of the same strain background (81). The C57/129P2 mice were bred in our lab.

Cell culture reagents were purchased from the following companies: phosphate-buffered saline (PBS), DMEM, and RPMI 1640 (Cellgro, Manassas, VA); trypsin-EDTA 0.25% (Gibco, Grand Island, NY); fetal bovine serum (FBS) (Lonza, Walkersville, MD); dimethyl sulfoxide (DMSO), bovine serum albumin (BSA), and soybean trypsin inhibitor (STI) (Sigma-Aldrich); and collagenase type IV (Life Technologies). The Plasmocin test kit, treatment, and prophylactic were purchased from InvivoGen (San Diego, CA). Cell culture vessels and cryogenic vials were bought from Nunc (Life Technologies). The cell strainer (100 μM) was purchased from Thermo Fisher Scientific, Inc. (Kalamazoo, MI).

The RNAqueous kit was purchased from Ambion (Austin TX). The cDNA synthesis kit, SYBR green Supermix, and 7500 RT-PCR System were obtained from Applied Biosystems (Foster City, CA). Reagents and supplies for the luciferase assay were purchased from the following: cuvette (Gene Pulser Cuvette, Bio-Rad, Hercules, CA), Dual-Luciferase Reporter Assay System (Promega, Madison, WI); and Synergy 2 luminometer (BioTek, Winooski, VT).

The protease inhibitor was purchased from Roche (New York, NY) and phosphatase inhibitor from Pierce (Rockford, IL). All of the dry and liquid chemicals utilized to make the Western blot (WB) buffers were purchased from Sigma-Aldrich unless otherwise noted. The following reagents were from Thermo Fisher Scientific, Inc.: Tris-buffered saline (TBS), Tween-20, methanol, and guanidine hydrochloride. For the Bradford assay, the Coomassie blue was purchased from Bio-Rad, and the DU-640 spectrophotometer was from Beckman Coulter (Indianapolis, IN). The pre-cast gels, XCell SureLock mini-gel electrophoresis and transfer systems were obtained from Life

Technologies. The polyvinylidene fluoride (PVDF, 0.45 µm) were from Millipore Corporation (Bedford, MA). The HyBlot film, enhanced chemiluminescence (ECL) SuperSignal West Pico and Femto substrates were obtained from Life Technologies. A Kodak X-Omat 2000A Processor (Rochester, NY) was used.

Name	Specificity	Dilution	Details	Manufacturer
Phospho-p44/42 MAPK (p-ERK)	Dually phosphorylated Thr202 and Tyr 204 of Erk1 or Th4185 and Tyr 187 of Erk2, and singly phosphorylated at Thr202	1:1000 (WB), 1:200 (IHC)	Rabbit, monoclonal	Cell Signaling #4376
p44/42 MAPK (total ERK)	Total p44/42 MAPK kinase (Erk1/Erk2)	1:1000 (WB)	Rabbit, polyclonal	Cell Signaling #9102
Phospho-Akt	Akt only when phosphorylated at threonine 308	1:1000 (WB)	Rabbit, monoclonal	Cell Signaling #4056
Akt	Total Akt 1, Akt2, and Akt 3	1:1000 (WB)	Rabbit, polyclonal	Cell Signaling #9272
NF-κB p65	Amino acids 1-286 of NF-κB p65 of human origin	1:100 (ICC)	Rabbit, polyclonal	Santa Cruz sc-7151
Bovine anti-rabbit IgG-HRP	Rabbit IgG	1:5000 (WB)	Bovine	Santa Cruz sc-2370
Biotinylated goat anti-rabbit	Rabbit IgG	1:200 (IHC)	Goat	Vector Lab BA-1000
Goat Anti-rabbit IgG-Alexa Fluor 488	Rabbit IgG	1:200 (ICC)	Rabbit, polyclonal	Life Tech. A-11034

TABLE 2. Antibodies used in acinar cell experiments.

In the IHC protocol, the ethanol, xylene, Tween 20, and hydrogen peroxide were from Thermo Fisher Scientific, Inc. The avidin/biotin blocking kit was purchased from Invitrogen (#004303, Life Technologies). The horseradish peroxidase streptavidin (SA-5704) was purchased from Vector Laboratories, Inc. (Burlingame, CA). The antibody

diluent (#S3022), diaminobenzidine (DAB, #K3468), and Vectashield mounting medium with DAPI were from DAKO (Santa Clara, CA). The Permount mounting media and Harris Hematoxylin were from Thermo Fisher Scientific, Inc. In regards to ICC, reagents were purchased as follows: VECTASHIELD mounting media with DAPI (Vector Lab), collagen and paraformaldehyde (Sigma). Information regarding the antibodies utilized is included in **Table 2**. Antibodies were purchased from Cell Signaling (Danvers, MA), Santa Cruz Biotechnology (Dallas, TX), Vector Laboratories, and Life Technologies.

2.2.2 Methods

2.2.2.1 Standard Cell Culture Methods

Acinar Cell Line - The AR42J acinar cell line was purchased from the American Type Culture Collection (ATCC CRL-1492, Manassas, VA) and was initially established from a transplantable exocrine tumor generated by azaserine treatment of Wistar/Lewis rats (94). The immortalized cell line maintains a differentiated exocrine phenotype in culture and is the only commercially available cell line for the study of acinar cell function *in vitro*. AR42J cells are a widely used, well-characterized model for the study of exocrine function *in vitro*. AR42J cells were grown in RPMI with 10% FBS. Cell cultures were maintained at 37˚C in a humidified 95% O_2/5% CO_2 atmosphere.

Thawing Cells – The cryogenic vial of cells was removed from the liquid nitrogen tank and immediately placed in a 37˚C waterbath. The cells were quickly thawed by swirling the vial within the warm bath until a small piece of ice remained. The cell solution was transferred to a cell culture vessel, and the volume of freeze media was diluted 1:10 with the appropriate growth media. The cell culture vessel was returned to the incubator for 24 hours (hr) and left undisturbed to facilitate cell attachment. The next day, the cell culture media was aspirated and replaced with fresh growth media. Cells were grown for a minimum of 5 days prior to use in experiments, allowing time for growth and adjustment from the stress of the freeze-thaw cycle.

Subculturing – Once cell cultures reached 70-80% confluence, they were passaged. The media was aspirated and the cells were washed once with 1X PBS. Refer to **Table 3** for volumes of subculturing reagents. The cells were coated with a thin layer of trypsin and allowed to incubate for 2-3 minutes (min) within the 37˚C incubator. Cells were checked for detachment by gently tapping the side of the flask. If the cells remained attached, the cells were incubated with trypsin for an additional time. Once the cells detached, trypsin was neutralized by adding FBS, and the harvested cell solution was mixed by trituration. Acinar cells were split at a 1:3 ratio, and the flask was filled with the appropriate volume of growth media (RPMI + 10% FBS). Periodically, cells were tested for mycoplasma infection using the PlasmoTest kit. Positive cultures were treated with Plasmocin Treatment, 25 µg/ml for 2 wk, following the manufacturer's protocol. Cell lines were re-tested and used only after a negative screening result. Plasmocin Prophylactic, 5 µg/ml, was added regularly to the growth media of cells previously infected with mycoplasma.

Flask Size (cm^2)	**PBS (mL)**	**Trypsin (mL)**	**FBS (mL)**	**Media (mL)**
T25	0.5	0.5	0.125	8
T75	1	1	0.25	20
T175	2	2	0.5	30

TABLE 3. Volumes of cell culture reagents used when passaging cells.

Freezing Cells – Harvested cell solutions were centrifuged for 5 min at 1000 rpm and 25˚C. The supernatant was discarded and the cell pellet resuspended in freeze media (FBS + 10% DMSO) so that there was a density of 1 million cells/1 mL freeze media/cryogenic vial. The vial of cells was placed in a freezing apparatus containing a chamber of isopropanol and set in a -80˚C freezer. After 24 hr, the frozen cells were transferred to the liquid nitrogen tanks and stored in the gaseous or liquid-phase for long-term cryopreservation.

2.2.2.2 Generation of PTHrP Knockout Mice

All animal protocols were approved by the UTMB Institutional Animal Care and Use Committee (IACUC), which is fully accredited by the Association for the Assessment and Accreditation of Laboratory Animal Care International. The generation of *PTHrP$^{flox/flox}$; Cre^{+}* (homozygous) mice has been described in detail by Bhatia *et* al (81). These transgenic mice contain a tamoxifen-inducible *Cre*-lox recombination system driven by the rat elastase 1 pancreatic promoter. Thus, there were two levels of specificity within this system. PTHrP knockout was induced in 6-8-wk-old male and female mice by injecting them with tamoxifen: 20 mg/ml, 100 μl/mouse, IP, once daily for 5 days (115). The control mice were of the same strain background and were injected with the vehicle (corn oil) following an identical schedule. One wk after completion of the injections, the mice were anesthetized with isoflurane and sacrificed per protocol.

2.2.2.3 Isolation of Primary Acinar Cells

The method for primary acinar cell isolation was derived from published protocols (80, 81). The pancreata from 4-5 mice were harvested and placed in an isolation buffer [PBS with Ca^{2+} and Mg^{2+}, 0.1% BSA, and 10 μg/ml STI]. The tissue was finely minced in isolation buffer and then digested with collagenase type IV, 1 mg/ml, using continuous brisk trituration for 15 min at 37˚C. Collagenase digestion was stopped through a 1:2 dilution with cold isolation buffer. The cells were washed three times with cold isolation buffer. The cells were filtered through a 100 μm mesh, re-suspended in 10 mL of DMEM with 10% FBS and 0.025% STI, and seeded into a six-well plate. The cells were allowed to attach for 24 hr before initiating treatment.

2.2.2.4 RNA Isolation and Reverse Transcription-Polymerase Chain Reaction (RT-PCR)

The RNAqueous kit was utilized for total RNA extraction, and the manufacturer's protocol was followed. The RT-PCR methods employed have been previously described by Bhatia *et al* (80, 81). Spectrophotometry was used to quantify RNA concentrations, and formaldehyde agarose gel electrophoresis was used to evaluate the quality of RNA

isolation. The Applied Biosystems cDNA synthesis kit and manufacturer's protocol were used to reverse transcribe 2.0 µg of RNA into complementary DNA (cDNA). The Applied Biosystems 7500 RT-PCR System was used to run the first-strand cDNA with the primers listed in **Table 4** and SYBR green Supermix. The threshold cycle (C_T) value for each gene was normalized to that of β-actin, and relative expression levels were calculated using the following formulas: n-fold change = 2^ ($-\Delta\Delta C_T$) where $\Delta\Delta C_T = \Delta C_{T\ (target\ sample)}\ \Delta C_T$ — (control).

Primer	Species	Forward Primer	Reverse Primer
IL-6	Mouse	TGGAGTCACAGAAGGAGTGGCTAAG	TCTGACCACAGTGAGGAATGTCCAC
Actin	Mouse	TCACCCACACTGTGCCCATCTACGA	GGATGCCACAGGATTCCATACCCA

TABLE 4. SYBR-green primers used in acinar cell RT-PCR.

2.2.2.5 Luciferase Reporter Assay

AR42J cells were harvested using the subculturing methods described in **Section 2.2.2.1**. The cells were centrifuged for 5 min at 1000 rpm and 25˚C. The supernatant was discarded; the pellet was resuspended in 0.5 mL of RPMI and transferred to a cuvette. A PTHrP-P3 plasmid, which contained 140 bp upstream of the P3 TATA box, was cloned into the pGL-2 vector and obtained from Dr. Z. Bouizar (116). AR42J cells were transfected with the P3 plasmid or empty vector (control), and co-transfected with a *Renilla* luciferase construct using electroporation (0.4-cm electrode gap, 250 V, 1,500 µF capacitance, and for 2 pulse lengths of 11 ms) (81). The cuvette was placed on ice for 10 min before seeding into a multi-well plate containing RPMI with 10% FBS. The cells were allowed to attach for 24 hr before initiating treatment.

After the completion of experimental treatments, cell lysates were prepared using the passive lysis buffer provided in the Dual-Luciferase Reporter Assay System, while following the manufacturer's protocol. Luciferase substrate was added to the cell lysate and activity was quantitated, in triplicate, using a luminometer. Readings for the empty vector were subtracted from their corresponding luciferase values. The firefly luciferase

activity (experimental reporter) was normalized to *Renilla* luciferase activity (control reporter).

2.2.2.6 Immunoblotting

Protein isolation - Cell culture plates were placed on ice and the media aspirated. The cells were gently washed once with cold PBS. At the time of use, ½ tablet of EDTA-free protease inhibitor and phosphatase inhibitor were added to 5 mL of lysis buffer [20 mM tris-HCl (pH 7.5), 150 mM NaCl, 1 mM Na_2EDTA, 1 mM EGTA, 1% Triton-X-100, 2.5 mM sodium pyrophosphate, 1 mM β-glycerophosphate, 1 mM Na_3VO_4]. For a six-well plate, 200 µL of lysis buffer was added to each well for a 10 min incubation on ice, agitating the plate every 2 min. The wells were then scrapped and contents transferred to a pre-chilled Eppendorf tube. The samples were centrifuged for 10 min at 13,000 rpm and 4˚C. The supernatant containing the cytoplasmic extract was saved.

Bradford assay and protein normalization – At the time of protein isolation, protein concentrations were determined using the colormetric Bradford Assay (117). A standard curve was first generated using BSA at concentrations of 1-20 µg/mL. For each protein sample, 2-5 µL of sample was added to 800 µL of Milli-Q (MQ) ultrapure water in a 12 x 75 mm glass test tube. While vortexing, 200 µL of 5X Coomassie blue dye was added to the tube. The binding of Coomassie blue to protein results in a shift of the absorption maximum, from 465 nm to 595 nm, that is directly proportional to protein concentration. Absorbance was measured at 595 nm using a spectrophotometer. The protein concentrations were calculated from the standard curve. Samples were diluted to equal concentrations (ideally 2.5 µg/uL) using lysis buffer and 6X modified Laemmli sample buffer (375 mM Tris•HCl pH 6.8, 10% SDS, 30% glycerol, 0.06% bromophenol blue, and the reducing agent, 0.6 M dithiothreitol). All samples were flash frozen in liquid nitrogen and stored at -80˚C.

Sodium dodecyl sulfate-polyacrylamide gel electrophoresis (SDS-PAGE) – Protein samples denatured for 5 min at 90˚C. Equal amounts of protein (30-50 µg) were loaded onto the 10-12% pre-cast, 1.5 mm, Tris-Glycine polyacrylamide mini-gels. The

running buffer consisted of 25 mM tris base (pH 8.3), 92 mM glycine, 0.1% SDS, and the reducing agent 5 mM sodium bisulfite. Electrophoresis was used to separate protein samples by size and charge, and the gel was run for 2 hr at a constant voltage of 125 V.

The PVDF membrane was wet with 100% methanol for 1 min followed by incubation in ultrapure MQ water for 5 min. The membrane was then kept in transfer buffer until use. The transfer buffer consisted of 12 mM tris base (pH 8.3), 96 mM glycine, and 10% methanol. The blotting process transferred proteins from the gel to the membrane and was run at 25 V for 3 hr on ice.

The apparatus was unpacked and the membrane was blocked for 1 hr, on the shaker, at 25˚C. The blocking buffer consisted of 5% BSA and TBS-T (0.1% Tween-20). The primary antibody (Ab) was prepared in blocking buffer using a 1:1000 dilution. The membrane was incubated with primary Ab overnight on a shaker at 4˚C. The membrane was washed with wash buffer (TBS with 0.2% Tween-20) for 15 min, three times. The appropriate species of horseradish peroxidase (HRP)-conjugated secondary Ab (Santa Cruz Biotechnology, Inc., Dallas, TX) was prepared in blocking buffer using a 1:5000 dilution, and the membrane was incubated in it on a shaker for 1 hr at 25˚C.

The membrane was washed with wash buffer for 15 min, three times. The membrane was developed using chemiluminescence SuperSignal substrates and autoradiography. If the membrane was to be re-probed, it was incubated in stripping buffer (6M GnHCl, 0.2% Triton-X, 20 mM Tris-HCl, pH 7.5, and 0.1 β-mercaptoethanol) for 5 min, on a shaker, twice (118). This was followed by 5 min washes, four times, in TBS-N (0.14 M NaCl, 10 mM Tris HCl, pH 7.5, 0.05% NP-40). The stripped membrane was then re-blocked, as described above, before proceeding with a new primary Ab incubation.

2.2.2.7 RAP Mouse Model

Under an IACUC approved protocol (IRB #0212089A), RAP was induced in mice using serial CR injections (111, 119). This widely used, reproducible model has been shown to induce the progressive histologic damage of CP, including acinar cell injury, fibrosis, and inflammation (120). Male and female, 6-8-wk-old mice of C57BL/6 or

C57/129P2 background were randomized into study groups, each with 5-6 mice. The average weight of the mice was used to calculate and prepare concentrated (10X) stock solutions of CR and apigenin, which were frozen in -20˚C. Daily aliquots were thawed on ice and diluted to 1X on the day of use.

Starting the first week of the experiment, RAP was induced by 5 consecutive hourly IP injections of CR (50 µg/kg mouse weight), given 3 days (d)/wk (on Monday/Wednesday/Friday), for the duration of 4 wk (**Figure 5**). Control mice received the vehicle (PBS) following the same schedule. After inducing RAP for one week, apigenin

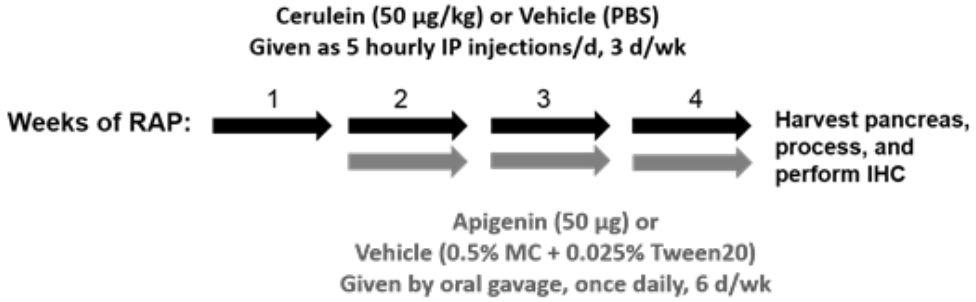

FIGURE 5. Diagram of RAP mouse model.

treatment was initiated and continued while inducing RAP. Apigenin (50 µg/mouse, ≈ 2.5 mg/kg) was administered by oral gavage, 6 d/wk, for the remaining 3 wk. Control mice received the vehicle (0.5% MC + 0.025% Tween20 in MQ water) according to the same schedule as apigenin. Thus, all mice were subjected to serial IP injections and repeated gavage of the active agent or its corresponding vehicle. At the end of 4 wk, the mice were sacrificed, the pancreata harvested and processed.

2.2.2.8 Immunohistochemistry (IHC)

Fresh pancreatic tissue was fixed in 10% formalin for 72 hr at 4˚C and then paraffin-embedded by the UTMB Histopathology Core. Briefly, the tissue blocks were cut and sections (5 µm) were baked onto slides overnight at 60˚C. The slides were deparaffinized and incubated in antigen retrieval solution (10 mM sodium citrate, pH 6.0) for 20 min at 98˚C, and allowed to cool to 25˚C. Endogenous peroxidases were quenched by incubating sections with 3% H_2O_2 for 10 min followed by a wash in MQ water. An avidin/biotin blocking kit was used to block non-specific binding in sections for 15 min. The sections

were incubated with primary Ab in Ab diluent for 1 hr. The sections were washed in TBS-T and incubated with biotinylated goat anti-rabbit IgG in Ab diluent for 15 min. The sections were washed in TBS-T and incubated with horseradish peroxidase streptavidin for 30 min. After washing the sections with TBS-T, brown color development was achieved by applying DAB to the slides for 5 min followed by a rinse with MQ water. The sections were counterstained blue with Harris Hematoxylin and rinsed with MQ water. The sections were dehydrated through a graded ethanol series and cleared in xylene (3 times, 5 min each). The coverslips were applied with Permount.

2.2.2.9 Immunocytochemistry (ICC)

Coverslips (12 mm diameter, 0.19 mm thickness) were placed in a 6-well plate, coated with collagen (15 µg/mL PBS) and allowed to set for 1 hr at 25˚C. AR42J cells were seeded onto the coverslip (5E4/0.5 mL RPMI) to attach undisturbed for 2.5 hr at 25˚C. The wells were then flooded in RPMI with 10% FBS, and the plate was returned to the incubator. The next day, ICC was initiated by washing the coverslips with ice-cold PBS twice. Cells were fixed with 4% paraformaldehyde for 15 min at 25˚C followed by washes in cold PBS (5 min, trice). Cells were permeabilized with 0.3% Triton X-100 for 10 min at 25˚C. Nonspecific binding was blocked by incubating cells in a 1% BSA/PBS for 20 min. The cells were incubated with primary Ab diluted in the blocking solution for 1 hr. After washing the cells in PBS, they were incubated with fluorescent secondary Ab for 30 min followed by the PBS washes. Additional washes in MQ water were completed to remove the salts from the PBS. The coverslips were attached to slides using Vectashield mounting medium with DAPI. The slides were stored in 4˚C, shielded from light.

2.2.2.10 Image Analysis

Images were captured using an Olympus BX51 microscope coupled to a DP71 Olympus digital camera and PictureFrame program Version 2.3 (Optronics, Goleta, CA). The same acquisition exposure-time conditions were used to capture images from the different treatment groups.

Immunohistochemical tissue staining was evaluated with the validated ImmunoRatio program, which is available as a free-ware web-based application (121) or as an Image Processing and Analysis in Java (ImageJ 1.46r, NIH) plug-in. The 400x images were uploaded to the online application, and the percentage of positively stained nuclei was calculated. The ImmunoRatio software utilized a color deconvolution algorithm, separating DAB from hematoxylin stain, and adaptive thresholding for nuclear area segmentation (122).

Immunocytochemical nuclear fluorescence was quantified using and a protocol adapted from methods published in the literature (123, 124). Images of cells were captured using bright field (BF), DAPI, and FITC filters. The DAPI image was opened in ImageJ and automatic brightness/contrast adjustment was performed. A region of interest (ROI) was drawn around the DAPI-stained nucleus and saved as an overlay. The FITC image was opened and the overlay was applied. An additional circle was drawn outside the cell, where there was no fluorescence, to represent background signal. ImageJ calculated the area, integrated density, and mean gray value for each ROI. The corrected total cell fluorescence (CTCF) was calculated using the formula CTCF = integrated density – (area of selected cell x mean fluorescence of background readings). An average of 25 representative nuclei was analyzed per treatment group. The nuclear fluorescence was graphed as the mean CTCF with error bars representing the standard error of the mean (SEM).

X-ray film was scanned into a computer and the densitometric quantification of Western blots was completed in ImageJ. The file was first converted to an 8-bit image. A rectangular ROI was drawn around the band within the first lane. The same ROI was duplicated and applied to the remaining lanes. Band density was plotted as histograms; a straight line was drawn across the base of each peak, eliminating background noise. The Wand tool was used to click inside each peak, highlighting the enclosed area to be measured. The peaks were labelled, and the densitometry data was imported into Excel (Microsoft, Redmond, WA). The relative density (to the positive control) and adjusted density (to the loading control) were calculated and graphed.

2.2.2.11 Statistical Analysis

Graphs were generated in GraphPad Prism 5 (GraphPad Software, Inc., La Jolla, CA), and the results were graphed as the mean value with error bars representing the SEM. Statistical analysis was completed with SPSS, Version 20 (IBM, Armonk, NY). Quantile-to-quantile (Q-Q) plots were generated to determine whether data was normally distributed. Parametric data was evaluated using one-way or two-way ANOVA and post hoc Mann-Whitney U tests. Nonparametric data was evaluated using Kruskal-Wallis test and post hoc Tukey-Kramer multiple comparisons tests. Statistical significance was set as $p < 0.05$.

2.3 Results

2.3.1 Apigenin decreased IL-6 levels via a PTHrP-dependent mechanism.

A genetic approach was utilized to evaluate PTHrP functionality relative to apigenin's anti-inflammatory activity. The pro-inflammatory cytokine IL-6 was chosen as the assay endpoint since it has been shown to correlate with pancreatitis severity in CR-induced animal models and humans with CP (125). A tamoxifen-inducible *Cre-lox* recombination system was employed to induce an acinar cell-specific PTHrP knockout mouse. Mice of the same background were treated with the vehicle of tamoxifen (corn oil), which did not activate *cre* recombinase. Thus, the wild-type control mice retained their PTHrP gene. Pancreata were harvested from each group (N = 4-5 mice), and the acini were isolated by collagenase digestion. The primary acini were treated *ex vivo* with vehicle (DMSO), cerulein (10^{-7} M), and/or apigenin (50 µM) for 4 hr. Total RNA was isolated from the cells and RT-PCR performed to determine IL-6 levels.

CR significantly stimulated IL-6 mRNA levels in WT mice with functional PTHrP, and this pro-inflammatory response was inhibited by apigenin ($p < 0.001$) (**Figure 6**). Compared to the vehicle, apigenin treatment reduced basal IL-6 levels. This was in contrast to the results produced from the PTHrP knockout mice. CR failed to stimulate IL-6 mRNA levels, and apigenin treatment had no effect on the cytokine level either. This suggested that apigenin was acting through a PTHrP-dependent mechanism.

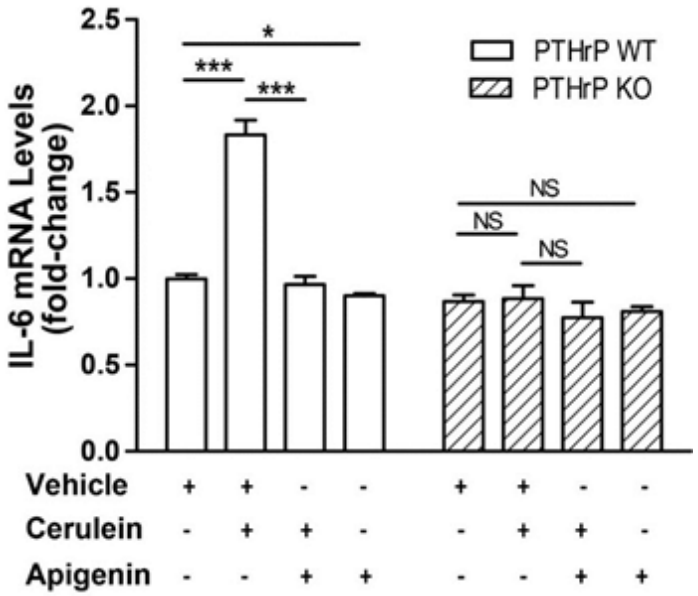

FIGURE 6. **Apigenin decreased IL-6 mRNA levels via PTHrP-dependent mechanisms.** Primary acini were isolated from PTHrP WT and PTHrP KO mice and treated *ex vivo* with vehicle (DMSO), CR (10^{-7} M), and/or apigenin (50 μM) for 4 hr. IL-6 levels were measured by RT-PCR. The data graphed was a combination of 3 independent assays. Two-way ANOVA determined a $p < 0.001$. One-way ANOVA with Tukey's test revealed $p < 0.05$ (*), $p < 0.001$ (***), and non-significant comparisons (NS).

2.3.2 Apigenin down-regulated PTHrP promoter activity.

Human PTHrP is synthesized from a single gene containing nine exons. Three isoforms of the protein can be generated by the expression of three distinct promoters and alternative splicing mechanisms; however, the P3 promoter has been found to be the most widely used sequence in both normal and tumor tissue (126). There is 90% homology between the human P3 promoter and the single PTHrP TATA promoter observed in rats and mice (127).

Apigenin's effect on PTHrP P3 promoter activity was assessed using a luciferase reporter assay. AR42J acinar cells were co-transfected with a PTHrP P3 promoter construct and a dual-luciferase reporter gene. The cells were treated with vehicle, apigenin, TGF-β, MAPK kinase inhibitor PD98059, and PI3K inhibitor LY294002. TGF-β was chosen as the stimulant since it is a crucial growth factor in the regenerative response of RAP, secreted by both acinar cells and activated PSCs. Furthermore, the P3 promoter has an EBS

1 site that binds Ets-1 and Smad 3, which are components of the classical TGF-β signaling pathway (126).

In comparison to the vehicle, apigenin did not significantly change PTHrP promoter activity (**Figure 7**). TGF-β stimulated P3 transcriptional activity, which was significantly inhibited by apigenin ($p < 0.01$). This inhibitor response was also seen by treatment with the MAPK kinase inhibitor PD98059. The PI3K/AKT pathway inhibitor LY294002 did not reflect any changes in reporter activity.

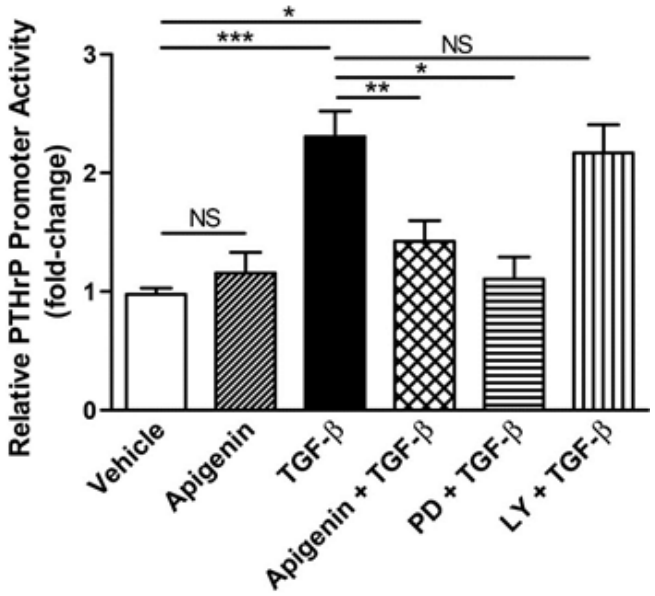

FIGURE 7. **Apigenin limited TGF-β stimulation of PTHrP P3 promoter activity.** AR42J cells were pre-treated with inhibitors PD98059 (PD, 10 μM) and LY294002 (LY, 25 μM) for 30 min. Cells were treated with vehicle (DMSO), apigenin (50 μM), and/or TGF-β (1 ng/mL) for 4 hr. Promoter activity was measured with the Dual-Luciferase Reporter Assay System. IL-6 levels were measured by RT-PCR. The data graphed was a combination of 3 independent assays. One-way ANOVA determined a $p < 0.001$, and Tukey's test revealed $p < 0.05$ (*), $p < 0.01$ (**), $p < 0.001$ (***), and non-significant comparisons (NS).

2.3.3 Apigenin did not significantly change pERK protein expression.

CR is a known activator of the MAPK pathway. Apigenin has been reported to be an inhibitor of the ERK pathway in breast, prostate, thyroid, colon, and pancreatic cancer cell lines (108, 128, 129). Therefore, the effect of apigenin on MAPK pathway activation was evaluated in AR42J cells. The acinar cells were pre-treated with vehicle, apigenin, or the inhibitors PD98059 and LY294002 followed by stimulation with CR for 5 min. Cells

without any treatment represented the negative control, and the positive control incorporated the treatment of cells with 10% FCS for 1 hr. In-well cell lysis was performed and cytoplasmic protein isolated. SDS-PAGE and immunoblotting for pERK and total ERK was completed. Densitometric analysis of the bands was done in ImageJ. Results were normalized to total ERK levels.

A representative blot was provided in **Figure 8A**. The negative control, vehicle and apigenin had minimal pERK expression. CR significantly increased pERK band intensity (at 42/44 kDa). Apigenin treatment appeared to down-regulate pERK expression in the blot; however, this was not a statistically significant difference when the results from 4 independent assays were combined (**Figure 8B**). The same trend was seen with PD98059 treatment but was not a statistically significant change. LY294002 appeared to slightly reduce pERK levels in the representative blot, but when combined with the assay replicates, had no effect on pERK expression at 5 min.

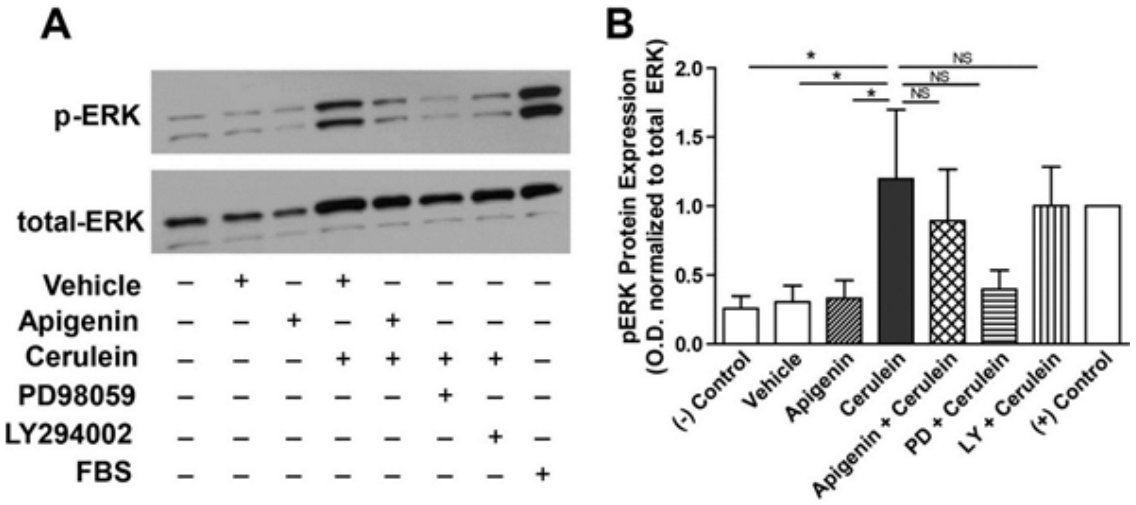

FIGURE 8. **Apigenin nor inhibitors PD98059 or LY294002 significantly reduced CR-induced pERK expression.**
AR42J cells were pre-treated with vehicle (DMSO) or apigenin (50 μM) for 1 hr. Inhibitors PD98059 (PD, 10 μM) and LY294002 (LY, 25 μM) pre-treatment was for 30 min. Cells were stimulated with CR (0.1 μM) for 5 min. Immunoblotting for pERK and total ERK was completed. A representative blot was provided in A). The data graphed in (B) was a combination of 4 independent assays. Kruskal-Wallis determined a $p < 0.01$, and Mann-Whitney tests revealed $p < 0.05$ (*) and non-significant comparisons (NS).

2.3.4 Apigenin reduced pERK nuclear localization *in vivo*.

For the next experiment, I decided to look at pERK in a mouse model of CP. Recurrent pancreatitis was induced by serial supraoptimal doses of CR, which has been shown to recapitulate the biochemical, morphologic, and pathophysiologic features of human disease (99, 101). Through hyperstimulation of the CCK receptor, pancreatic injury is generated by a deranged secretory response. Pancreatic enzymes become prematurely activated, leading to parenchymal autodigestion that incites inflammation and fibrosis. Repeated bouts of pancreatitis shifts homeostasis from a physiologic to pathologic response to injury with progression toward the irreversible damage of CP.

The mice were subjected to RAP for 1 wk prior to the initiation of apigenin therapy, simulating a clinically relevant scenario. Apigenin was administered at a dose of 2.5 mg/kg, given daily, by oral gavage, 6 d/wk. The repeated induction of pancreatitis was continued with apigenin therapy for an additional 3 wk. At termination of the study, the mice were sacrificed and pancreata were harvested, fixed, paraffin-embedded, and sectioned. DAB-immunohistochemical staining for pERK was completed with counter-staining using hematoxylin. Ten, non-overlapping 400x images were taken of each slide. Representative images per treatment group were included in **Figure 9A, C, E, and G**. The ImmunoRatio program was used for image analysis, providing an automated means of quantifying the percentage of acinar cell nuclei staining positive for pERK. ImmunoRatio output included a pseudo-colored image, identifying the detection of acinar nuclei (purple) and DAB-stained nuclei (orange) (**Figure 9B, D, F, and H**). The program also provided a labeling index, which represented the percentage of positively stained nuclei (**Figure 9I**).

Activation of the MAPK pathway involves a phosphorylation cascade of sequential serine/threonine kinases, which transduces signaling from the cell surface receptor-ligand interactions to cytoplasmic and nuclear targets. The down-stream effector, pERK, can translocate to the nucleus and phosphorylate additional transcription factors required for the expression of genes involved in cell growth, differentiation, apoptosis, and inflammation. In regard to this experiment, basal pERK expression appeared to be mostly

cytoplasmic within the vehicle and apigenin groups. CR-induced RAP-induced pancreatic MAPK pathway activation and significant translocation of pERK to the nucleus. Daily oral

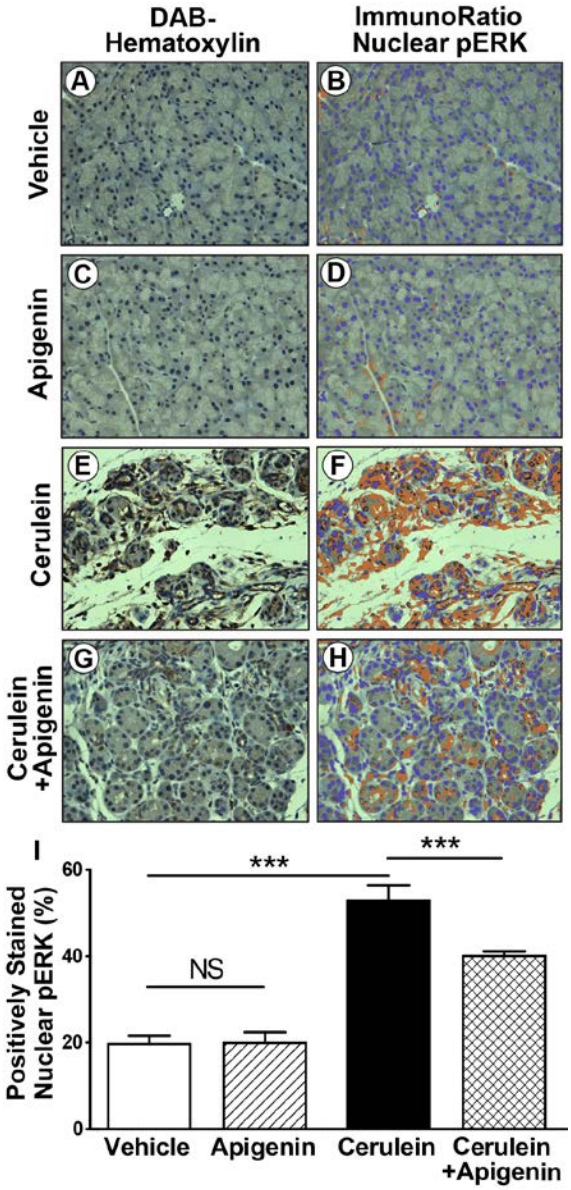

FIGURE 9. Apigenin reduced nuclear pERK positivity.

Mice were subjected to 4 wk of CR-induced RAP. After 1 wk of pancreatitis, apigenin therapy was initiated (2.5 mg/kg, oral gavage, once daily, 6 d/wk) and continued the duration of the experiment. Pancreata were harvested and processed; 2-3 pancreata/group were stained for pERK by DAB-IHC and counterstaining with hematoxylin was completed. Representative 400x microscopic images of each group were taken: (A) vehicles (PBS IP, 0.5% MC + 0.025% Tween20 by oral gavage); (C) apigenin (+PBS); (E) CR (+ apigenin's vehicle); and (G) CR + apigenin. Image analysis was performed with ImmunoRatio, and data output consisted of the pseudo-colored images where the purple color represented nuclei recognized and brown was DAB-stained nuclei (B, D, F, H). The percent area of positively stained nuclei was graphed in (I). One-way ANOVA determined a $p < 0.001$, and Tukey's tests revealed $p<0.001$ (***) and non-significant comparisons (NS).

apigenin therapy not only reduced pERK nuclear translocation ($p < 0.001$) but helped preserve pancreatic architecture. The histologic changes observed in the RAP experiment will be discussed in more depth within the next chapter.

2.3.5 Apigenin reduced NF-κB pathway activation.

Apigenin's effect on NF-κB was also evaluated since it has been identified as a pro-inflammatory pathway activated in CP independent of intra-acinar trypsinogen activation (130). In quiescent cells, cytoplasmic NF-κB (p65/p50 subunits) is inactivated by its complex with the inhibitor of NF-κB (IκB). Growth factors like TNF-α activate IκB kinase (IKK), which induces phosphorylated ubiquitination of IκB, releasing NF-κB from the inhibitory complex. Free p65/p60 translocates to the nucleus, where the transcription factors interact with gene targets (131). Thus, nuclear localization of NF-κB serves as a conjugate for pathway activation.

ICC and image analysis were employed to assess NF-κB localization. AR42J cells were pre-treated with apigenin followed by stimulation with TNF-α. Immunostaining was performed with a p65 primary Ab and Alexa fluor 488 fluorescent secondary Ab. A series of 400x microscope images were taken using different filters. A BF image served as a reference to cell size and shape. The mounting medium contained DAPI, which

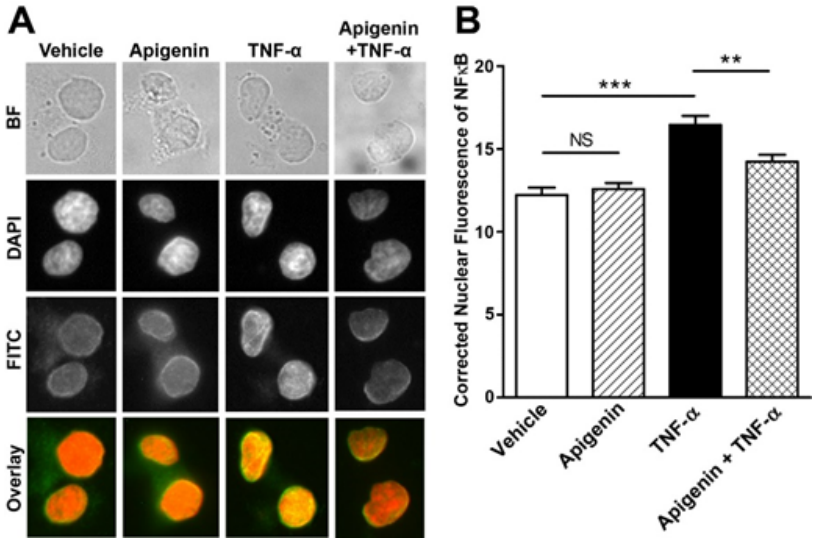

FIGURE 10. **Apigenin reduced NF-κB nuclear localization.**
AR42J cells were pre-treated with vehicle (DMSO) or apigenin (50 μM) for 1 hr followed by stimulation with TNF-α (10 ng/mL) for 30 min. Fluorescent ICC was performed, and 400x were taken using BF, DAPI, and FITC filters (A). A minimum of 25 nuclei were analyzed per group, and the assay was independently replicated twice. The area of nuclear p65 staining was quantified and graphed in (B). Kruskal-Wallis determined a $p < 0.001$, and Mann-Whitney tests revealed $p < 0.01$ (**), $p < 0.001$ (***), and non-significant comparisons (NS).

preferentially stained nuclei; this image was used to generate an outline of the ROI. The ROI overlay was applied to the FITC image, and density of nuclear fluorescent signal was quantified in ImageJ. The overlay image was created by pseudo-coloring the DAPI image red and the FITC image green so that the appearance of yellow indicated overlap of the stains and was interpreted as nuclear p65 expression (**Figure 10A**). Automated image analysis verified apigenin limited TNF-α induced nuclear translocation of NF-κB ($p < 0.01$) (**Figure 10B**).

2.4 Discussion

PTHrP has been identified as a pro-inflammatory mediator in both AP and CP (80, 81). The generation of the $PTHrP^{flox/flox}$; Cre^{+} (homozygous) mice enabled evaluation of the relationship between PTHrP function and apigenin's known anti-inflammatory activity. Hyperstimulation of acini with the CCK analog, CR, disrupts normal secretory function, leading to cellular injury, necrosis, and activation of an immune response through the synthesis and secretion of cytokines like IL-6. The acini isolated from PTHrP WT mice responded to CR by increasing mRNA levels, and apigenin inhibited generation of this response. Also, apigenin reduced IL-6 mRNA levels significantly below that of the vehicle. Thus, apigenin may be resetting a 'threshold' required to activate intracellular signaling pathways that result in generation of inflammatory mediators.

Knockout of PTHrP abolished acinar cell response to CR, and apigenin treatment did not change IL-6 mRNA levels. Therefore, it can be deduced that apigenin exerts it anti-inflammatory, in part, by down-regulating IL-6 transcription. Measurement of mRNA levels not only reflects transcriptional activity but post-translational modifications. It is possible that apigenin may be altering the regulation of IL-6 transcript stability and turnover. A future experiment should include the performance of a time-course study involving a RNA polymerase inhibitor like 5,6-dichlorobenzimidazole riboside. By measuring the mRNA levels at each time point, with and without apigenin treatment, the decay rates could be determined.

I have attempted several PTHrP rescue experiments with inconsistent results. Since the transgenic mice have a genetic deletion of the peptide rather than receptor knockout, primary acinar cells should respond to exogenous PTHrP by increasing IL-6 transcript. I have found that acini isolated from WT mice respond to PTHrP (10^{-7} M for 15 min) by increasing IL-6 levels; however, this pro-inflammatory response is by orders of magnitude weaker than CR (data not shown). Acini from PTHrP knockout mice failed to rescue with PTHrP at one dose (10^{-7}M) and one time point (15 min) tested. A PTHrP time-course and dose-titration studies are needed to determine whether the lack of an effect of exogenous PTHrP is due to experimental design or altered biology of the acini isolated from the knockout animals.

The luciferase reporter gene assay was used to assess the effects of apigenin on PTHrP P3 promoter activity. Apigenin suppressed TGF-β stimulation of P3 activity. The MAPK kinase inhibitor PD98059 reduced P3 activity as well. The combination of these results provided an indirect link between the ERK pathway and apigenin's transcriptional regulation of PTHrP. Decreased promoter activation leads to reduced transcription, translation, and production of the protein.

Future studies should include assays that directly assess the binding of transcription factors to the promoter. Regulation of promoter activity has been shown to be mediated by the binding and cooperation of multiple transcription factors (Ets-1, Sp1, and Smads) and co-activators like CREB-binding protein (CBP)/p300 (126). Ets-1 is activated by both TGF-β and MAPK (126), providing a potential mechanistic target for apigenin. Future studies could employ a chromatin immunoprecipitation assay using an Ets-1 antibody, followed by RT-PCR using primers for the PTHrP promoter sequence, to evaluate whether apigenin treatment inhibits Ets binding to the endogenous PTHrP promoter in acinar cells. Pathway inhibitors like PD98059, LY294002, SB203580 (for p38 inhibition), and SP600125 (for JNK inhibition) could also be incorporated, providing additional information regarding preferential MAPK pathway use in PTHrP transcriptional regulation.

MAPK/ERK pathway inhibition by apigenin was investigated further *in vitro* using SDS-PAGE immunoblotting. These studies showed that pre-treatment of AR42J cells with 50 μM of apigenin was insufficient to significantly inhibit pERK activation by CR. We observed significant variability between the independent assay replicates, hence the large error bars on the graph (**Figure 8**). This variability may be due, in part, to technical problems since CR activates pERK rapidly (2.5-5 min) in acinar cells.

Using a mouse model of RAP, assessment of MAPK pathway activation revealed that apigenin significantly reduced pERK nuclear localization. The MAPK pathway is a critical link between extracellular stimuli, such as CR or CCK, intracellular response, and regulation of cell proliferation, differentiation, and apoptosis. Signal transduction is transferred through the sequential phosphorylation of a kinase cascade, classically leading to pERK translocation from the cytoplasm to the nucleus, where it can phosphorylate transcription factors (132). In quiescent cells, ERK is largely anchored in the cytoplasm; upon activation, pERK transiently enters the nucleus and returns to the cytoplasm due to an inherent nuclear export sequence at its N-terminus (133, 134). Thus, the positive pERK nuclear staining correlated with MAPK activation by RAP, and apigenin inhibition of this response correlated with a reduction in pancreatic injury.

The use of ERK inhibitors has further solidified the importance of the MAPK pathway activity in the perpetuation of pancreatitis. Rats pre-treated with MEK inhibitors PD98059 or U0126 for 30 min prior to CR-induced AP, and consequently redosed with hourly CR injections, exhibited less severe pancreatitis as measured by lower pancreatic wet weight, limited severity of pancreatitis-related morphology, and reduced serum amylase (135). Wet weight is an indirect measurement of pancreatic edema. In addition, rats were treated with vinblastine to generate neutropenia, and U0126 pretreatment reduced pancreatic wet weight and ERK expression in protein homogenate (135), providing evidence for intra-pancreatic MAPK/ERK pathway stimulation.

Apigenin's effect on NF-κB pathway activation was investigated using ICC staining and quantification of nuclear localization. Apigenin was found to reduce NF-κB translocation. This finding is relevant since the immunostaining of pancreatic tissue from

CP patients has shown significant nuclear p65 positivity of acini (130). Wu *et al*'s findings support the concept that apigenin resets a threshold for activation of intracellular pathways involved in the generation of an inflammatory response; apigenin was found to reduce both basal and TNF-α-stimulated NF-κB DNA binding, transcriptional activity, IκB phosphorylation, and nuclear p65/p50 nuclear translocation in pancreatic cancer cell line AsPc-1 (136). Thus, apigenin is most likely acting through multiple mechanisms to limit pancreatic injury in RAP, and thereby progression to CP.

CHAPTER 3:

APIGENIN'S REGULATION OF PSC ACTIVITY

3.1 Introduction

3.1.1 Fate of Activated PSCs

According to the SAPE hypothesis, the sentinel event of AP injures acinar cells. This induces a pro-inflammatory and pro-fibrotic response mediated, in part, by the myofibroblastic transformation of PSCs. The physiologic wound-healing response becomes pathologic when repeated stress sustains the activation of PSCs, perpetuating their activation, proliferation, synthetic activity, and fibrotic response to pancreatic injury. PSC activation has been well-characterized, but controversy exists as to what is the fate of activated PSCs. Options include reversion to a quiescent state, senescence, and/or apoptosis (93).

PSC inactivation has been demonstrated *in vitro*; PSCs treated with retinol and its metabolites reduced cellular proliferation, α-SMA expression, collagen 1/FN/laminin expression, and activation of MAPK pathways involving ERK, p38, and JNK (137). Pancreatic cryostat sections from rats with dibutyltin dichloride-induced CP exhibited increased colocalization of senescence-associated β-galactosidase, α-SMA, fibrosis, and CD4 and CD8 inflammatory infiltrate (138).

Vonlaufen *et al* have provided stronger *in vivo* evidence supporting the importance of PSC apoptosis in pancreatitis resolution. Rats were subjected to 10 wk of alcohol feeding followed by an LPS challenge, and recovery was monitored with and without the continuation of alcohol. IHC for caspase 3 and dUTP nick-end labeling (TUNEL) staining were used to assess PSC apoptosis in pancreatic sections. The withdrawal of ethanol for 3 or 7 d resulted in a significant increase in PSC apoptosis accompanied by reduced collagen and hydroxyproline deposition; whereas continued alcohol feeding prevented PSC apoptosis (139).

Additional research is needed to identify mechanisms of PSC inactivation as this is a potential target for therapeutic drug development in RAP. Within the oncologic literature, apigenin has been reported to possess anti-proliferative and pro-apoptotic properties (108); therefore, we hypothesized that the preservation of pancreatic architecture seen in our

animal model of RAP was mediated, in part, through growth inhibition, apoptosis induction, and suppression of PTHrP-mediated PSC response to pancreatic injury.

3.2 Materials and Methods

3.2.1 Materials

The majority of the materials have been listed in **Section 2.2.1**. Any additional reagents have been included in this section. The C57BL/6 mice were purchased from Harlan Laboratories (Houston, TX) and The Jackson Laboratory (Bar Harbor, ME).

The following IHC reagents were purchased from the companies indicated: rabbit serum (Sigma-Aldrich), hematoxylin 7211 (Thermo Fischer Scientific, Inc.), VECTASTAIN Elite ABC kit and VectaMount (Vector Laboratories). Information regarding the antibodies utilized was included in **Table 5**.

Name	Specificity	Dilution	Details	Manufacturer
Fibronectin	C-terminus of fibronectin of human origin (C-20)	1:600 (IHC)	Goat, polyclonal	Santa Cruz sc-6952
Biotinylated rabbit anti-goat	Goat IgG	1:400 (IHC)	Rabbit	Vector Lab BA-5000

TABLE 5. Antibodies used in PSC experiments.

The following cell culture reagents were purchased from Invitrogen: streptomycin, penicillin, gentamicin, and amphotericin B (Life Technologies). The insulin-transferrin-selenium-ethanolamine was from Gibco, and the 1% non-essential amino acid was from Sigma-Aldrich. The lentiviral vector for Simian virus 40 (SV40) large T antigen (plasmid #12245) and human telomerase (#12246) were obtained from Addgene (Cambridge MA).

The cell proliferation assays were conducted with the following: Z1 Particle Counter (Beckman Coulter, Hialeah, FL), alamarBlue reagent (DAL1025, Thermo Fisher Scientific, Inc.), and SpectraMax M2 Microplate Reader (Molecular Device, Sunnyvale, CA). The Cell Death Detection ELISA^{PLUS} assay, Version 11.0, was purchased from Roche

Applied Science (Indianapolis, NY), and absorbance output was read with an ELx808 Automated Microplate Reader (Bio-TEK Instruments, Inc., Winooski, VT).

To assess the efficiency of RNA isolation, a NanoDrop spectrophotometer (Nanodrop Technologies, Wilmington, DE) and RNA Nano chip with Agilent 2100 Bioanalyzer (Agilent Technologies, Santa Clara, CA) were utilized. The TaqMan Reverse Transcription Reagents Kit (Life Technologies), Faststart Universal SYBR green Master Mix (Roche), and ABI Prism 7500 Sequence Detection System (Life Technologies) were used to complete qPCR.

3.2.2 Methods

3.2.2.1 RAP Mouse Model

The RAP model has been previously described in **Section 2.2.2.7**. The mouse strains C57/129P2 and C57BL/6 were utilized for the RAP experiments repeated in triplicate.

3.2.2.2 Immunohistochemistry (IHC)

A protocol for tissue fixation and automated IHC was discussed in **Section 2.2.2.8**. A method of manual immunohistochemical staining for FN has been previously published (111). Any differences between the two methods have been included below.

The sections were deparaffinized with xylene, rehydrated using an ethanol gradient, and washed in MQ water for 3 min, trice. Heat-mediated antigen retrieval was performed by incubating the sections with the same citrate buffer for 30 min at 97˚C. The slides were allowed to cool to 25˚C and then washed in MQ water for 5 min, twice. Endogenous peroxidase activity was quenched by incubating sections with 3% H_2O_2 for 20 min at room temperature (RT). To block nonspecific binding, the sections were incubated with a solution of 5% rabbit serum, 1% BSA, and PBS for 3 hr at RT. The sections were incubated with primary Ab in Ab diluent overnight in a humidity chamber at 4˚C.

Two 5-min washes with PBS-0.1% Tween 20 (PBS-T) were followed by two washes with PBS. The sections were incubated with secondary Ab for 30 min in a humidity

chamber at RT. The slides were washed with PBS-T and PBS as before. The VECTASTAIN Elite ABC kit and DAB were utilized for color development. The slides were washed with MQ water for 3 min twice followed by counter-staining with hematoxylin 7211. The sections were dehydrated using an ascending graded series of ethanol followed by xylene. VectaMount was used to attach the coverslips to the slide.

3.2.2.3 Image Analysis

The BX51 microscope coupled to a DP71 Olympus digital camera was used to capture 10 non-overlapping 400x images of each pancreas. ImageJ software and Ruifrok's color deconvolution plug-in (140) were used to isolate the brown staining from the compound image of DAB and hematoxylin stained pancreata. The ROI was set as the entire 400x image. The images were analyzed using a sequence of commands: background substraction; automated brightness/color adjustment; color deconvolution using the 'H DAB' vector with selection of the brown channel; minimal thresholding, and automated measurement of the percent area of isolated brown staining within the ROI (119).

3.2.2.4 Primary Human PSC Isolation and Culture

The method for establishing primary PSC cultures has been published (119). Under an Institutional Review Board-approved protocol, discarded pancreatic tissue (500 mm^3) from patients with CP was attained fresh from the operating room at UTMB. The tissue was transported in tumor media, which consisted of the following: DMEM supplemented with streptomycin 200 µg/ml, penicillin 200 U/mL, gentamicin 50 µg/mL, amphotericin B 0.25 µg/mL, 1% insulin-transferrin-selenium-ethanolamine, 1% non-essential amino acids, and 10% FBS. The tissue was finely minced and explanted onto a collagen-coated (15 µg/mL) flask which had been prepared at least 30 min prior to use. The flask was filled with enough tumor media to cover the tissue, preventing desiccation. Cell culture conditions were maintained at 37˚C and a 5% CO_2 humidified atmosphere. The tumor media was replaced every 3-5 days for a month.

The human PSCs were isolated using a standard outgrowth method as described by Apte (82) and Bachem (83), whom both have shown that PSCs grown on plastic auto-

activate. PSC culture purity was confirmed by immunostaining for α-SMA, vimentin, and GFAP. The primary PSCs were immortalized for repeat experimentation. This was achieved by transducing the cells with lentivirus containing SV40 Large T antigen and human telomerase (141). The transformed PSCs were selected by growing them in DMEM supplemented with 10% FBS and ampicillin (100 µg/mL).

3.2.2.5 Cell Proliferation Assays

Cell proliferation was evaluated over time through cell counting (119). Human PSCs were seeded in quadruplicate in a 12-well plate ($1.5x10^5$ cells/well) containing DMEM with 10% FBS. The next day, the media was aspirated and changed to DMEM with 1% FBS. Apigenin (30 µM) or vehicle (DMSO) treatment was initiated for 24, 48, and 72 hr. For each time point, the cells were recovered using trypsin and quantified with a Coulter counter.

Cell viability was assessed using the colorimetric alamarBlue assay (119). Human PSCs were plated in sextuplicate in a 96-well plate ($3x10^3$ cells/well) containing DMEM with 10% FBS. The next day, the media was aspirated and changed to DMEM with 1% FBS. The PSCs were treated with escalating doses of apigenin (0-50 µM) for 48 hr. The cells were incubated with alamarBlue reagent (10% of the well volume) for 4 hr at 37˚C, shielded from light. Viable cells were able to maintain a reducing environment and convert the cell-permeable active ingredient, resazurin, to a highly fluorescent product, resorufin. Fluorescent intensity is directly proportional to cell number and was measured at excitation and emission wavelengths of 544/590 nm by a microplate reader. To account for background fluorescence, the average reading from wells containing media (no cells) was subtracted from the assay output. Apigenin did not interfere with the assay as it has been shown to be weakly fluorescent in aqueous solutions (142). The data was used to generate a dose-response curve by plotting fluorescence versus [apigenin].

3.2.2.6 Cell Death Assay

Methods used to evaluate cell death have been previously published (119). Human PSCs were plated in triplicate in 96-well plate ($8x10^3$ cells/well) containing DMEM with

10% FBS. The media was changed to DMEM with 1% FBS the next day. The PSCs were treated with apigenin over time (50 µM for 1-6 hr) and at different concentrations (0-50 µM for 14-16 hr) by performing serial dilutions. In-well cell lysis and an enzyme-linked immunosorbent assay (ELISA) were completed using Ab-directed at mononucleosomes and oligonucleosomes specific to the process of apoptosis rather than necrosis. A negative control consisted of untreated cells, and the ELISA kit incorporated a DNA-histone positive control. Background was quantified by measuring the absorbance of Incubation Buffer rather than a sample, and this average reading was subtracted from the assay output. Absorbance was measured at a wavelength of 405 nm using a microplate reader. Apigenin did not interfere with the assay's output as its two intrinsic absorbance bands (Band I 300-390 nm, Band II 250-280 nm) lie outside of the spectra utilized (142). The data was used to generate a dose-response by plotting absorbance versus log [apigenin].

3.2.2.7 Real Time PCR (qPCR)

RNA isolation was once again performed with the RNAqueous kit, and qPCR was completed by the UTMB Molecular Genomics Core. RNA quantity and quality was assessed with a NanoDrop spectrophotometer and Nanochip with Agilent 2100 Bioanalyzer. The TaqMan cDNA synthesis kit was used to reverse transcribe 1.0 µg of RNA into cDNA while using the following reaction conditions: 25˚C for 10 min, 48˚C for 30 min, and 95˚C for 5 min. Real-time PCR (qPCR) was performed with the ABI Prism 7500 Sequence Detection System, primers listed in **Table 6**, SYBR green master mix, and the following conditions: 50˚C for 2 min, 95˚C for 10 min, followed by 40 cycles at 95˚C for 15 sec and 60˚C for 1 min. Results were reported relative to the housekeeping gene 18S. The threshold cycle and n-fold change formulas were calculated as described in **Section 2.2.2.4**.

3.2.2.8 Statistical Analysis

The apigenin concentrations were converted to a logarithmic scale and entered into GraphPad with their associated fluorescence/absorbance assay results. Then, nonlinear regression was utilized to create a best-fit curve for the dose-response data. This enabled

determination of half maximal inhibitory concentration (IC_{50}) and half maximal effective concentration (EC_{50}). Additional methods for statistical analysis have been described in previous chapters.

Primer	Species	Forward Primer	Reverse Primer
Collagen type 1α1	Human	GGCAGCCTTCCTGATTTCTG	CTTGGCAAAACTGCACCTTCA
Fibronectin	Human	ATGGTGTCAGATACCAGTGCTACTG	TCGACAGGACCACTTGAGCTT
TGF-β1	Human	GCACGTGGAGCTGTACCAGAA	CTGAGGTATCGCCAGGAATTG
PCNA	Human	GGGCGTGAACCTCACCAGTA	TCATTGCCGGCGCATT
IL-6	Human	ATGAACTCCTTCTCCACAAGCG	CCCCAGGGAGAAGGCAAC
IL-8	Human	GGCAGCCTTCCTGATTTCTG	CTTGGCAAAACTGCACCTTCA

TABLE 6. SYBR-green primers used in PSC qPCR.

3.3 Results

3.3.1 Apigenin reduced pancreatic injury and fibrosis *in vivo*.

Apigenin was tested using the well-established animal model of secretagogue-induced RAP. Stromal fibrosis was evaluated by performing DAB-immunohistochemical staining for FN, a fibrillar component of the ECM matrix. Hematoxylin counterstaining was performed to provide contrast and define the parenchymal architecture. The blue dye preferentially bound to basophilic structures such as DNA in the nucleus and RNA in the ribosomes and RER, both of which are predominant in the acinar cell.

Each study group consisted of 5-6 mice, and this experiment was repeated independently a total of 3 times. Four weeks of CR-induced RAP produced significant histologic evidence of pancreatic injury (**Figure 11A**). An overall loss in acini was observed, and those remaining appeared atrophic and disorganized. Intralobular ducts were decreased in number with distorted epithelial lining and periductal fibrosis. The islets were relatively spared (not shown), which is a common finding in early CP. Increased cellularity was noted, reflecting lymphoplasmacytic infiltration. The diffuse periacinar, perilobular, and periductal fibrosis was identified by the brown immunohistochemical staining for FN. In contrast, the normal pancreatic architecture was observed in the vehicle control group

(**Figure 11B**). The parenchyma was composed of plump, homogenous acini without signs of inflammation or fibrosis.

Apigenin therapy appeared to protect the pancreas from recurrent injury induced by CR (**Figure 11C**). The acinar units appeared to be preserved with minimal atrophy. Less cellularity, interstitial edema, and stromal fibrosis was noted. Mice treated with apigenin alone (**Figure 11D**) exhibited pancreatic histology comparable to the vehicle controls. Ten non-overlapping representative images of each pancreatic section were taken, and the percent area of brown (FN) staining was quantified using ImageJ and a color deconvolution plug-in. As seen in **Figure 11E**, Apigenin treatment significantly reduced pancreatic fibrosis during RAP by 58% ($p < 0.001$).

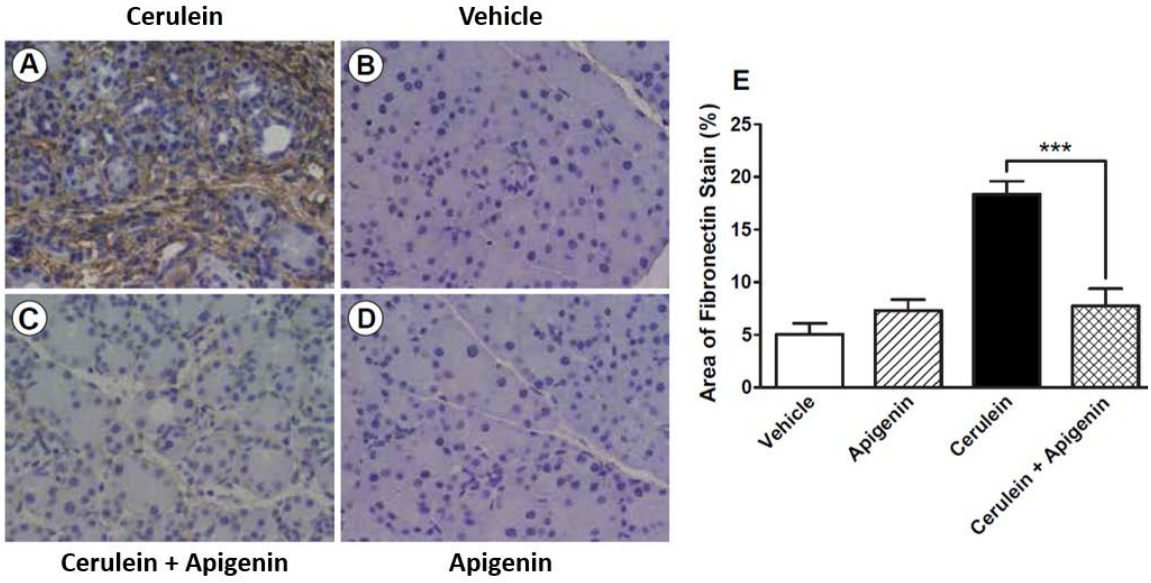

FIGURE 11. Apigenin preserved pancreatic architecture and limited fibrosis during RAP *in vivo*.
Mouse pancreatic tissue was stained for FN by DAB-IHC and counter-stained with hematoxylin. Representative sections from each study group were provided, with images taken at 400x (A-D). The vehicle for CR was PBS, and the vehicle for apigenin was 0.5% MC + 0.025% Tween 20 in MQ water. Treatment groups consisted of: A) CR (+ apigenin's vehicle); B) both vehicles; C) CR + apigenin (2.5 mg/kg); and D) apigenin (+ CR's vehicle). The percent area of brown FN staining was quantified in ImageJ and graphed as mean ± SEM in E). The animal experiment was repeated in triplicate, and a significant p-value < 0.001 was indicated as ***. Reproduced with permission (119).

3.3.2 Apigenin inhibited PSC proliferation and viability over time and with increased doses.

Activated PSCs are responsible for the dysregulated deposition and remodeling of ECM components in CP (93). Therefore, the effect of apigenin on PSC proliferation and viability was evaluated *in vitro*. For the proliferation assay, PSCs were treated with apigenin (30 µM) or vehicle (DMSO) for 24-78 hr. At each time point, the cells were rinsed with PBS, trypsinized, and the cell number was determined by an automated Coulter counter. PSCs treated with the vehicle displayed log phase cell growth; however, PSC proliferation was inhibited by apigenin over the 78-hr time period (**Figure 12A**).

Cell viability was assessed with the colormetric alamarBlue assay, and data output was used to generate a dose-response curve (**Figure 12B**). PSCs were treated with increasing doses of apigenin (0-50 µM) for a 48-hr time period, and PSC viability was inhibited in a dose-dependent manner. Using nonlinear transformation, a best-fit curve was generated in SPSS, allowing determination of the concentration at which apigenin results in 50% inhibition of PSC viability. By combining the results from 10 independent alamarBlue assays, the IC_{50} of apigenin was determined to be 18.6 ± 1.6 µM (mean ± SEM) (111, 119).

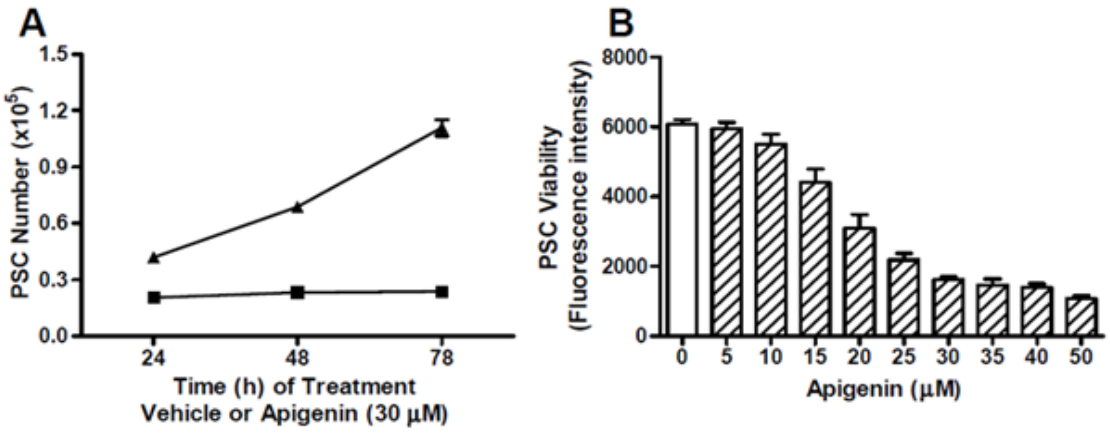

FIGURE 12. PSC proliferation and viability were inhibited by apigenin in a time- and dose-dependent manner.
A) PSCs were treated with apigenin (30 µM, ■) or vehicle (DMSO,▲) for 24, 48, and 72 hr. At each time point, PSCs were washed with PBS, trypsinized, and counted. Each condition was performed in quadruplicate. B) PSCs were treated with escalating doses of apigenin for 48 hr. B) PSC viability was measured using the alamarBlue assay, from which the dose-response curve was generated representing a single assay. Apigenin's IC_{50} (18.6 ± 1.6 µM) was determined from a total of 10 independent assays. Reproduced with permission (111, 119).

3.3.3. Apigenin induced PSC apoptosis over time and with increased doses.

Perpetual activation of PSCs produces the desmoplastic reaction to pancreatic injury. The PSCs express a high mitotic index accompanied by decreased cell death (93). The effect of apigenin on PSC apoptosis was evaluated *in vitro.* Programmed cell death was quantified using an ELISA directed at nucleosomes, which are generated from endonuclease-dependent DNA fragmentation. For the first experiment, PSCs were treated with apigenin (50 µM) for various time points (**Figure 13A**). Compared to basal levels, apigenin induced significant PSC apoptosis at 3.5, 5, and 6 hr ($p < 0.05$).

Next, PSCs were treated with increasing doses of apigenin (0-50 µM) for 48 hr, and the ELISA was completed. Absorbance was directly proportional to apoptosis and reflected a dose-response to apigenin (**Figure 13B**). SPSS was used to perform nonlinear regression and generation of a best-fit curve. Apigenin's EC_{50} (24.5 ± 2.5 µM) was derived from 7 independent assays, and it represented the concentration at which half the maximal amount of apoptosis was induced (111, 119).

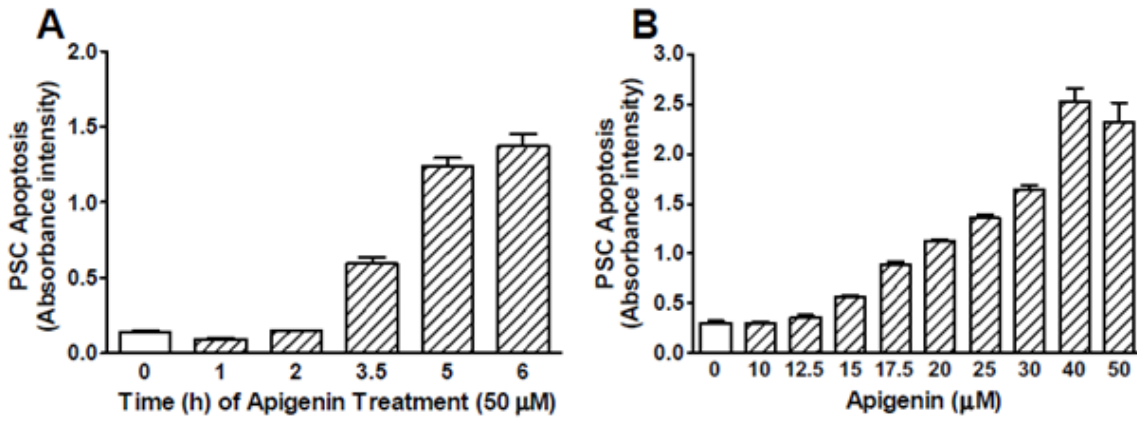

FIGURE 13. **PSC apoptosis was induced by apigenin in a time- and dose-dependent manner.** A) PSCs were treated with apigenin (50 µM) for 1-6 hr. Apoptosis was measured using the Cell Death Detection ELISA^{PLUS} assay. B) PSCs were treated with apigenin escalating doses of apigenin for 14-16 hr. Apoptosis was evaluated as in A), from which a dose-response curve was generated representing a single assay. Apigenin's EC_{50} (24.5 ± 2.5 µM) was determined from a total of 7 independent assays. Reproduced with permission (111, 119).

3.3.4. Apigenin limited PTHrP-mediated induction of PSC ECM synthesis, proliferation, and inflammation.

PTHrP has been shown to be a pro-fibrogenic and pro-inflammatory mediator of pancreatitis (80, 81). The effect of apigenin on PSC transcriptional response to PTHrP was evaluated *in vitro*. Human PSCs were pre-treated with vehicle (DMSO) or apigenin (50 μM) for 1 hr followed by stimulation with PTHrP (10-7M) for 12 hr. RNA was isolated and qPCR performed to measure the mRNA levels of ECM proteins collagen type 1α1 and FN, cell proliferation marker PCNA, TGF-β1, and pro-inflammatory cytokines IL-6 and IL-8 (**Figure 14 A-F**, respectively). Apigenin reduced basal mRNA levels of all endpoints except FN. Furthermore, apigenin significantly reduced PSC transcriptional response to PTHrP ($p < 0.001$). Compared to the vehicle, PTHrP minimally stimulated IL-8, and thus

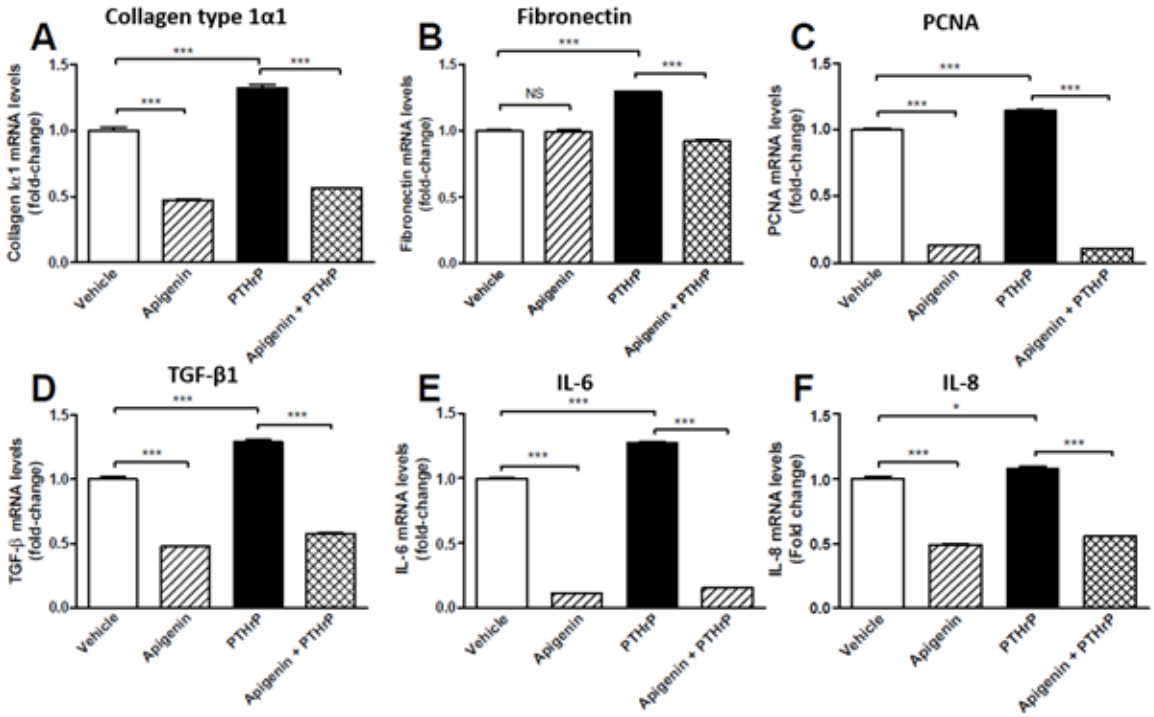

FIGURE 14. **PSC reduced PTHrP-induced fibrogenesis, proliferation, and inflammation.** PSCs were pre-treated with vehicle (DMSO) or apigenin (50 μM) for 1 hr and then stimulated with PTHrP (10^{-7} M) for 12 hr. Total RNA isolation and qPCR were performed to determine the mRNA levels of collagen type 1α1 (A), FN (B), proliferating cell nuclear antigen (C), TGF-β1 (D), IL-6 (E), and IL-8 (F). Fold-change was reported relative to the vehicle. The graphs represented the combined results of 2 independent assays. P-values were indicated as * ($p < 0.05$), *** ($p < 0.0001$), and NS ($p > 0.05$, non-significant). Reproduced with permission (119).

apigenin's effect is most likely independent of PTHrP (119). The graphs represented the combined results from 2 independent assays.

3.4 Discussion

Testing of apigenin in a mouse model of CR-induced RAP revealed that it was a promising lead compound for therapeutic drug development. Oral apigenin treatment (of 2.5 mg/kg) was initiated 1 wk after the induction of RAP and continued for the duration of 4 wk. This preclinical study design modeled the potential clinical application of apigenin in pancreatitis patients who are at risk for progression to CP. After 4 wk of RAP, apigenin therapy had appeared to protect the pancreas from recurrent injury. Pancreatic architecture was preserved with limited evidence of histologic damage by pancreatitis. Apigenin reduced acinar atrophy, inflammatory infiltrate, and stromal fibrosis. DAB-immunohistochemical staining for FN confirmed a significant reduction in stromal fibrosis, which reflected the pathologic activity of activated PSCs.

To my knowledge, a single study exists in the literature evaluating the use apigenin in the setting of pancreatitis. Lampropoulos *et al* utilized a biliopancreatic ductal ligation rodent model of AP to assess the effect of single, 5 mg oral dose of apigenin (110). The authors reported how apigenin "seemed to protect the pancreatic tissue", significantly limiting inflammatory infiltrate and MPO activity, which is a redox-related lysosomal enzyme highly expressed by neutrophils (110). There is evidence within the literature of other classes of flavonoids reducing the severity of pancreatitis. Pretreatment with the flavonol quercetin (at single oral doses of 25, 50, 100 mg/kg) attenuated CR-induced AP by significantly modulating the following parameters: serum amylase/lipase, pancreatic edema (measured by wet weight), inflammation (measured by MPO activity, immunostaining for TNF-α, and serum levels of TNF-α, IL-1β, IL-6, and IL-10), lipid peroxidation, and histologic damage involving edema, inflammatory infiltration, acinar vacuolization and necrosis (143).

Another study induced AP in rats using ethanol feeding and jugular vein infusion of CCK (50 ng/kg body weight/1 hr). Black tea extract, which contains apigenin, protected

the pancreas through the following mechanisms: reduction in autodigestive injury as evidenced by lower serum amylase/lipase levels, lipid peroxidation, and histologic severity scores; anti-inflammatory activity, reducing pro-inflammatory cytokines TNF-α and IL-6; and antioxidant activity, which was assessed by cytotoxic nitric oxide production, superoxide dismutase/catalase enzymatic function, and glutathione levels (144). Also of pertinence, the black tea extract reduced the degree of DNA fragmentation in pancreatic homogenate, reinforcing the reduction in acinar cell necrosis observed histologically (144). Thus, the chemical structure of flavonoids provides a strong basis for analog development.

Apigenin's known anti-proliferative and pro-apoptotic effects were beneficial to the control of PSC activity, thereby limiting the fibrotic response seen in the CR-induced RAP model. Apigenin significantly inhibited PSC proliferation and viability in a time- and dose-dependent fashion. Transformation of PSCs from a quiescent to activated state involves a physiologic increase in mitotic index (93, 145). The treatment of PSCs *in vitro* with green tea polyphenol epigallocatechin-3-gallate resulted in suppressed ethanol-mediated induction of α-SMA expression, collagen production, TGF-β excretion, and mitogenic p38 MAPK pathway activation measured by Western blot (146).

Within the oncologic literature, apigenin has been shown to exert its anti-proliferative activity by inducing reversible G2/M and G0/G1 cell-cycle arrest through the down-regulation of cyclin-dependent kinases and induction of p53 protein stability (108). Similarly, apigenin induced PSC apoptosis in a time- and dose-dependent fashion. Molecular mechanisms by which apigenin shifts activated cells toward programmed cell death include increasing the Bax/Bcl-2 ratio, which results in a release of cytochrome c, Apaf-1 induction, caspase-3 activation, and poly-ADP ribose polymerase (PARP)-cleavage (108).

In my *in vitro* PSC RT-PCR experiments, apigenin inhibited PTHrP-mediated increases in ECM production (collagen type 1α, FN), proliferation (PCNA), and generation of pro-inflammatory growth factor TGF-β and cytokines IL-6 and IL-8. Apigenin also reset the threshold for transcription of all endpoints except FN, which most likely was not captured in the 12-hr time frame. This provided indirect evidence of the importance of

PTHrP in autocrine and paracrine signaling. As described in the RAP model, the progression of pancreatitis involves the critical interaction between acinar cell injury and PSC response to it. By inhibition of PSC proliferation and induction of apoptosis, apigenin minimizes the pro-inflammatory, pro-fibrotic response to acinar cell injury, which is in part mediated through reduced responsiveness to PTHrP.

CHAPTER 4:

DEVELOPMENT AND TESTING OF APIGENIN ANALOGS

4.1 Introduction

Apigenin is a plant-derived compound ubiquitously found in many fruits, vegetables and beverages. The average American diet includes a daily flavanoid intake of 189.7 mg/d, of which 0.8% (≈ 1.5 mg/d) is derived from flavones like apigenin (147). As a class, flavones' clinical application as therapeutics agents is limited by their poor aqueous solubility, low oral bioavailability and metabolic stability. Apigenin lacks sugar moieties (aglycone), and its hydrophobicity permits its passive diffusion across intestinal membranes; greatest absorption has been noted in the duodenum (148). Flavonoids then bind to albumin within the portal circulation and are transported to the liver. Undergoing extensive Phase II hepatic metabolism, metabolites are generated through conjugation reactions with glucuronic acid and sulfate (149), which are primarily excreted in the urine (150). Early drug development involves modification of a lead compound's molecular structure to optimize its functionality. With regards to apigenin, rings A and C have been identified as potential targets for chemical modification (**Figure 15**) (151-153). Studies have shown that polymethoxylated flavones/derivatives with nonpolar groups attached to the A ring exhibited an enhanced antiproliferative effect on human cancer cell lines (154) and improved metabolic stability (155).

4.2 Materials and Methods

4.2.1 Materials

The majority of the materials have already been listed in **Section 3.2.1**. The C57BL/6 mice were purchased from Harlan Laboratories and The Jackson Laboratory. Apigenin analogs were synthesized and provided through collaboration with medicinal chemist, Dr. Jia Zhou. The chemistry-related materials for analog synthesis were described in detail elsewhere (111).

4.2.2 Methods

4.2.2.1 Generation of apigenin analogs

Apigenin analogs were designed and synthesized with the goal of improving upon the lead compound's unfavorable physiochemical properties. This was achieved by generating a "focused library of O-alkyl-amino-tethered apigenin derivatives at the 4'-O position of the ring" (111). Apigenin's chemical structure (4',5,7-trihydroflavone) was first modified by adding nonpolar alkyl groups at the 5' and 7' position of ring A (**Figure 15**). Through a series of additional synthetic reactions, the 4' position of ring C was altered to

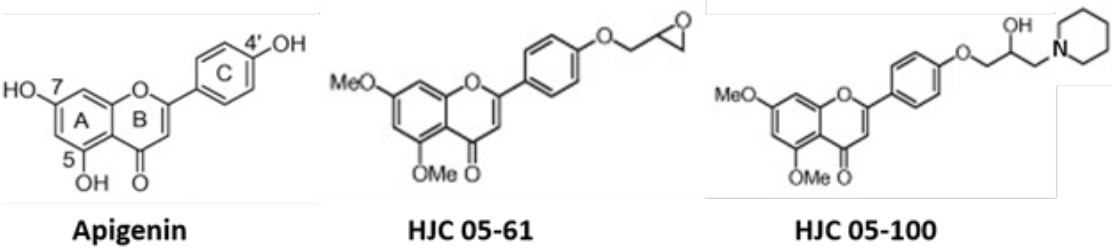

FIGURE 15. **Chemical structures of apigenin and analogs tested *in vitro* and *in vivo*.**

include an epoxide group (HJC 05-61) or terminal amino moiety (HJC 05-100) for improvement in aqueous solubility. The synthetic routes utilized to produce the two analogs have been described in detail by Chen *et al,* and all derivatives were refined to a purity >95% as determined by high performance liquid chromatography (HPLC) (111).

For each analog, traditional medicinal chemistry metrics were calculated to predict the compounds' drug-likeness, providing an estimate of property optimization beyond that of the lead structure. The calculated logarithm of the partition coefficient (cLogP) is a measure of lipophilicity, which is an important property drug absorption, distribution, metabolism and excretion. The topological polar surface area (tPSA) is the surface sum of

Compound	**Lipophilicity (cLogP)**	**Polarity (tPSA)**
Apigenin	2.33	90.9
HJC 05-61	2.50	70.4
HJC 05-100	3.03	81.4

TABLE 7. Prediction of molecular properties.
cLogP: http://146.107.217.178/lab/alogps/start.html.
tPSA: http://www.molinspiration.com/cgi-bin/properties. Reproduced with permission (111).

all of the polar atoms within the molecule. Both analogs had increased lipophilicity and reduced polarity (**Table 7**), which were compliant with Lipinski's 'Rule of 5' favorable drug-like properties. HPLC was also performed on selected derivatives to evaluate aqueous solubility. HJC 05-100 (in the form of hydrochloride salt) exhibited significantly improved solubility (84.1 mg/mL) compared to apigenin (2.16 μg/mL) (111).

4.2.2.2 Previously Described *In Vitro* Methods

The immortalized human PSC line that was previously established by our laboratory (**Section 3.2.2.4**) was utilized to test the biologic potency of the analogs *in vitro*. The alamarBlue assay was performed as before (**Section 3.2.2.5)** and used to complete preliminary screening of the multiple analogs synthesized. Two promising apigenin analogs, designated HJC 05-61 and HJC 05-100, were selected for additional testing, and their dose-response were characterized using the cell viability and apoptosis assays (**Section 3.2.2.6**) (111).

4.2.2.3 RAP Mouse Model and Image Analysis

Apigenin and the analogs HJC 05-100 and HJC 05-61 were tested *in vivo* using the preclinical mouse model of RAP, which has been outlined in **Section 3.2.2.1**. Briefly, RAP was induced by serial CR injections as before. After the first week of RAP, treatment with apigenin and the 2 analogs was initiated at a much lower dose of 10 μg/mouse (≈ 0.5 mg/kg) and continued for the remaining 3 wk of the experiment (**Figure 16**). At termination, the

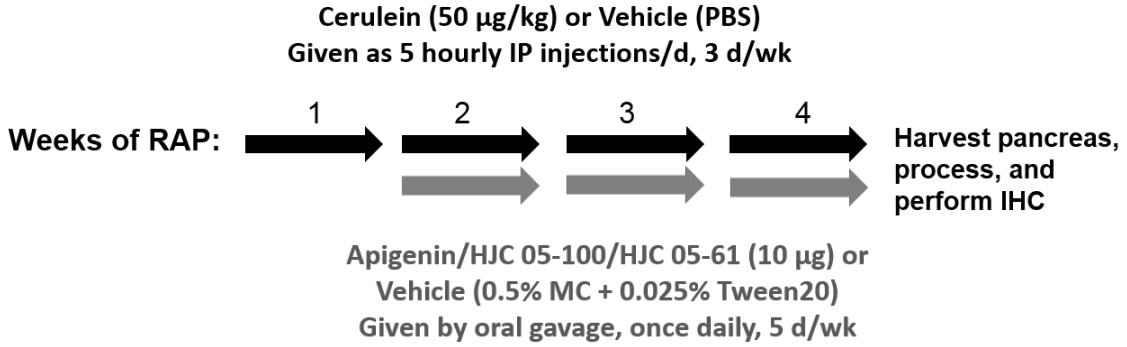

FIGURE 16. Diagram of RAP mouse model for proof-of-concept testing.

mice were sacrificed, pancreata harvested, processed and stained for FN using the immunohistochemical methods described in **Section 3.2.2.2**. Five representative, non-

overlapping 400x images of each pancreas were taken with the Olympus BX51 microscope coupled to a DP71 Olympus digital camera. The images were analyzed using the ImageJ color deconvolution program (140), and the percent area of FN staining was determined (111).

4.2.2.4 Statistical Analysis

Using the cell viability and apoptosis assay data, best-fit curves were generated through logarithmic transformation and nonlinear regression. This allowed determination of the analogs' IC_{50} and EC_{50} relative to that of apigenin. The IHC data was analyzed with two-way ANOVA and post hoc Tukey-Kramer multiple comparisons test. Statistical significance was set at $p < 0.05$, and the data was graphed as the mean value ± SEM.

4.3 Results

4.3.1 Apigenin analogs were screened using the alamarBlue assay.

Drs. Zhou and Chen synthesized more than 30 apigenin analogs that needed to be screened for increased potency relative to apigenin. The alamarBlue cell viability test was used to accomplish this task, and selected concentrations of 5, 10, and 20 µM were analyzed. Viable cells maintained a reducing environment and were able to convert the permeable, non-fluorescent dye to a red, highly fluorescent product. Fluorescence intensity was then measured, which was directly proportional to the number of viable PSCs. As an

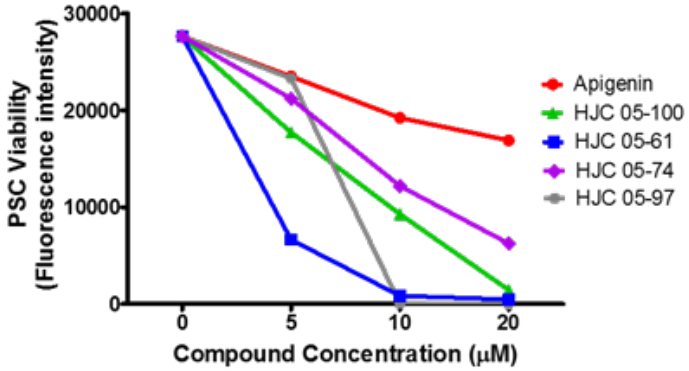

FIGURE 17. **Screening of apigenin analogs with the alamarBlue cell viability assay.** PSCs were treated with apigenin or analogs over a range of doses (0-20 µM) for 48 hr. The different apigenin analogs were designated by HJC 05-#. PSC viability was assessed was measured using the alamarBlue assay.

example, the results from one screening assay were provided in **Figure 17**. The analogs tested inhibited PSC viability at lower concentrations than apigenin. Analog HJC 05-61 appeared to be the most potent in the screen, reducing viability drastically by 10 µM.

4.3.2 Apigenin analogs HJC 05-61 and HJC 05-100 were more potent at reducing PSC viability.

The alamarBlue assay was employed again to fully characterize the dose-response of apigenin analogs HJC 05-61 and HJC 05-100. PSCs were treated with increasing doses of apigenin/analog (0-50 µM) for 48 hr. Both analogs inhibited PSC viability at lower concentrations than apigenin (**Figure 18A**). Best-fit curves were determined by graphing fluorescent output versus the log of compound concentrations and performing nonlinear regression (**Figure 18B**). The analogs' increased potency in reducing PSC viability was reflected in their lower IC_{50} values when compared to apigenin: HJC 05-100 (8.0 ± 1.8 µM) and HJC 05-61 (2.5 ± 0.6 µM) versus apigenin (18.6 ± 1.6 µM) (111, 119).

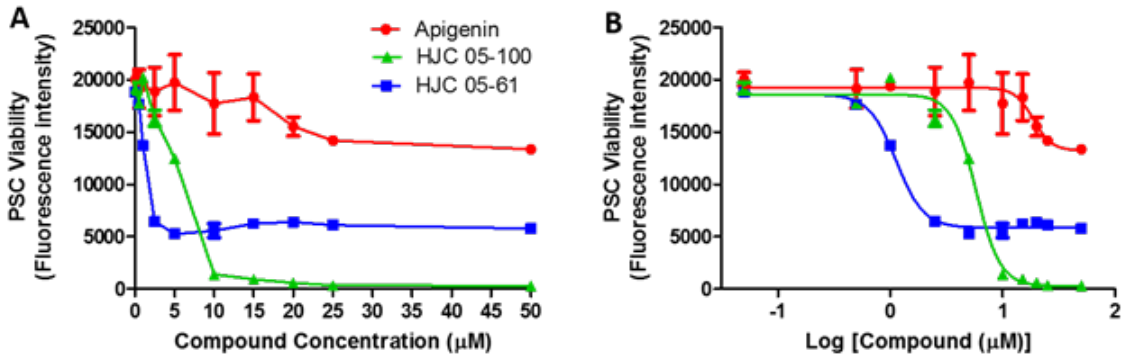

FIGURE 18. Analogs HJC 05-61 and HJC 05-100 were more potent than apigenin at inhibiting PSC viability.
A) PSCs were treated with escalating doses of apigenin, analog HJC 05-100, and analog HJC 05-61 for 24 hr. PSC viability was measured using the alamarBlue assay, from which the dose-response curves were generated. The graph represented a single assay. B) Transformation of the compound concentrations to a logarithmic scale and nonlinear regression enabled generation of a best-fit curve. The IC_{50} of apigenin, HJC 05-100, and HJC 05-61 were 18.6 ± 1.6 µM, 8.0 ± 1.8 µM, and 2.5 ± 0.6 µM, respectively. The IC_{50} were reported as the mean ± SEM and derived from at least 3 independent assays. Reproduced with permission (111).

4.3.3 Analog HJC 05-61 was more potent at inducing PSC apoptosis.

The Cell Death ELISA^{PLUS} was utilized to quantify the degree or programmed cell death. This was proportional to the assay's endpoint of absorbance (**Figure 19A**). HJC 05-61 was more potent than apigenin, inducing PSC apoptosis at much lower concentrations. HJC 05-100 induced minimal cell death at low concentrations, and between 25-35 µM, a steep dose-response was observed followed by significant cell death at higher concentrations. SPSS was employed to generate a best-fit curve for the data in **Figure 19B**, and the EC_{50} values were determined from 2 independent assays: HJC 05-100 (9.6 ± 1.8 µM), apigenin (24.5 ± 2.5 µM) and HJC 05-100 (35.2 ± 5.5 µM) (111, 119).

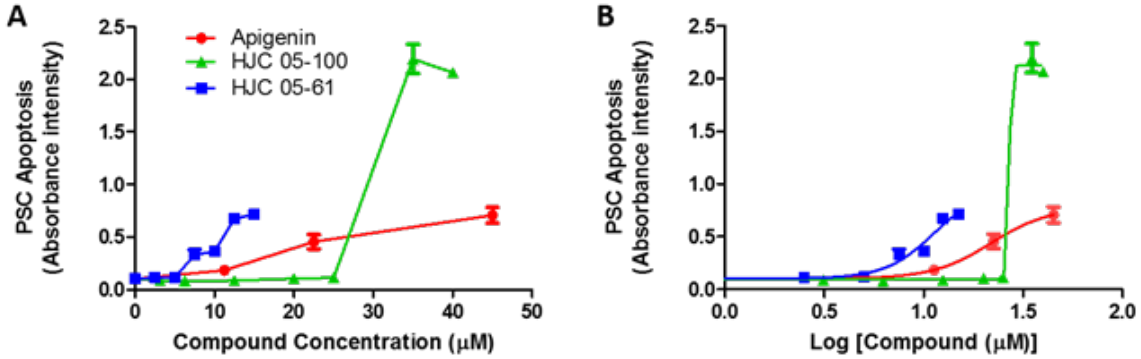

FIGURE 19. **Analog HJC 05-61 was more potent than apigenin at inducing PSC apoptosis.** A) PSCs were treated with increasing doses of apigenin, analog HJC 05-100, and analog HJC 05-61 for 14 hr. PSC apoptosis was measured using the Cell Death ELISA^{PLUS} assay, and the graph depicted the results of a single assay. B) Logarithmic transformation of the compound concentrations and nonlinear regression enabled generation of best-fit curves. The EC_{50} of apigenin (24.5 ± 2.5 µM), HJC 05-100 (35.2 ± 5.5 µM), and HJC 05-61 (9.6 ± 1.8 µM) were determined from 2 independent assays. Reproduced with permission (111).

4.3.4 Apigenin and analogs reduced fibrosis in a preclinical mouse model of RAP.

The next step involved testing the analogs *in vivo* using the CR-induced RAP model. For this experiment, each group consisted of 5-6 mice. The control groups consisted of IP injections of PBS, which was the vehicle for CR. Pancreatitis was induced 1 wk prior to initiation of treatment with apigenin, HJC 05-100, HJC 05-61 or vehicle (0.5% MC + 0.025% Tween20 in MQ water). This experiment differed from previous RAP studies in that 1/5 the dose (10 µg ≈ 0.5 mg/kg) of apigenin and analogs was administered by oral gavage, once daily, 5 d/wk. The fibrotic response to pancreatic injury was evaluated

through immunohistochemical staining for FN. Normal pancreatic architecture was noted in all of the PBS controls (images not shown). Secretagogue induced pancreatitis produced heterogenous, atrophic acini, periacinar and perilobular fibrosis and edema (**Figure 20A**). Both apigenin and the analogs decreased the degree of fibrosis while helping preserve acini at the low dose of 0.5 mg/kg (**Figure 20B-D**). At the low dose of 0.5 mg/kg, apigenin-like structures were as effective as the apigenin in reducing the percent area of FN staining ($p < 0.001$) (**Figure 20E**) (111).

4.4 Discussion

The *in vitro* and *in vivo* results presented in this dissertation provide several mechanisms and disease targets of apigenin that support its preclinical development as a pharmacologic agent in the treatment of RAP, thereby limiting the progression to CP. However, as a lead compound, apigenin's favorable biological activity is diminished by its unsatisfactory 'druggability' profile. Its low oral bioavailability and poor metabolic stability are reinforced by the fact that apigenin is ubiquitous in our diets yet fails to reach potent therapeutic levels. Thus, drug design was aimed at optimizing these shortcomings to facilitate the transition of apigenin-like compounds from bench to bedside.

Collaboration with a medicinal chemist enabled the generation of analogs based on apigenin's chemical structure with improved druglikeness. The compounds' aqueous solubility were augmented through the reduction of the compound's polar surface area and increase in its lipophilicity, achieved by reducing the number of hydrogen-bond donors and acceptors. Improvement in potency required functional biologic testing. This was accomplished by using the *in vitro* alamarBlue assay to screen for improved inhibition of PSC viability at lower doses than that of apigenin. Selected anti-proliferative and pro-apoptotic effects of apigenin derivatives on PSC activity was characterized by determination of their IC_{50} and EC_{50}. From the dose-response curves, HJC 05-61 was consistently more potent than apigenin at regulating PSC activity. HJC 05-100 exhibited

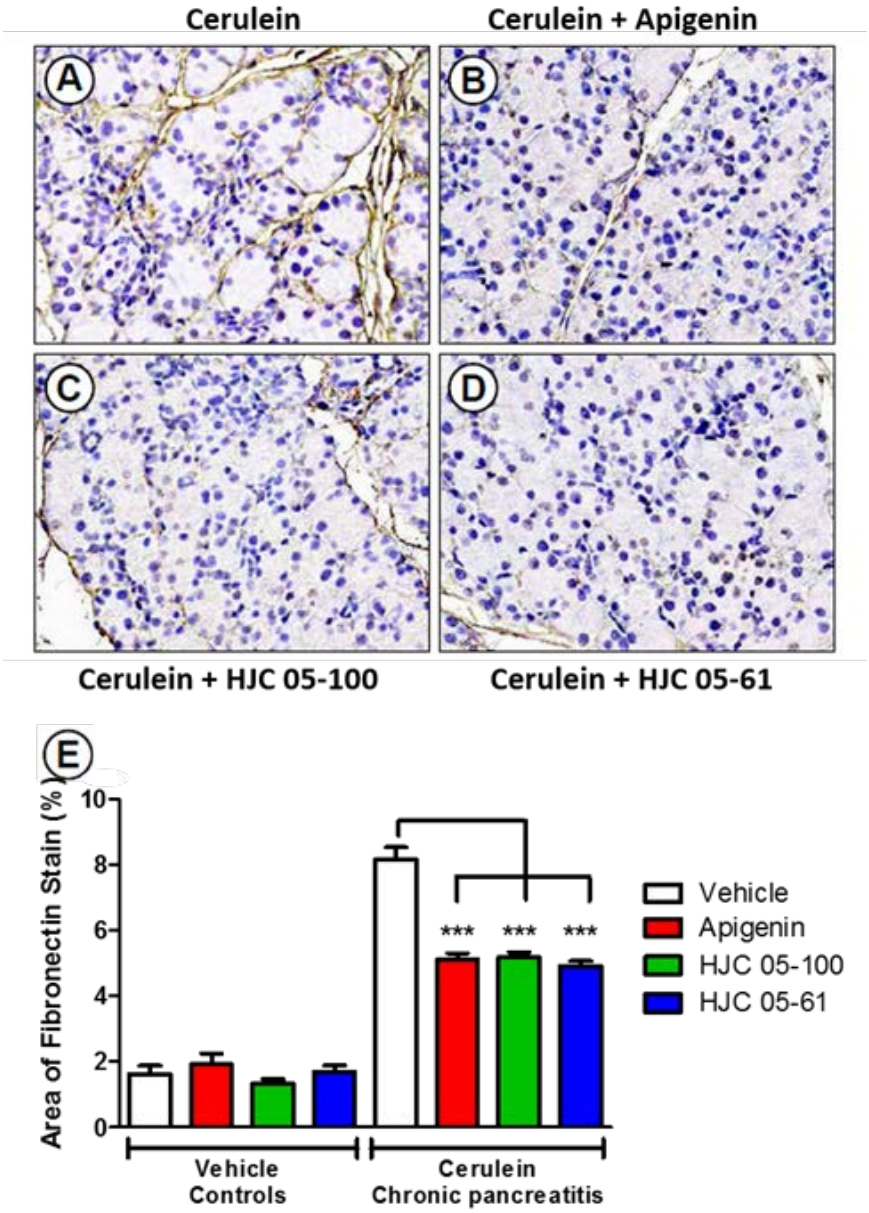

FIGURE 20. **Apigenin and analogs reduced stromal fibrosis during RAP *in vivo*.**
Mouse pancreatic tissue was stained for FN by DAB-IHC and counter-stained with hematoxylin. Representative sections from the RAP groups were imaged at 400x with automated brightness/contrast adjustment in ImageJ (A-D). The vehicle for CR was PBS, and the vehicle for apigenin/analogs was 0.5% MC + 0.025% Tween20. Control groups displayed normal pancreatic architecture (not shown). Apigenin and the analogs were given at the low dose of 0.5 mg/kg. RAP was induced in the following groups A) CR (+ vehicle); B) CR + apigenin; C) CR + HJC 05-100; and D) CR + HJC 05-61. The percent area of brown FN staining was quantified in ImageJ and graphed as mean ± SEM in E). A p-value < 0.001 was indicated as ***. There was no significant difference between apigenin and the analogs. Reproduced with permission (111).

more potent anti-proliferative activity but induced PSC apoptosis over a narrow therapeutic window of 25-35 μM. Chemical modification of attaching an amino group to the 4' C ring of apigenin's structure most likely altered the mechanism by which apoptosis was activated.

A proof-of-concept study was completed, testing apigenin and analogs HJC 05-100 and HJC 05-61 in the CR-induced RAP rodent model. The compounds were administered at a lower dose (0.5 mg/kg) compared to what was tested in the previous RAP experiments (2.5 mg/kg). Although this study design did not facilitate determination of the analogs' potency *in vivo*, it did demonstrate that the analogs were as effective as apigenin in protecting the pancreas from recurrent injury. FN staining was significantly reduced by the apigenin-like compounds accompanied by histologic preservation of acinar units and pancreatic architecture. Thus, optimization of apigenin's chemical structure and drug-like properties was executed.

CHAPTER 5:

CONCLUSIONS AND FUTURE DIRECTIONS

5.1 Conclusions

Apigenin and apigenin-like compounds have been developed as pharmacologic agents for the treatment of RAP. Apigenin treatment induces a protective pancreatic phenotype by inhibiting pro-inflammatory and pro-fibrotic mediators involved in the physiologic response to repeated pancreatic injury. The current working model by which apigenin inhibits (-) signaling pathways and molecular targets is provided in **Figure 21**.

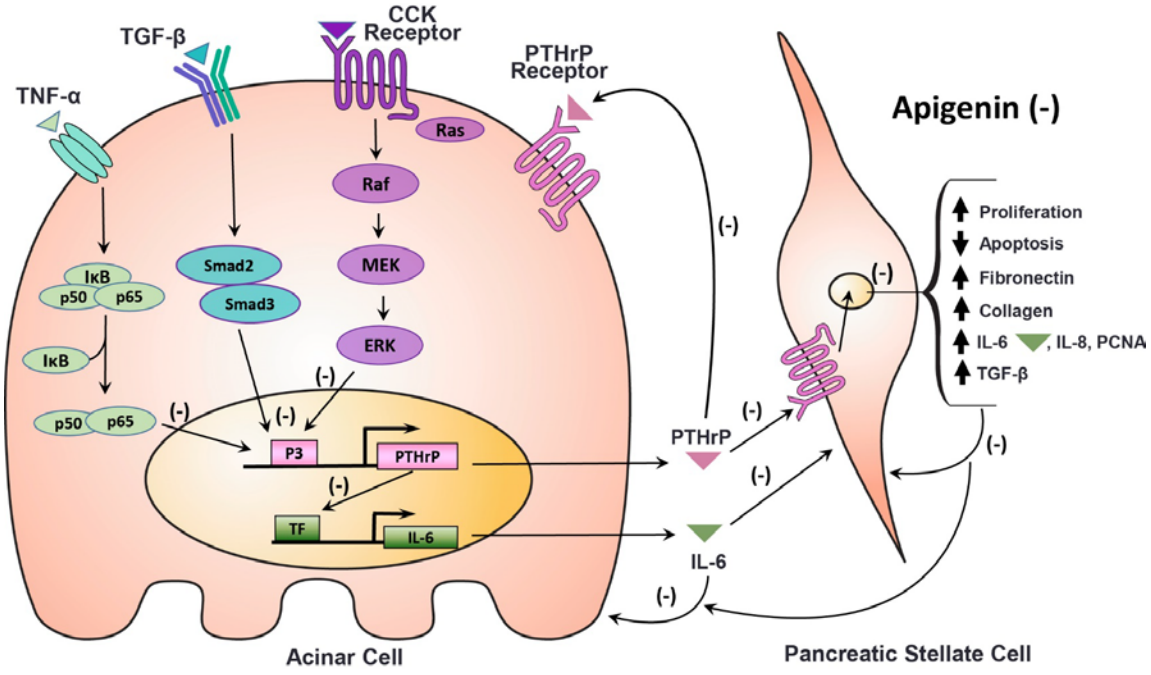

Figure 21. Schematic of apigenin's mechanisms of action in acini and PSCs.
The (-) icon indicates down-regulation by apigenin.

Experimental activation of acinar cell secretory pathways was induced by multiple stimuli including TNF-α, TGF-β, and CR, a CCK analog. Binding of ligand to its appropriate receptor activated the NF-κB, SMAD, and the MAPK/ERK signaling pathways, respectively. A point of convergence of these pathways involves transcriptional regulation of the P3 promoter for PTHrP. Apigenin was shown to inhibit TNF-α induced p65 nuclear translocation, reduce TGF-β stimulation of P3 promoter activity, and limit CR-induced pERK nuclear localization, which was indicative of decreased MAPK pathway activation. Given the limited time and dose evaluated, the Western blot data did not support apigenin's regulation of ERK phosphorylation, but this result is viewed with skepticism

due to the large variation in results between experimental replicates. Apigenin treatment of primary acini isolated from wild-type and PTHrP knockout mice illustrated how the decrease in IL-6 mRNA levels occurred via a PTHrP-dependent mechanism.

Rather than limiting my drug development investigation to a single cell type, a holistic approach was taken to evaluate and identify mechanisms involved in the preservation of pancreatic architecture and limitation of pathogenic response to RAP. Even though acinar cell injury leads to the secretion of pro-inflammatory and pro-fibrotic mediators like PTHrP and IL-6, it is the perpetual activation of dysregulated PSC activity that amplifies and contributes to pathologic disease progression from RAP to CP. Apigenin significantly reduced stromal fibrosis in our CR-induced mouse model of RAP. *In vitro* studies revealed that this related to the inhibition of PSC viability and induction of PSC apoptosis in a time- and dose-dependent manner. This was, in part, due to apigenin inhibiting a PTHrP-mediated transcriptional response in PSCs. Apigenin reduced mRNA levels of ECM proteins collagen type 1α1 and FN, PCNA, and cytokines TGF-β1, IL-6, and IL-8. Furthermore, apigenin appeared to reset the basal threshold for transcriptional response to PTHrP, significantly lowering basal mRNA levels of all of the aforementioned endpoints except FN, whose late phase expression was most likely not captured at the 12-hr time point. Reduced transcription translates into a reduced production of pro-inflammatory and pro-fibrotic mediators that stimulate acini and PSCs in autocrine and paracrine fashion.

Apigenin analogs with improved aqueous solubility and lipophilicity were designed, synthesized, and screened for increased biologic potency. HJC 05-100 and HJC 05-61 were characterized by the generation of dose-response curves. HJC 05-61 was found to be more potent than apigenin *in vitro*, inhibiting PSC viability and inducing apoptosis at lower doses than apigenin. HJC 05-100 induced significant apoptosis over a narrow index of concentrations, and this was interpreted as structural modification resulting in differences in apoptotic pathway activation. At the low dose of 0.5 mg/kg, apigenin and the analogs effectively reduced pancreatic fibrosis during RAP, demonstrating a proof-of concept. Additional *in vivo* studies are needed to determine the potency of each analog.

5.2 Future Directions

Immediate drug discovery efforts should be directed at the optimization of apigenin analogs' absorption, distribution, metabolism, elimination, and toxicity (ADME/Tox) profiles. For example, intestinal absorption can be estimated using the cell-based Caco-2 permeability model, where the chemical compound diffuses (by concentration gradient) from the apical chamber, through a confluent layer of Caco-2 cells attached to a semipermeable membrane, and into the basolateral chamber (156). Apigenin has been shown to undergo extensive Phase II metabolism, thereby limiting its metabolic stability and bioavailability. Therefore, drug design and biologic testing of analogs using liver microsomes and hepatocytes should continue concurrently. *In vivo* pharmacokinetic studies will need to be completed in both rodent and non-rodent animals to account for inter-species variation (157). Successful testing will lead to the linear progression of pharmacodynamic studies, mechanism-based disease modeling, and Phase I clinical trials.

Patients at risk for RAP and progression to CP will most likely benefit from apigenin analog therapy. Clinicians are aware that this is difficult to predict, but cues from epidemiological studies, the etiology of pancreatitis, characteristics of disease pathogenesis, and lifestyle factors can aide in clinical decision making. For example, a patient likely to have recurrence of pancreatitis would be an African American male with a past medical history of hereditary pancreatitis, family history of pancreatitis, and a social history positive for drinking 2-4 beers daily, smoking, and a diet consisting of meat and potatoes. A retrospective study with a median follow-up of 4.6 years found that patients with a severe sentinel event of AP, smokers, and alcoholics had a significant risk for recurrent pancreatitis and progression to CP (158).

In conclusion, the preclinical testing of apigenin and analogs has shown promise as pharmacologic agents in the treatment of RAP. Additional mechanistic knowledge gained from the study of PTHrP-mediated inflammation and fibrosis in acinar and PSCs will provide more targets for drug design and analog optimization.

REFERENCES

1. Steer MR. Exocrine pancreas. In: Townsend CM, Jr., Beauchamp RD, Evers BM, Mattox KL, editors. Sabiston textbook of surgery: the biological basis of modern surgical practice. 18th ed. PA: Saunders Elsevier; 2008. p. 1589-1623.

2. Vickers SM, Arnoletti JP, Brunicardi FC. Pancreas anatomy and physiology. In: Mulholland MW, Lillemoe KD, Doherty GM, Maier RV, Upchurch GR, Jr., editors. Greenfield's surgery: scientific principle and practice. 4th ed. PA: Lippincot Williams & Wilkins; 2006. p. 820-839.

3. Thompson JC, Townsend CM, Jr. Endocrine pancreas. In: Townsend CM, Jr., Beauchamp RD, Evers BM, Mattox KL, editors. Sabiston textbook of surgery: the biological basis of modern surgical practice. 18th ed. PA: Saunders Elsevier; 2008. p. 976-996.

4. Rovery M. Limited proteolyses in pancreatic chymotrypsinogens and trypsinogens. *Biochimie* 1988;70(9):1131-1135.

5. Gorry MC, Gabbaizedeh D, Furey W, Gates LK, Jr., Preston RA, Aston CE, Zhang Y, Ulrich C, Ehrlich GD, Whitcomb DC. Mutations in the cationic trypsinogen gene are associated with recurrent acute and chronic pancreatitis. *Gastroenterology* 1997;113(4):1063-1068.

6. Whitcomb DC, Gorry MC, Preston RA, Furey W, Sossenheimer MJ, Ulrich CD, Martin SP, Gates LK, Jr., Amann ST, Toskes PP, Liddle R, McGrath K, Uomo G, Post JC, Ehrlich GD. Hereditary pancreatitis is caused by a mutation in the cationic trypsinogen gene. *Nature Genetics* 1996;14(2):141-145.

7. Saluja AK, Lerch MM, Phillips PA, Dudeja V. Why does pancreatic overstimulation cause pancreatitis? *Annual Review of Physiology* 2007;69249-269.

8. Dufresne M, Seva C, Fourmy D. Cholecystokinin and gastrin receptors. *Physiological Reviews* 2006;86(3):805-847.

9. Petersen OH. Calcium signalling and secretory epithelia. *Cell Calcium* 2014;55(6):282-289.

10. Petersen OH. Specific mitochondrial functions in separate sub-cellular domains of pancreatic acinar cells. *Pflugers Archiv European Journal of Physiology (Berlin)* 2012;464(1):77-87.

11. Lee M, Chung S, Uhm DY, Park MK. Regulation of zymogen granule exocytosis by Ca2+, cAMP, and PKC in pancreatic acinar cells. *Biochemical and Biophysical Research Communications* 2005;334(4):1241-1247.

12. Sans MD, Xie Q, Williams JA. Regulation of translation elongation and phosphorylation of eEF2 in rat pancreatic acini. *Biochemical and Biophysical Research Communications* 2004;319(1):144-151.

13. Namkung W, Yoon JS, Kim KH, Lee MG. PAR2 exerts local protection against acute pancreatitis via modulation of MAP kinase and MAP kinase phosphatase signaling. *American Journal of Physiology: Gastrointestinal and Liver Physiology* 2008;295(5):G886-894.

14. Hietaranta AJ, Saluja AK, Bhagat L, Singh VP, Song AM, Steer ML. Relationship between NF-kappaB and trypsinogen activation in rat pancreas after supramaximal caerulein stimulation. *Biochemical and Biophysical Research Communications* 2001;280(1):388-395.

15. Han B, Ji B, Logsdon CD. CCK independently activates intracellular trypsinogen and NF-kappaB in rat pancreatic acinar cells. *American Journal of Physiology: Cell Physiology* 2001;280(3):C465-472.

16. Sah RP, Dawra RK, Saluja AK. New insights into the pathogenesis of pancreatitis. *Current Opinions in Gastroenterology* 2013;29(5):523-530.

17. Lupia E, Pigozzi L, Goffi A, Hirsch E, Montrucchio G. Role of phosphoinositide 3-kinase in the pathogenesis of acute pancreatitis. *World Journal of Gastroenterology* 2014;20(41):15190-15199.

18. Singh VP, Saluja AK, Bhagat L, van Acker GJ, Song AM, Soltoff SP, Cantley LC, Steer ML. Phosphatidylinositol 3-kinase-dependent activation of trypsinogen modulates the severity of acute pancreatitis. *Journal of Clinical Investigations* 2001;108(9):1387-1395.

19. Dabrowski A. Exocrine pancreas; molecular basis for intracellular signaling, damage and protection--Polish experience. *Journal of Physiology & Pharmacology* 2003;54 Suppl 3167-181.

20. Witt H, Apte MV, Keim V, Wilson JS. Chronic pancreatitis: challenges and advances in pathogenesis, genetics, diagnosis, and therapy. *Gastroenterology* 2007;132(4):1557-1573.

21. Lowenfels AB, Maisonneuve P, Cavallini G, Ammann RW, Lankisch PG, Andersen JR, Dimagno EP, Andren-Sandberg A, Domellof L. Pancreatitis and the risk of pancreatic cancer. International Pancreatitis Study Group. *New England Journal of Medicine* 1993;328(20):1433-1437.

22. Forsmark CE. Management of chronic pancreatitis. *Gastroenterology* 2013;144(6):1282-1291 e1283.

23. Braganza JM, Lee SH, McCloy RF, McMahon MJ. Chronic pancreatitis. *Lancet* 2011;377(9772):1184-1197.

24. Etemad B, Whitcomb DC. Chronic pancreatitis: diagnosis, classification, and new genetic developments. *Gastroenterology* 2001;120(3):682-707.

25. Aimoto T, Uchida E, Nakamura Y, Yamahatsu K, Matsushita A, Katsuno A, Cho K, Kawamoto M. Current surgical treatment for chronic pancreatitis. *Journal of Nippon Medical School = Nihon Ika Daigaku Zasshi* 2011;78(6):352-359.

26. Conwell DL, Lee LS, Yadav D, Longnecker DS, Miller FH, Mortele KJ, Levy MJ, Kwon R, Lieb JG, Stevens T, Toskes PP, Gardner TB, Gelrud A, Wu BU, Forsmark CE, Vege SS. American Pancreatic Association practice guidelines in chronic pancreatitis: evidence-based report on diagnostic guidelines. *Pancreas* 2014;43(8):1143-1162.

27. Everhart JE, Ruhl CE. Burden of digestive diseases in the United States part I: overall and upper gastrointestinal diseases. *Gastroenterology* 2009;136(2):376-386.

28. Wehler M, Nichterlein R, Fischer B, Farnbacher M, Reulbach U, Hahn E, Schneider T. Factors associated with health-related quality of life in chronic pancreatitis. *The American Journal of Gastroenterology* 2003;Sect. 138-146.

29. Schneider A, Lohr JM, Singer MV. The M-ANNHEIM classification of chronic pancreatitis: introduction of a unifying classification system based on a review of previous classifications of the disease. *Journal of Gastroenterology* 2007;42(2):101-119.

30. Dufour MC, Adamson MD. The epidemiology of alcohol-induced pancreatitis. *Pancreas* 2003;27(4):286-290.

31. Schneider A, Whitcomb DC. Hereditary pancreatitis: a model for inflammatory diseases of the pancreas. *Best Practice and Research-Clinical Gastroenterology* 2002;16(3):347-363.

32. Peery AF, Dellon ES, Lund J, Crockett SD, McGowan CE, Bulsiewicz WJ, Gangarosa LM, Thiny MT, Stizenberg K, Morgan DR, Ringel Y, Kim HP, Dibonaventura MD, Carroll CF, Allen JK, Cook SF, Sandler RS, Kappelman MD, Shaheen NJ. Burden of gastrointestinal disease in the United States: 2012 update. *Gastroenterology* 2012;143(5):1179-1187 e1171-1173.

33. Bordalo O, Goncalves D, Noronha M, Cristina ML, Salgadinho A, Dreiling DA. Newer concept for the pathogenesis of chronic alcoholic pancreatitis. *American Journal of Gastroenterology* 1977;68(3):278-285.

34. Haber PS, Apte MV, Applegate TL, Norton ID, Korsten MA, Pirola RC, Wilson JS. Metabolism of ethanol by rat pancreatic acinar cells. *Journal of Laboratory & Clinical Medicine* 1998;132(4):294-302.

35. Bhopale KK, Falzon M, Ansari GA, Kaphalia BS. Alcohol oxidizing enzymes and ethanol-induced cytotoxicity in rat pancreatic acinar AR42J cells. *In Vitro Cellular & Developmental Biology Animal* 2014;50(4):373-380.

36. Werner J, Laposata M, Fernandez-del Castillo C, Saghir M, Iozzo RV, Lewandrowski KB, Warshaw AL. Pancreatic injury in rats induced by fatty acid ethyl ester, a nonoxidative metabolite of alcohol. *Gastroenterology* 1997;113(1):286-294.

37. Camello-Almaraz MC, Pozo MJ, Murphy MP, Camello PJ. Mitochondrial production of oxidants is necessary for physiological calcium oscillations. *Journal of Cellular Physiology* 2006;206(2):487-494.

38. Bhardwaj P, Yadav RK. Chronic pancreatitis: role of oxidative stress and antioxidants. *Free Radical Research* 2013;47(11):941-949.

39. Braganza JM, Wickens DG, Cawood P, Dormandy TL. Lipid-peroxidation (free-radical-oxidation) products in bile from patients with pancreatic disease. *Lancet* 1983;2(8346):375-379.

40. Guyan PM, Uden S, Braganza JM. Heightened free radical activity in pancreatitis. *Free Radical Biology & Medicine* 1990;8(4):347-354.

41. Norton ID, Apte MV, Lux O, Haber PS, Pirola RC, Wilson JS. Chronic ethanol administration causes oxidative stress in the rat pancreas. *Journal of Laboratory & Clinical Medicine* 1998;131(5):442-446.

42. Morris-Stiff GJ, Bowrey DJ, Oleesky D, Davies M, Clark GW, Puntis MC. The antioxidant profiles of patients with recurrent acute and chronic pancreatitis. *American Journal of Gastroenterology* 1999;94(8):2135-2140.

43. Siriwardena AK, Mason JM, Sheen AJ, Makin AJ, Shah NS. Antioxidant therapy does not reduce pain in patients with chronic pancreatitis: the ANTICIPATE study. *Gastroenterology* 2012;143(3):655-663 e651.

44. Perez S, Pereda J, Sabater L, Sastre J. Redox signaling in acute pancreatitis. *Redox Biology* 2015;51-14.

45. Siriwardena AK. Reappraisal of xenobiotic-induced, oxidative stress-mediated cellular injury in chronic pancreatitis: a systematic review. *World Journal of Gastroenterology* 2014;20(11):3033-3043.

46. Sahel J, Sarles H. Modifications of pure human pancreatic juice induced by chronic alcohol consumption. *Digestive Diseases and Sciences* 1979;24(12):897-905.

47. Sarles H, Bernard JP, Johnson C. Pathogenesis and epidemiology of chronic pancreatitis. *Annual Review of Medicine* 1989;40453-468.

48. Guy O, Robles-Diaz G, Adrich Z, Sahel J, Sarles H. Protein content of precipitates present in pancreatic juice of alcoholic subjects and patients with chronic calcifying pancreatitis. *Gastroenterology* 1983;84(1):102-107.

49. De Caro A, Multigner L, Dagorn JC, Sarles H. The human pancreatic stone protein. *Biochimie* 1988;70(9):1209-1214.

50. Graf R, Schiesser M, Scheele GA, Marquardt K, Frick TW, Ammann RW, Bimmler D. A family of 16-kDa pancreatic secretory stress proteins form highly organized fibrillar structures upon tryptic activation. *Journal of Biological Chemistry* 2001;276(24):21028-21038.

51. Schiesser M, Bimmler D, Frick TW, Graf R. Conformational changes of pancreatitis-associated protein (PAP) activated by trypsin lead to insoluble protein aggregates. *Pancreas* 2001;22(2):186-192.

52. Kloppel G. Chronic pancreatitis, pseudotumors and other tumor-like lesions. *Modern Pathology* 2007;20 Suppl 1S113-131.

53. Kloppel G, Maillet B. Pathology of acute and chronic pancreatitis. *Pancreas* 1993;8(6):659-670.

54. Ammann RW, Muellhaupt B. Progression of alcoholic acute to chronic pancreatitis. *Gut* 1994;35(4):552-556.

55. Ammann RW, Heitz PU, Kloppel G. Course of alcoholic chronic pancreatitis: a prospective clinicomorphological long-term study. *Gastroenterology* 1996;111(1):224-231.

56. Kloppel G, Maillet B. Pseudocysts in chronic pancreatitis: a morphological analysis of 57 resection specimens and 9 autopsy pancreata. *Pancreas* 1991;6(3):266-274.

57. Whitcomb DC. Genetic polymorphisms in alcoholic pancreatitis. *Digestive Diseases* 2005;23(3-4):247-254.

58. Masamune A, Watanabe T, Kikuta K, Shimosegawa T. Roles of pancreatic stellate cells in pancreatic inflammation and fibrosis. *Clinical Gastroenterology and Hepatology* 2009;7(11 Suppl):S48-54.

59. Whitcomb DC. Hereditary pancreatitis: new insights into acute and chronic pancreatitis. *Gut* 1999;45(3):317-322.

60. Comfort MW, Gambill EE, Baggenstoss AH. Chronic relapsing pancreatitis; a study of 29 cases without associated disease of the biliary or gastrointestinal tract. *Gastroenterology* 1946;6376-408.

61. Witt H, Luck W, Hennies HC, Classen M, Kage A, Lass U, Landt O, Becker M. Mutations in the gene encoding the serine protease inhibitor, Kazal type 1 are associated with chronic pancreatitis. *Nature Genetics* 2000;25(2):213-216.

62. Cohn JA. Reduced CFTR function and the pathobiology of idiopathic pancreatitis. *Journal of Clinical Gastroenterology* 2005;39(4 Suppl 2):S70-77.

63. Stevens T, Conwell DL, Zuccaro G. Pathogenesis of chronic pancreatitis: an evidence-based review of past theories and recent developments. *American Journal of Gastroenterology* 2004;99(11):2256-2270.

64. Ohmuraya M, Hirota M, Araki M, Mizushima N, Matsui M, Mizumoto T, Haruna K, Kume S, Takeya M, Ogawa M, Araki K, Yamamura K. Autophagic cell death of pancreatic acinar cells in serine protease inhibitor Kazal type 3-deficient mice. *Gastroenterology* 2005;129(2):696-705.

65. Sutton R, Criddle D, Raraty MG, Tepikin A, Neoptolemos JP, Petersen OH. Signal transduction, calcium and acute pancreatitis. *Pancreatology* 2003;3(6):497-505.

66. Ward JB, Sutton R, Jenkins SA, Petersen OH. Progressive disruption of acinar cell calcium signaling is an early feature of cerulein-induced pancreatitis in mice. *Gastroenterology* 1996;111(2):481-491.

67. Raraty M, Ward J, Erdemli G, Vaillant C, Neoptolemos JP, Sutton R, Petersen OH. Calcium-dependent enzyme activation and vacuole formation in the apical granular region of pancreatic acinar cells. *Proceedings of the National Academy of Sciences of the United States of America* 2000;97(24):13126-13131.

68. Maleth J, Rakonczay Z, Jr., Venglovecz V, Dolman NJ, Hegyi P. Central role of mitochondrial injury in the pathogenesis of acute pancreatitis. *Acta Physiologica* 2013;207(2):226-235.

69. Odinokova IV, Sung KF, Mareninova OA, Hermann K, Evtodienko Y, Andreyev A, Gukovsky I, Gukovskaya AS. Mechanisms regulating cytochrome c release in pancreatic mitochondria. *Gut* 2009;58(3):431-442.

70. Kubisch CH, Sans MD, Arumugam T, Ernst SA, Williams JA, Logsdon CD. Early activation of endoplasmic reticulum stress is associated with arginine-induced acute pancreatitis. *American Journal of Physiology: Gastrointestinal & Liver Physiology* 2006;291(2):G238-245.

71. Kubisch CH, Logsdon CD. Secretagogues differentially activate endoplasmic reticulum stress responses in pancreatic acinar cells. *American Journal of Physiology: Gastrointestinal & Liver Physiology* 2007;292(6):G1804-1812.

72. Sah RP, Garg SK, Dixit AK, Dudeja V, Dawra RK, Saluja AK. Endoplasmic reticulum stress is chronically activated in chronic pancreatitis. *Journal of Biological Chemistry* 2014;289(40):27551-27561.

73. Lampel M, Kern HF. Acute interstitial pancreatitis in the rat induced by excessive doses of a pancreatic secretagogue. *Virchows Archive A: Pathological Anatomy and Histopathology* 1977;37397-117.

74. O'Konski MS, Pandol SJ. Effects of caerulein on the apical cytoskeleton of the pancreatic acinar cell. *Journal of Clinical Investigation* 1990;86(5):1649-1657.

75. Saluja A, Hashimoto S, Saluja M, Powers RE, Meldolesi J, Steer ML. Subcellular redistribution of lysosomal enzymes during caerulein-induced pancreatitis. *American Journal of Physiology* 1987;253(4 Pt 1):G508-516.

76. Mareninova OA, Hermann K, French SW, O'Konski MS, Pandol SJ, Webster P, Erickson AH, Katunuma N, Gorelick FS, Gukovsky I, Gukovskaya AS. Impaired autophagic flux mediates acinar cell vacuole formation and trypsinogen activation in rodent models of acute pancreatitis. *Journal of Clinical Investigations* 2009;119(11):3340-3355.

77. Hoque R, Mehal WZ. Inflammasomes in pancreatic physiology and disease. *American Journal of Physiology: Gastrointestinal Liver Physiology* 2015;308G643-G651.

78. Dios ID. Inflammatory role of the acinar cells during acute pancreatitis. *World Journal of Gastrointestinal Pharmacology and Therapeutics* 2010;6(1):15-20.

79. Bhatia M, Brady M, Shokuhi S, Christmas S, Neoptolemos JP, Slavin J. Inflammatory mediators in acute pancreatitis. *Journal of Pathology* 2000;190(2):117-125.

80. Bhatia V, Kim SO, Aronson JF, Chao C, Hellmich MR, Falzon M. Role of parathyroid hormone-related protein in the pro-inflammatory and pro-fibrogenic response associated with acute pancreatitis. *Regulatory Peptides* 2012;175(1-3):49-60.

81. Bhatia V, Rastellini C, Han S, Aronson JF, Greeley GH, Jr., Falzon M. Acinar cell-specific knockout of the Pthrp gene decreases the pro-inflammatory and pro-fibrotic response in pancreatitis. *American Journal of Physiology: Gastrointestinal Liver Physiology* 2014;307(5):G533-549.

82. Apte MV, Haber PS, Applegate TL, Norton ID, McCaughan GW, Korsten MA, Pirola RC, Wilson JS. Periacinar stellate shaped cells in rat pancreas: identification, isolation, and culture. *Gut* 1998;43(1):128-133.

83. Bachem MG, Schneider E, Gross H, Weidenbach H, Schmid RM, Menke A, Siech M, Beger H, Grunert A, Adler G. Identification, culture, and characterization of pancreatic stellate cells in rats and humans. *Gastroenterology* 1998;115(2):421-432.

84. Phillips PA, McCarroll JA, Park S, Wu MJ, Pirola R, Korsten M, Wilson JS, Apte MV. Rat pancreatic stellate cells secrete matrix metalloproteinases: implications for extracellular matrix turnover. *Gut* 2003;52(2):275-282.

85. Kennedy RH, Bockman DE, Uscanga L, Choux R, Grimaud JA, Sarles H. Pancreatic extracellular matrix alterations in chronic pancreatitis. *Pancreas* 1987;2(1):61-72.

86. Apte MV, Phillips PA, Fahmy RG, Darby SJ, Rodgers SC, McCaughan GW, Korsten MA, Pirola RC, Naidoo D, Wilson JS. Does alcohol directly stimulate pancreatic fibrogenesis? Studies with rat pancreatic stellate cells. *Gastroenterology* 2000;118(4):780-794.

87. Jalleh RP, Aslam M, Williamson RC. Pancreatic tissue and ductal pressures in chronic pancreatitis. *British Journal of Surgery* 1991;78(10):1235-1237.

88. Watanabe S, Nagashio Y, Asaumi H, Nomiyama Y, Taguchi M, Tashiro M, Kihara Y, Nakamura H, Otsuki M. Pressure activates rat pancreatic stellate cells. *American Journal of Physiology - Gastrointestinal & Liver Physiology* 2004;287(6):G1175-1181.

89. Bachem MG, Zhou Z, Zhou S, Siech M. Role of stellate cells in pancreatic fibrogenesis associated with acute and chronic pancreatitis. *Journal of Gastroenterology & Hepatology* 2006;21 Suppl 3S92-96.

90. Masamune A, Shimosegawa T. Pancreatic stellate cells--multi-functional cells in the pancreas. *Pancreatology* 2013;13(2):102-105.

91. Masamune A, Kikuta K, Watanabe T, Satoh K, Satoh A, Shimosegawa T. Pancreatic stellate cells express Toll-like receptors. *Journal of Gastroenterology* 2008;43(5):352-362.

92. Shimizu K. Pancreatic stellate cells: molecular mechanism of pancreatic fibrosis. *Journal of Gastroenterology & Hepatology* 2008;23 Suppl 1S119-121.

93. Apte M, Pirola R, Wilson J. Pancreatic stellate cells: a starring role in normal and diseased pancreas. *Frontiers in Physiology* 2012;31-14.

94. Longnecker DS, Lilja HS, French J, Kuhlmann E, Noll W. Transplantation of azaserine-induced carcinomas of pancreas in rats. *Cancer Letters* 1979;7(4):197-202.

95. Phillips PA, Yang L, Shulkes A, Vonlaufen A, Poljak A, Bustamante S, Warren A, Xu Z, Guilhaus M, Pirola R, Apte MV, Wilson JS. Pancreatic stellate cells produce acetylcholine and may play a role in pancreatic exocrine secretion. *Proceedings of the National Academy of Sciences of the United States of America* 2010;107(40):17397-17402.

96. Berna MJ, Seiz O, Nast JF, Benten D, Blaker M, Koch J, Lohse AW, Pace A. CCK1 and CCK2 receptors are expressed on pancreatic stellate cells and induce collagen production. *Journal of Biological Chemistry* 2010;285(50):38905-38914.

97. Scheele G, Adler G, Kern H. Exocytosis occurs at the lateral plasma membrane of the pancreatic acinar cell during supramaximal secretagogue stimulation. *Gastroenterology* 1987;92(2):345-353.

98. Yamaguchi H, Kimura T, Mimura K, Nawata H. Activation of proteases in cerulein-induced pancreatitis. *Pancreas* 1989;4(5):565-571.

99. Neuschwander-Tetri BA, Burton FR, Presti ME, Britton RS, Janney CG, Garvin PR, Brunt EM, Galvin NJ, Poulos JE. Repetitive self-limited acute pancreatitis induces pancreatic fibrogenesis in the mouse. *Digestive Diseases and Sciences* 2000;45(4):665-674.

100. Neuschwander-Tetri BA, Bridle KR, Wells LD, Marcu M, Ramm GA. Repetitive acute pancreatic injury in the mouse induces procollagen alpha1(I) expression colocalized to pancreatic stellate cells. *Laboratory Investigation* 2000;80(2):143-150.

101. Aghdassi AA, Mayerle J, Christochowitz S, Weiss FU, Sendler M, Lerch MM. Animal models for investigating chronic pancreatitis. *Fibrogenesis Tissue Repair* 2011;4(1):26.

102. Mizunuma T, Kawamura S, Kishino Y. Effects of injecting excess arginine on rat pancreas. *Journal of Nutrition* 1984;114(3):467-471.

103. Weaver C, Bishop AE, Polak JM. Pancreatic changes elicited by chronic administration of excess L-arginine. *Experimental and Molecular Pathology* 1994;60(2):71-87.

104. Foster JR. A review of animal models of nonneoplastic pancreatic diseases. *Toxicologic Pathology* 2014;42(1):243-259.

105. Watanabe S, Abe K, Anbo Y, Katoh H. Changes in the mouse exocrine pancreas after pancreatic duct ligation: a qualitative and quantitative histological study. *Archives of Histology & Cytology* 1995;58(3):365-374.

106. Lieber CS, Jones DP, Decarli LM. Effects of Prolonged Ethanol Intake: Production of Fatty Liver Despite Adequate Diets. *Journal of Clinical Investigation* 1965;441009-1021.

107. Sarles H, Lebreuil G, Tasso F, Figarella C, Clemente F, Devaux MA, Fagonde B, Payan H. A comparison of alcoholic pancreatitis in rat and man. *Gut* 1971;12(5):377-388.

108. Shukla S, Gupta S. Apigenin: a promising molecule for cancer prevention. *Pharmaceutical Research* 2010;27(6):962-978.

109. Wang YC, Huang KM. In vitro anti-inflammatory effect of apigenin in the Helicobacter pylori-infected gastric adenocarcinoma cells. *Food & Chemical Toxicology* 2013;53376-383.

110. Lampropoulos P, Lambropoulou M, Papalois A, Basios N, Manousi M, Simopoulos C, Tsaroucha AK. The role of apigenin in an experimental model of acute pancreatitis. *Journal of Surgical Research* 2013;183(1):129-137.

111. Chen H, Mrazek AA, Wang X, Ding C, Ding Y, Porro LJ, Liu H, Chao C, Hellmich MR, Zhou J. Design, synthesis, and characterization of novel apigenin analogues that suppress pancreatic stellate cell proliferation in vitro and associated pancreatic fibrosis in vivo. *Bioorg Med Chem* 2014;22(13):3393-3404.

112. Vasavada RC, Cavaliere C, D'Ercole AJ, Dann P, Burtis WJ, Madlener AL, Zawalich K, Zawalich W, Philbrick W, Stewart AF. Overexpression of parathyroid hormone-related protein in the pancreatic islets of transgenic mice causes islet hyperplasia, hyperinsulinemia, and hypoglycemia. *Journal of Biological Chemistry* 1996;271(2):1200-1208.

113. Mannstadt M, Juppner H, Gardella TJ. Receptors for PTH and PTHrP: their biological importance and functional properties. *American Journal of Physiology* 1999;277(5 Pt 2):F665-675.

114. Mathison A, Liebl A, Bharucha J, Mukhopadhyay D, Lomberk G, Shah V, Urrutia R. Pancreatic stellate cell models for transcriptional studies of desmoplasia-associated genes. *Pancreatology* 2010;10(4):505-516.

115. Kruse ML, Hildebrand PB, Timke C, Folsch UR, Schafer H, Schmidt WE. Isolation, long-term culture, and characterization of rat pancreatic fibroblastoid/stellate cells. *Pancreas* 2001;23(1):49-54.

116. Cataisson C, Gordon J, Roussiere M, Abdalkani A, Lindermann R, Dittmer J, Foley J, Bouizar Z. Ets-1 activates parathyroid hormone-related protein gene expression in tumorigenic breast epithelial cells. *Molecular and Cellular Endocrinology* 2002;204155-168.

117. Bradford MM. A rapid and sensitive method for the quantitation of microgram quantities of protein utilizing the principle of protein-dye binding. *Analytical Biochemistry* 1976;72248-254.

118. Yeung YG, Stanley ER. A solution for stripping antibodies from polyvinylidene fluoride immunoblots for multiple reprobing. *Analytical Biochemistry* 2009;389(1):89-91.

119. Mrazek AA, Porro LJ, Bhatia V, Falzon M, Spratt H, Zhou J, Chao C, Hellmich MR. Aigenin inhibits pancreatic stellate cell activity in pancreatitis. *Journal of Surgical Research* 2015;196(1):8-16.

120. Gao X, Cao Y, Yang W, Duan C, Aronson JF, Rastellini C, Chao C, Hellmich MR, Ko TC. BMP2 inhibits TGF-beta-induced pancreatic stellate cell activation and extracellular matrix formation. *American Journal of Physiology: Gastrointestinal and Liver Physiology* 2013;304(9):G804-813.

121. Isola J, Tuominen VJ. ImmunoRatio. Cited June 28, 2015; 1.0c: Institute of Biomedical Technology, University of Tampere. Available from: http://153.1.200.58:8080/immunoratio/

122. Tuominen VJ, Ruotoistenmaki S, Viitanen A, Jumppanen M, Isola J. ImmunoRatio: a publicly available web application for quantitative image analysis of estrogen receptor (ER), progesterone receptor (PR), and Ki-67. *Breast Cancer Research* 2010;12(4):R56.

123. Gavet O, Pines J. Progressive activation of CyclinB1-Cdk1 coordinates entry to mitosis. *Developmental Cell* 2010;18(4):533-543.

124. Potapova TA, Sivakumar S, Flynn JN, Li R, Gorbsky GJ. Mitotic progression becomes irreversible in prometaphase and collapses when Wee1 and Cdc25 are inhibited. *Molecular Biology of the Cell* 2011;22(8):1191-1206.

125. Lesina M, Wormann SM, Neuhofer P, Song L, Algul H. Interleukin-6 in inflammatory and malignant diseases of the pancreas. *Seminars in Immunology* 2014;26(1):80-87.

126. Richard V, Rosol TJ, Foley J. PTHrP gene expression in cancer: do all paths lead to Ets? *Critical Reviews in Eukaryotic Gene Expression* 2005;15(2):115-132.

127. Karperien M, Farih-Sips H, Hendriks JA, Lanske B, Papapoulos SE, Abou-Samra AB, Lowik CW, Defize LH. Identification of a retinoic acid-inducible element in the murine PTH/PTHrP (parathyroid hormone/parathyroid hormone-related peptide) receptor gene. *Molecular Endocrinology* 1999;13(7):1183-1196.

128. Van Dross R, Xue Y, Knudson A, Pelling JC. The chemopreventive bioflavonoid apigenin modulates signal transduction pathways in keratinocyte and colon carcinoma cell lines. *The Journal of Nutrition* 2003;133(11 Suppl 1):3800S-3804S.

129. Pham H, Chen M, Takahashi H, King J, Reber HA, Hines OJ, Pandol S, Eibl G. Apigenin inhibits NNK-induced focal adhesion kinase activation in pancreatic cancer cells. *Pancreas* 2012;41(8):1306-1315.

130. Sah RP, Dudeja V, Dawra RK, Saluja AK. Cerulein-induced chronic pancreatitis does not require intra-acinar activation of trypsinogen in mice. *Gastroenterology* 2013;144(5):1076-1085.e1072.

131. Karin M, Yamamoto Y, Wang QM. The IKK NF-kappa B system: a treasure trove for drug development. *Nature Reviews Drug Discovery* 2004;3(1):17-26.

132. Kondoh K, Torii S, Nishida E. Control of MAP kinase signaling to the nucleus. *Chromosoma* 2005;114(2):86-91.

133. Fukuda M, Gotoh I, Gotoh Y, Nishida E. Cytoplasmic localization of mitogen-activated protein kinase kinase directed by its NH2-terminal, leucine-rich short amino acid sequence, which acts as a nuclear export signal. *Journal of Biological Chemistry* 1996;271(33):20024-20028.

134. Adachi M, Fukuda M, Nishida E. Nuclear export of MAP kinase (ERK) involves a MAP kinase kinase (MEK)-dependent active transport mechanism. *Journal of Cell Biology* 2000;148(5):849-856.

135. Clemons AP, Holstein DM, Galli A, Saunders C. Cerulein-induced acute pancreatitis in the rat is significantly ameliorated by treatment with MEK1/2 inhibitors U0126 and PD98059. *Pancreas* 2002;25(3):251-259.

136. Wu D-G, Yu P, Li J-W, Jiang P, Sun J, Wang H-Z, Zhang L-D, Wen M-B, Bie P. Apigenin potentiates the growth inhibitory effects by IKK-beta-mediated NF-kappaB activation in pancreatic cancer cells. *Toxicology Letters* 2014;224(1):157-164.

137. McCarroll JA, Phillips PA, Santucci N, Pirola RC, Wilson JS, Apte MV. Vitamin A inhibits pancreatic stellate cell activation: implications for treatment of pancreatic fibrosis. *Gut* 2006;55(1):79-89.

138. Fitzner B, Muller S, Walther M, Fischer M, Engelmann R, Muller-Hilke B, Putzer BM, Kreutzer M, Nizze H, Jaster R. Senescence determines the fate of activated rat pancreatic stellate cells. *Journal of Cellular Molecular Medicine* 2012;16(11):2620-2630.

139. Vonlaufen A, Phillips PA, Xu Z, Zhang X, Yang L, Pirola RC, Wilson JS, Apte MV. Withdrawal of alcohol promotes regression while continued alcohol intake promotes persistence of LPS-induced pancreatic injury in alcohol-fed rats. *Gut* 2011;60(2):238-246.

140. Ruifrok AC, Johnston DA. Quantification of histochemical staining by color deconvolution. *Analytical and Quantitative Cytology and Histology* 2001;23(4):291-299.

141. Salmon P, Oberholzer J, Occhiodoro T, Morel P, Lou J, Trono D. Reversible immortalization of human primary cells by lentivector-mediated transfer of specific genes. *Molecular Therapy: The Journal of the American Society of Gene Therapy* 2000;2(4):404-414.

142. Park HR, Daun Y, Park JK, Bark KM. Spectroscopic properties of flavonoids in various aqueous-organic solvent mixtures. *Bulletin of the Korean Chemical Society* 2013;34(1):211-220.

143. Carvalho KM, Morais TC, de Melo TS, de Castro Brito GA, de Andrade GM, Rao VS, Santos FA. The natural flavonoid quercetin ameliorates cerulein-induced acute pancreatitis in mice. *Biological and Pharmaceutical Bulletin* 2010;33(9):1534-1539.

144. Das D, Mukherjee S, Das AS, Mukherjee M, Mitra C. Aqueous extract of black tea (Camellia sinensis) prevents ethanol+cholecystokinin-induced pancreatitis in a rat model. *Life Sciences* 2006;78(19):2194-2203.

145. Erkan M, Adler G, Apte MV, Bachem MG, Buchholz M, Detlefsen S, Esposito I, Friess H, Gress TM, Habisch HJ, Hwang RF, Jaster R, Kleeff J, Kloppel G, Kordes C, Logsdon CD, Masamune A, Michalski CW, Oh J, Phillips PA, Pinzani M, Reiser-Erkan C, Tsukamoto H, Wilson J. StellaTUM: current consensus and discussion on pancreatic stellate cell research. *Gut* 2012;61(2):172-178.

146. Asaumi H, Watanabe S, Taguchi M, Tashiro M, Nagashio Y, Nomiyama Y, Nakamura H, Otsuki M. Green tea polyphenol (-)-epigallocatechin-3-gallate inhibits ethanol-induced activation of pancreatic stellate cells. *European Journal of Clinical Investigation* 2006;36(2):113-122.

147. Chun OK, Chung SJ, Song WO. Estimated dietary flavonoid intake and major food sources of U.S. adults. *Journal of Nutrition* 2007;137(5):1244-1252.

148. Zhang J, Liu D, Huang Y, Gao Y, Qian S. Biopharmaceutics classification and intestinal absorption study of apigenin. *International Journal of Pharmaceutics* 2012;436(1-2):311-317.

149. Gradolatto A, Canivenc-Lavier MC, Basly JP, Siess MH, Teyssier C. Metabolism of apigenin by rat liver phase I and phase ii enzymes and by isolated perfused rat liver. *Drug Metabolism and Disposition* 2004;32(1):58-65.

150. Gradolatto A, Basly JP, Berges R, Teyssier C, Chagnon MC, Siess MH, Canivenc-Lavier MC. Pharmacokinetics and metabolism of apigenin in female and male rats after a single oral administration. *Drug Metabolism and Disposition* 2005;33(1):49-54.

151. Chan KF, Zhao Y, Burkett BA, Wong IL, Chow LM, Chan TH. Flavonoid dimers as bivalent modulators for P-glycoprotein-based multidrug resistance: synthetic apigenin homodimers linked with defined-length poly(ethylene glycol) spacers increase drug retention and enhance chemosensitivity in resistant cancer cells. *Journal of Medicinal Chemistry* 2006;49(23):6742-6759.

152. Wong IL, Chan KF, Tsang KH, Lam CY, Zhao Y, Chan TH, Chow LM. Modulation of multidrug resistance protein 1 (MRP1/ABCC1)-mediated multidrug resistance by bivalent apigenin homodimers and their derivatives. *Journal of Medicinal Chemistry* 2009;52(17):5311-5322.

153. Lin AS, Nakagawa-Goto K, Chang FR, Yu D, Morris-Natschke SL, Wu CC, Chen SL, Wu YC, Lee KH. First total synthesis of protoapigenone and its analogues as potent cytotoxic agents. *Journal of Medicinal Chemistry* 2007;50(16):3921-3927.

154. Manthey JA, Guthrie N. Antiproliferative activities of citrus flavonoids against six human cancer cell lines. *Journal of Agricultural and Food Chemistry* 2002;50(21):5837-5843.

155. Walle T. Methylation of dietary flavones greatly improves their hepatic metabolic stability and intestinal absorption. *Molecular Pharmaceutics* 2007;4(6):826-832.

156. Li AP. Screening for human ADME/Tox drug properties in drug discovery. *Drug Discovery Today* 2001;6(7):357-366.

157. Di L, Kerns EH, Carter GT. Drug-like property concepts in pharmaceutical design. *Current Pharmaceutical Design* 2009;15(19):2184-2194.

158. Bertilsson S, Sward P, Kalaitzakis E. Factors that affect disease progression after first attack of acute pancreatitis. *Clinical Gastroenterology Hepatology* 2015[Apr 22-epub ahead of print].

CURRICULUM VITAE

NAME: Amy Ann Mrazek **DATE:** 7/19/2015

PRESENT POSITION AND ADDRESS: House officer, PGY III
Department of Surgery, Route 0534
University of Texas Medical Branch
301 University Blvd.
Galveston, TX 77555

BIOGRAPHICAL:

Date of birth: July 22, 1983
Place of birth: Corpus Christi, TX
Citizenship: United States of America
Home address: 4328 Avenue O, Galveston, TX 77550
Phone number: (409) 789-6994, cell. (409) 643-0084, pager
Email: aamrazek@utmb.edu

EDUCATION:

01/2013 – 08/2015	Ph.D. Candidate Mentors: Mark R. Hellmich, Ph.D., and Celia Chao, M.D. Human Pathophysiology and Translational Medicine University of Texas Medical Branch (UTMB), Galveston, TX
07/2010 - 06/2018	General Surgery Residency Training T32 Research Fellow University of Texas Medical Branch, Galveston, TX
08/2006 - 06/2010	M.D. University of Texas Medical Branch, Galveston, TX
08/2001 - 12/2005	B.S. Dual major in chemistry and biomedical science Texas A&M University – Corpus Christi, TX

PROFESSIONAL WORK HISTORY AND RESEARCH ACTIVITIES:

07/2012 – 07/2015	T32 Research Fellow Field: Gastrointestinal molecular mechanisms in the study of pancreatitis PI: Mark R. Hellmich, Ph.D. Grant support: T32 DK763920

	Department of Surgery University of Texas Medical Branch, Galveston, TX
06/2007 – Present	House Officer Supervisor: Kristene Gugliuzza, M.D. Department of General Surgery University of Texas Medical Branch, Galveston, TX
06/2007 – 04/2009	Research assistant Field: Sepsis and immunosenescence Mentor: Hiroshi Saito, Ph.D. Department of General Surgery University of Texas Medical Branch, Galveston, TX
03/2005 – 07/2005	College intern in the DeBakey Summer Surgery Program Mentors: William Fisher, M.D., and Charles Brunicardi, M.D. Baylor College of Medicine, Houston, TX
12/2004 – 04/2006	Research assistant Field: Microvascular research Supervisor: Wassim Choucair, M.D. Cardiology Associates of Corpus Christi, Corpus Christi, TX

TEACHING RESPONSIBILITIES AT UTMB:

Teaching: Medical students as a resident
Student Research Mentees: Gi He, college summer intern, 2014
Minal Cheema, high school summer student, 2013, 2014

MEMBERSHIP IN SCIENTIFIC SOCIETIES:

2014 – Present	Translational Research Scholars Program, UTMB
2013 - Present	Multi-disciplinary Translational Team on H2S and Colorectal Cancer, member
2013 – Present	Association of Academic Surgeons, member
2010 – Present	American College of Surgeons, member Association of Women Surgeons American Medical Association

HONORS:

2014	Singleton Surgical Society "1st Place in Basic Science Research", UTMB
2013	Singleton Surgical Society "1st Place in Basic Science Research", UTMB

2007 Medical Student Research Program "Best overall poster/presentation", Sigma Xi
2006 School of Medicine Alumni Scholarship, UTMB
2006 Student Research Award, Coastal Heart Foundation
2005 S*umma cum laude*, Texas A&M University-Corpus Christi
2005 Student Affairs Leadership Scholarship, Texas A&M University-Corpus Christi
2005 Behmann Brothers Foundation Scholarship
2001 – 2005 Presidential Top Scholarship, Texas A&M University-Corpus Christi
2004 Chemistry Scholar Award of South Texas Region, American Chemical Society

PUBLICATIONS:

Articles in Peer-Review Journals:

1. Bohanon FJ, **Mrazek AA**, Shabana MT, Mims S, Radhakrishnan GL, Kramer GC, Radhakrishnan RS. Heart rate variability analysis is more sensitive at identifying neonatal sepsis than conventional vital signs. Am J Surg, June 2015, accepted for publication.

2. **Mrazek AA**, Porro LJ, Bhatia V, Falzon M, Spratt H, Zhou J, Chao C, Hellmich MR. Apigenin inhibits pancreatic stellate cell activity in pancreatitis. J Surg Res. S0022-4804(15)00140-7, Feb 2015. PMID: 25799526.

3. Starr ME, Takahashi H, Okamura D, Zwischenberger BA, **Mrazek AA**, Ueda J, Stromberg AJ, Evers BM, Esmon CT, Saito H. Increased coagulation and suppressed generation of activated protein C in aged mice during intra-abdominal sepsis. Am J Physiol Heart Circ Physiol 308:H83-91, 2015. PMCID: PMC4338937.

4. Chen H*****, **Mrazek AA***, Wang X, Ding C, Ding Y, Porro LJ, Liu H, Chao C, Hellmich MR, Zhou J. Design, synthesis, and characterization of novel apigenin analogues that suppress pancreatic stellate cell proliferation in vitro and associated pancreatic fibrosis in vivo. Bioorg Med Chem. 22(13): 3393-404, Jul 2014. PMCID: PMC4091635. **** indicates shared primary authorship***.

5. **Mrazek AA**, Carmical JR, Wood TG, Hellmich MR, Eltorky M, Chao C. Colorectal cancer-associated fibroblasts are genotypically distinct. Curr Cancer Ther Rev. 10(2):97-218, Jan 2014. PMCID: PMC4270051.

6. Djukom C, Porro L, **Mrazek A**, Townsend CM Jr, Hellmich MR, Chao C. Dual inhibition of PI3K and mTOR signaling pathways decreases human pancreatic neuroendocrine tumor metastatic progression. Pancreas. 43(1): 88-92, Jan 2014. PMCID: PMC3864633.

Reviews:

1. **Mrazek AA**, Chao C. Surviving cutaneous melanoma: a clinical review of follow-up practices, surveillance, and management of recurrence. Surg Clin North Am. 94(5): 989-1002, Oct 2014. PMCID: PMC4173121.

2. Porro LJ, **Mrazek AA**, Chao C. Triple negative breast cancer: a review of clinicopathologic characteristics and treatment options. The Open Breast Cancer Journal. 6:1-8, June 2014. Accessed at: http://Benthamopen.com/ABSTRACT/TOBCANJ-6-1.

Dissertation: **Mrazek AA**. Preclinical development of a pharmacology agent for the treatment of recurrent acute pancreatitis. July 2015. UTMB. Galveston, TX.

Publication in preparation: **Mrazek AA,** Bhatia V, Falzon M, Chao C, Hellmich MR. Apigenin Reduces Parathyroid Hormone Related Protein-Mediated Inflammation in Pancreatitis. Cell Mol Gastroenterol Hepatol 2015, *in preparation*.

ORAL PRESENTATIONS:

1. **Mrazek AA**, Bhatia V, Falzon M, Hellmich MR, Chao C. Apigenin reduces PTHrP-mediated inflammation, PSC proliferation, and ECM synthesis in pancreatitis. Academic Surgical Congress, Las Vegas, NV, February 3, 2015.

2. **Mrazek AA**, Bohanon FJ, Chen H, Zhou J, Porro L, Hellmich MR, Chao C. Apigenin minimizes SMAD-dependent and independent TGF-β signaling by acinar cells in an in vitro model of chronic pancreatitis. American College of Surgeons Clinical Congress, San Francisco, CA, October 29, 2014.

3. Bohanon FJ, **Mrazek AA**, Porro L, Hye G, Spratt H, Hellmich MR, Chao C. Aminooxyacetic acid in combination with oxaliplatin significantly decreases colorectal liver metastasis in vivo. American College of Surgeons Clinical Congress, San Francisco, CA, October 28, 2014.

4. **Mrazek AA**, Carmical JR, Wood TG, Hellmich MR, Eltorky M, Chao C. Colorectal cancer-associated fibroblasts are genotypically distinct. Singleton Surgical Society Resident/Fellow Competition, UTMB, Galveston, TX, June 13, 2014.

5. **Mrazek AA**, Bohanon FJ, Chen H, Zhou J, Porro L, Hellmich MR, Chao C. Apigenin decreases pErk and pAkt expression by acinar cells in an in vitro model of chronic pancreatitis. South Texas Chapter of the American College of Surgeons, Austin, TX, February 21, 2014.

6. Bohanon FJ, **Mrazek AA**, Hye G, Hellmich MR, Chao C. Aminooxyacetic acid in combination with oxaliplatin decreases colorectal cancer liver metastasis. Oral presentation by Dr. Bohanon. South Texas Chapter of the American College of Surgeons, Austin, TX, February 21, 2014.

7. **Mrazek AA**, Bohanon FJ, Chen H, Zhou J, Porro L, Hellmich MR, Chao C. Apigenin decreases pErk and pAkt expression by acinar cells in an in vitro model of chronic pancreatitis. UTMB Dept. of Surgery Grand Rounds, Galveston, TX, February 12, 2014.

8. Bohanon FJ, Mrazek AA, Hye G, Hellmich MR, Chao C. Aminooxyacetic acid in combination with oxaliplatin decreases colorectal cancer liver metastasis. Oral presentation by Dr. Bohanon. UTMB Dept. of Surgery Grand Rounds, Galveston, TX, February 12, 2014.

9. **Mrazek AA**, Falzon M, Chen H, Zhou J, Bohanon FJ, Porro L, Bhatia V, Wang X, Hellmich MR, Chao C. Apigenin inhibits the pro-inflammatory and pro-fibrogenic responses in both acinar cells and pancreatic stellate cells in experimentally induced pancreatitis. Academic Surgical Congress, San Diego, CA, February 6, 2014.

10. **Mrazek AA**, Shabana MT, Radhakrishnan GL, Kramer GC, Radhakrishnan RS. Heart rate variability analysis is more sensitive at identifying neonatal sepsis than conventional vital signs. 9th Annual Academic Surgical Congress, San Diego, CA, February 4, 2014.

11. **Mrazek A**, Porro L, Carmical JR, Gomez G, Gajjar A, Hellmich MR, Chao C. Genetic and epigenetic changes in carcinoma-associated fibroblasts derived from human colorectal cancers. ACS Clinical Congress, Washington, DC, October 8, 2013.

12. **Mrazek A**. Apigenin and analogs effectively suppress pancreatic stellate cell proliferation, induce apoptosis, and decrease fibrosis in chronic pancreatitis. Singleton Surgical Society Resident/Fellow Competition, UTMB, Galveston, TX, June 14, 2013.

13. Porro LJ, **Mrazek A**, Szabo C, Coletta C, Modis K, Gajjar A, Gomez G, Ekhaese O, Gore D, Chao C, Hellmich MR. Patient-derived tumor xenograft for preclinical drug trials. Oral presentation by Dr. Porro. Singleton Surgical Society Resident/Fellow Competition, UTMB, Galveston, TX, June 14, 2013.

14. Mrazek A. Apigenin analogs modulate fibrosis in chronic pancreatitis. UTMB Dept. of Surgery Grand Rounds, Galveston, TX, January 9, 2013.

POSTER PRESENTATIONS:

1. Johnson P, Chao C, Phillips CM, **Mrazek AA**, Zatarain JR, Szabo C, Luthra G, Pinchuk IV, Hellmich MR. Increased levels of cystathionine-β-synthase arise from cancer stem-like cells in colon cancer. Digestive Diseases Week, Washington, DC, May 17-19, 2015.

2. Zatarain JR, **Mrazek AA**, Johnson P, Pang L, Ding Y, Zhou J, Szabo C, Hellmich MR, Chao C. H2S inhibition of cystathionine-β-synthase using novel prodrug decreases colorectal cancer xenograft growth with less toxicity than aminooxyacetic acid. Digestive Diseases Week, Washington, DC, May 17-19, 2015.

3. **Mrazek AA**, Bhatia V, Falzon M, Chao C, Hellmich MR. Apigenin reduces parathyroid hormone-related peptide-mediated inflammation in pancreatitis. Clinical and Translational Research Forum, Galveston, TX, March 11, 2015.

4. Chao C, Bohanon FJ, **Mrazek AA**, Coletta C, Szabo C, Hellmich MR. Cysthionine-beta-synthetase inhibition in combination with standard-chemotherapy decreases colorectal cancer metastasis to the liver. Poster presentation by Dr. Hellmich. Third International Conference on Hydrogen Sulfide in Biology and Medicine, Kyoto, Japan, June 4-6, 2014.

5. **Mrazek AA**, Bhatia V, Falzon M, Bohanon FJ, Chao C, Hellmich MR. Apigenin attenuates cerulein-induced parathyroid hormone-related protein (PTHrP) and IL-6 in a model of murine pancreatitis. Digestive Diseases Week, Chicago, IL, May 3-6, 2014.

6. **Mrazek AA**. Porro LJ, Wang XF, Chen H, Ives KL, Aronson JF, Chao C, Zhou J, Hellmich MR. Apigenin and analogs effectively suppress pancreatic stellate cell proliferation, induce apoptosis and decrease fibrosis in chronic pancreatitis. Clinical and Translational Research Forum, Galveston, TX, February 12, 2014.

7. **Mrazek AA**, Porro L, Chen H, Zhou J, Hellmich MR, Chao C. Apigenin and analogs effectively suppress pancreatic stellate cell proliferation, induce apoptosis, and decrease fibrosis in chronic pancreatitis. Texas Regional CTSA Consortium (TRCC) Inaugural TL1 & KL2 Scholars Meeting, San Antonio, TX, November 15, 2013.

8. **Mrazek AA**, Wang X, Porro L, Chen H, Zhou J, Hellmich MR, Chao C. Apigenin and analogs effectively suppress pancreatic stellate cell proliferation, induce apoptosis, and decrease fibrosis in chronic pancreatitis. Association of Women Surgeons Fall Conference, Washington, DC, October 6, 2013.

9. **Mrazek A**, Wang X, Porro L, Chen H, Zhou J, Hellmich MR, Chao C. Apigenin analogs effectively suppress pancreatic stellate cell proliferation and induce apoptosis. Digestive Diseases Week, Orlando, FL, May 19, 2013.

10. **Mrazek AA**, Porro LJ, Wang XF, Chen H, Ives KL, Aronson JF, Chao C, Zhou J, Hellmich MR. Apigenin inhibits pancreatic stellate cell proliferation, stimulates apoptosis and inhibits fibrosis associated with chronic pancreatitis. Clinical and Translational Research Forum, Galveston, TX, February 20, 2013.

11. Porro LJ, Djukom C, **Mrazek A**, Hellmich M, Chao C. Dual inhibition of AKT and mTOR signaling pathways decreases human pancreatic neuroendocrine tumor (PNET) metastatic progression. Clinical & Translational Science Awards 1st Annual Poster Session, Galveston, TX, February 20, 2013.

12. Djukom C, Porro L, **Mrazek A**, Hellmich M, Chao C. Dual inhibition of AKT and mTOR signaling pathways decreases human pancreatic neuroendocrine tumor (PNET) metastatic progression. Joint 43rd Meeting of the American Pancreatic Association and the 17th Meeting of the International Association of Pancreatology, Miami, FL, November 1, 2012.

13. **Mrazek A**, Edge D, Takahashi H, Starr ME, Evers BM, Saito H. Age-associated increase in coagulation during sepsis: role of thrombomodulin. 49th Annual National Student Research Forum, Galveston, TX, April 2008.

14. **Mrazek A**, Edge D, Takahashi H, Starr ME, Evers BM, Saito H. Age-associated increase in coagulation during sepsis: role of thrombomodulin. 11th Annual Forum on Aging Poster Session, Galveston, TX, October 2007.

15. **Mrazek A**, Edge D, Takahashi H, Starr ME, Evers BM, Saito H. Age-associated increase in coagulation during sepsis: role of thrombomodulin and PI3K pathway. Medical Student Research Program Poster Presentation, Galveston, TX, June 2007

16. **Mrazek A**, Kelly M, Johnson P, Islam S, Johnson D, Choucair W. Imaging of the microvasculature. Annual Arrhythmia and Heart Failure Symposium, Corpus Christi, TX, 2006.

SUMMARY OF DISSERTATION:

Chronic pancreatitis (CP) is an irreversible disease process defined by acinar cell necrosis, inflammation and fibrosis. With disease progression, patients develop pancreatic insufficiency secondary to the destruction of functional pancreatic tissue and its replacement with scarring. Patients with CP have a poor quality of life, and their treatment options are limited to supportive care and symptom palliation. There are currently no drugs on the market directly targeting the pathogenesis of CP. The objective of this research is to develop a pharmacologic agent for the treatment of recurrent acute pancreatitis (RAP), thereby limiting progression to CP. Apigenin is a natural compound with known anti-inflammatory, anti-proliferative, and pro-apoptotic properties. In a mouse model of RAP, the natural compound, apigenin, protected the pancreas from histologic damage while minimizing fibrosis. It was hypothesized that apigenin minimized the sequelae of RAP by inhibiting the inflammatory and fibrotic response to recurrent injury. Parathyroid hormone related protein (PTHrP) is a pro-inflammatory and pro-fibrotic mediator of acute and CP. The first aim was to identify PTHrP-related mechanisms by which apigenin limits inflammation in acinar cells. Apigenin reduced activation of the MAPK/ERK and NF-κB pathways, leading to suppression of PTHrP P3 promoter activity and IL-6 transcription. The second aim was to determine how apigenin limits pancreatic stellate cell (PSC)-mediated fibrosis. Apigenin inhibited PSC proliferation, induced PSC death, reduced PSC transcription of extracellular matrix proteins collagen and fibronectin, proliferative cofactor PCNA, and cytokines TGF-β, IL-6, and IL-8. The last aim was to develop apigenin-like compounds with more favorable drug-like properties. Analogs with improved aqueous solubility were tested *in vitro* and *in vivo* for increased potency. Analog HJC 05-61 was more potent than apigenin at limiting PSC viability and inducing PSC apoptosis. In a proof-of-concept RAP mouse study, apigenin derivatives were as effective as apigenin in preserving pancreatic architecture and limiting fibrosis. Thus apigenin and analogs protect the pancreas during RAP by limiting the pro-inflammatory and pro-fibrotic

response to pancreatic injury. This is in part mediated through down-regulation of PTHrP and PSC activity, both of which participate in autocrine and paracrine signaling that perpetuates pancreatitis.